UNIVERSITÀ DEGLI STUDI DI MILANO-BICOCCA

Facoltà di Scienze Matematiche, Fisiche e Naturali

DOTTORATO IN SCIENZE AMBIENTALI

(XXII Ciclo)

Monitoring of greenhouse gas emissions from agricultural and forest soils

Tutor: Dott. Roberto Comolli

Dottoranda:

Chiara Ferré

Anno Accademico 2008-2009

UNIVERSITÀ DEGLI STUDI DI MILANO-BICOCCA

Facoltà di Scienze Matematiche, Fisiche e Naturali

DOTTORATO IN SCIENZE AMBIENTALI

(XXII Ciclo)

Monitoring of greenhouse gas emissions from agricultural and forest soils

Tutor: Dott. Roberto Comolli

Dottoranda:

Chiara Ferré

Anno Accademico 2008-2009

CONTENTS

INTRODUCTION

Global climate change is becoming a central issue in contemporary science as well as politics. There is a long-lasting debate about the cause of the climate change: anthropogenic activity versus the natural cycle (Damon and Kunen, 1976; Crowley, 2000; Cuffey, 2004). However, driven by the rapidly accumulated observations worldwide, a scientific consensus is coming a conclusion that the contemporary climate change (e.g. temperature increase) is mainly caused by anthropogenic emissions of the greenhouse gases, including carbon dioxide (CO_2), nitrous oxide (N_2O) and methane (CH_4) (Crutzen et al., 1979; Intergovernmental Panel on Climate Change 2007).

Soil is the major organic carbon pool in terrestrial ecosystems (Schlesinger and Andrews, 2000); it contains larger amount of organic carbon (1500 Pg C) than both terrestrial vegetation (550 Pg C) and the atmosphere (780 Pg C) (Houghton, 2003). Soil plays an important role as a source or sink of greenhouse gases in almost all terrestrial ecosystems. The ranges of the soil sources and sinks, in particular, are highly uncertain. Although fluxes of trace gases between soil and atmosphere can be measured with some reliability by using various approaches, it is not trivial to estimate atmospheric budgets from field fluxes due to the fact that the fluxes generally show a high spatial and temporal variability.

The dominant terrestrial source of CO_2 is soil; carbon dioxide is produced in soil primarily by heterotrophic organisms and by respiration of living roots and most CO_2 produced in soils is released into the atmosphere. Soil respiration is estimated to be within the range of 64–72 Gt C y^{-1}, accounting for the 20-40% of annual input of C-CO_2 from terrestrial and marine sources to the atmosphere (Houghton and Woodwell, 1989; Raich and Schlesinger, 1992).

Soil CO_2 efflux has been measured in various forest ecosystems all over the world (Raich and Schlesinger, 1992; Vose et al., 1995; Thierron and Laudelout, 1996; Davidson et al. 1998; Russell and Voroney 1998; Epron et al., 1999). High spatial and temporal variability of soil CO_2 efflux has been reported (Raich et al., 1990; Hanson et al., 1993; Thierron and Laudelout, 1996) and has been attributed to species composition, stand age, management practices, and climatic and edaphic conditions (Edwards and Ross-Todd 1983; Ewel et al. 1987; Hanson et al. 1993; Toland and Zak 1994). Temperature has a strong impact on soil respiration rates, and the potential for increased rates of CO_2 production by soils in response to global warming suggests that a positive feedback could occur between global warming and atmospheric CO_2 concentrations (Schlese, 1982; Jenkison et al., 1991; Raich and Schlesinger, 1992; Trumbore et al., 1996; Kirschbaum, 2000). Soil respiration is also controlled by moisture (Parker et al., 1983; Davidson et al., 2000), soil organic matter quantity and quality (Taylor et al., 1989; Coûteau et al., 1995), root and microbial bio-

mass, root nitrogen content (Ryan et al., 1996), soil acidity, texture and site productivity (Raich and Schlesinger, 1992; Raich and Potter, 1995).
Forests have been estimated to contain up to 80% of all aboveground organic C and about 40% of all underground C (Dixon et al., 1994), so that little changes in C pools of such soils can significantly affect the global C cycle; in temperate forests soil CO_2 efflux has been estimated to account for 60–90% of the total ecosystem respiration (Law et al., 2001; Valentini et al., 2000).
The total soil CO_2 efflux is the sum of heterotrophic and autotrophic respiration. Many studies have suggested that root respiration significantly contributes to net CO_2 fluxes from soils (Raich and Schlesinger, 1992; Hendricks et al., 1993; Epron et al., 1999; Högberg et al., 2001; Cisneros-Dozal et al., 2006), but estimates of such contribution is highly variable and reliable, and reproducible quantification remains hard to define. The partitioning of soil respiration in its two components, as well as the knowledge of temperature dependence of each component are relevant for the comprehension of the soil C balance, for the prediction of ecosystem response to climate change and for the understanding of the potential feedbacks of the global change on soil processes.
Soil also plays a role in contributing to the atmospheric concentrations of other greenhouse gases, such as CH_4 and N_2O. Rice fields are one of the most important sources of atmospheric CH_4, with a global emission estimated between 60 and 150 Tg year-1 (IPCC, 2007), accounting for 15–20% of the world's total anthropogenic CH_4 emission. Methane emissions in rice fields can be quite different in different sites, and in seasonal and management types (Wassmann et al., 2000). The most important variables which affect CH_4 emission include soil type, rice variety, temperature, soil redox potential (Eh), water management, and fertilization with organic carbon and nitrogen (Aulakh et al., 2001; Kimura et al., 2004; Minami, 1994; Neue and Roger, 2000; Yan et al., 2005). These variables affect production, transport, and oxidation of CH_4 in the rice field.
Methane oxidation occurs in well aerated soils, leading to a CH_4 uptake from the atmosphere into the soils, due to oxidizer microorganisms (King and Schnell, 1998; Dunfield et al., 1999), mainly localized in the uppermost layers of mineral soils (Steinkamp et al., 2001; Butterbach-Bahl and Papen, 2002).
N_2O is predominantly produced by the microbiological processes of nitrification and denitrification and agricultural soil is a major source of nitrous oxide. Since nitrous oxide derives from microbial processes, its production is controlled by factors which affect the growth of microorganisms, as temperature, pH, rainfall (Sahrawat and Keeney, 1986), but it is also affected by fertilizer rate, tillage practice, soil type, oxygen concentration, availability of carbon, vegetation, land use practices, use of chemicals, irrigation practices and water holding capacity of the soil (Sahrawat and Keeney, 1986; Simojoki and Jaakkola, 2000). Forest soils have been identified to be sources for NO_x (Brumme and Beese, 1992; Skiba et al., 1994; Papen and Butterbach-Bahl, 1999; Gasche and Papen, 1999), but also net N_2O or NO consumption by soils has been observed (Baumgärtner et al., 1996; Schiller and Hastie, 1996; Papen et al., 2001). Early studies found N_2O emission from paddy fields to be negligible (Smith et al., 1982), but recent studies suggest that rice cultivation is a significant anthropogenic source not only of atmospheric methane (CH_4) but also of

N_2O (Cai et al., 1997). In the last years, more measurements of N_2O emission from rice paddies have been performed although the number of field measurements is still relatively small compared with those of CH_4 emission from paddy rice fields or N_2O emission from upland fields.

Although CH_4 and especially N_2O are at far lower atmospheric concentrations than CO_2, their global warming potentials are sufficiently high that small changes have a large effect on radiative forcing. These gases are important to the atmospheric chemistry and earth's radiative balance because of their long atmospheric life times (10 yr for CH_4 and 120 yr for N_2O). Both species absorb terrestrial thermal radiation: N_2O is the strongest climate gas with a global warming potential (GWP) of 310, compared to the GWPs of CH_4 and CO_2, of 21 and 1, respectively. Concerning CO_2, there are only few studies that include CO_2 emissions from paddy soils; the mechanism of CO_2 efflux is not fully understood and the budget of CO_2 between the atmosphere and the rice paddies have not been well documented.

Gaseous emissions of N and C from soil are essentially the result of microbial activity, which includes nitrification, denitrification, respiration, methanotrophy and methanogenesis.

The study of microbial communities has for a long time been limited by the availability of suitable methods. Therefore, the knowledge of biogeochemical processes and fluxes was much more mature than the knowledge of the microbial communities responsible of these processes. Nevertheless, substantial progress has been made by applying molecular and biochemical techniques to the microbiota; independent culture techniques, based upon structural component analysis, have been developed to characterize changes in soil community diversity (Kennedy and Gewin, 1997), such as fatty acid-based methods (methyl ester (FAME) analysis and phospholipid fatty acid (PLFA and PLEL) analysis), and PCR-based methods (Øvreas, 2000).

The need of precise estimates of greenhouse gas production rates and emissions from natural as well as managed ecosystems has risen to a critical level. Future agreements between nations, concerning the reduction of their greenhouse gas emissions, will depend upon precise estimates of the present level of these emissions in both natural and managed terrestrial environments.

From this point of view, also the question of soil spatial variability has to be taken into account. A representative estimate of gas efflux from the soil surface is dependent on the understanding of the spatial variability of emission rates.

Spatial heterogeneity is, in fact, a substantial problem in monitoring and modelling of gas emissions in terrestrial ecosystems. Soil CO_2, CH_4 and N_2O fluxes are highly variable in space and time, affected by soil environmental factors like temperature, moisture, pH, redox potential, substrate concentration gradients, biochemical reactions (Li, 2000 and 2001; Li et al., 2004), climate, vegetation, as well as by anthropogenic activity. While studies on spatial variability have been conducted for soil respiration in both forest and agricultural ecosystem (Lee et al., 2006; Stoyan, 2000; Shibistova, 2002) demonstrating a high heterogeneity of CO_2 efflux, concerning N_2O and CH_4 emissions, the investigation of spatial trend presents greater difficulties. To get a representative value of soil effluxes of these

gases within an ecosystem, a large number of measurement chambers is required, resulting in high costs for equipment, checking and maintenance. The study and the knowledge of spatial pattern for the major soil properties affecting emissions of greenhouse gases can be used to estimate the spatial distribution for efflux rates of such gases, bypassing the difficulties in studying the spatial variability of gas emissions in a direct way. Information about the spatial heterogeneity of soil properties as well as of vegetation types can be useful for understanding ecosystems dynamics, assessing the contribution of gaseous emissions and identifying the appropriate sampling design.

The main objective of this thesis is the monitoring of GHG emissions from two ecosystem types: a forest and a rice paddy ecosystem. The forest site is a EMEP (European Monitoring and Evaluation Program - monitoring and evaluation of long range transmission of air pollution) experimental station, taking part of the activity of GHG-AGOLU of FP7-JRC project, while the agricultural ecosystem was included in the CarboEurope project and represents also a Level 3 site in the frame of NitroEurope project. The gas monitoring was carried out in 2008.

The thesis is composed by 4 chapters, corresponding to specific objectives. The first chapter is relative to the study of the spatial variability of the main soil chemical and physical properties on the basis of which the gas monitoring points were selected. The second and the third chapters are relative to cropland site. In particular, the second chapter includes monitoring data of CH_4, N_2O and CO_2 fluxes from the paddy field, both during the crop growth season and the fallow period, and the validation results of the DeNitrification–DeComposition (DNDC) model (Li et al., 1992), a process-oriented biogeochemical model used for simulating soil gas emissions from the paddy field, are reported. The third chapter contains the study of characterization of microbial community composition using phospholipid fatty acid analysis (PLFA), at eight sampling dates representative of different soil conditions and crop stages and consequently characterized by distinct soil greenhouse emission rates.

The fourth and last chapter includes the monitoring study of soil respiration in a forest site and its partitioning into autotrophic and heterotrophic components, applying the indirect linear regression method (Rodeghiero and Cescatti, 2006).

These studies were performed in the framework of a series of activities related to the CarboEurope-IP, Nitroeurope and FP7-JRC projects, in collaboration between the JRC Institute for Environmental and Sustainability - Climate Change Unit of Ispra (Italy) and the Department of Environmental and Land Sciences of the Milan Bicocca University.

REFERENCES

- Aulakh, M.S., Wassmann, R., Rennenberg, H., 2001. Methane transport capacity of twenty-two rice cultivars from five major Asian rice-growing countries. Agriculture, Ecosystems and Environment 70, 193-260.
- Baumgärtner, M., Koschorreck, M., Conrad, R., 1996. Oxidative consumption of nitric oxide by heterotrophic bacteria in soil. FEMS Microbiology Ecology 19, 165–170.
- Brumme, R., Beese, F., 1992. Effects of liming and nitrogen fertilization on emission of CO_2 and N_2O from temperate forest soils. Journal of Geophysical Research 97, 12851–12858.
- Butterbach-Bahl, K., Papen, H., 2002. Four years continuous record of CH_4-exchange between the atmosphere and untreated and limed soil of a N-saturated spruce and beech forest ecosystem in Germany. Plant and Soil 240, 77–90.
- Cai, Z., Xing, G., Yan, X., Xu, H., Tsuruta, H., Yagi, K., Minami, K., 1997. Methane and nitrous oxide emissions from rice paddy fields as affected by nitrogen fertilizers and water management. Plant and Soil 196, 7–14.
- Cisneros-Dozal, L.M., Trumbore, S., Hanson, P.J., 2006. Partitioning sources of soil-respired CO_2 and their seasonal variation using a unique radiocarbon tracer. Global Change Biology 12, 194–204.
- Coûteau, M.M., Bottner, P., Berg, B., 1995. Litter decomposition, climate and litter quality. Trends in Ecology and Evolution 10, 63-66.
- Crowley, T.J., 2000. Causes of climate change over the past 1000 years. Science 289, 270–277.
- Crutzen, P.J., Heidt, L.E., Krasnec, J.P., Pollock, W.H., Seiler, W., 1979. Biomass burning as a source of the atmospheric gases CO, H_2, N_2O, CH_3Cl, and COS. Nature 282, 253–256.
- Cuffey, K.M., 2004. Into an Ice Age. Nature 431, 133–134.
- Damon, P.E., Kunen, S.M., 1976. Global Cooling? Science 193, 447–453.
- Davidson, E.A., Verchot, L.V., Cattanio, J.H., Ackerman, I.L., Carvalho, J.E.M., 2000. Effects of soil water content on soil respiration in forests and cattle pastures of eastern Amazonia. Biogeochemistry 48(1), 53–69.
- Davidson, E.A.., Belk, E., Boone, R.D., 1998. Soil water content and temperature as independent or confounded factors controlling soil respiration in a temperate mixed hardwood forest. Global Change Biology 4(2), 217–227.
- Dixon, R.K., Brown, S., Houghton, R.A., Solomon, A.M., Trexler, M.C., Wisniewski, J., 1994. Carbon pools and flux of global forest ecosystems. Science 263, 185–190.
- Dunfield, P.F., Liesack, W., Henckel, T., Knowles, R., Conrad, R., 1999. High-affinity methane oxidation by soil enrichment culture containing a type II methanotroph. Applied and Environmental Microbiology 65, 1009–1014.
- Edwards, N.T., Ross-Todd, B.M., 1983. Soil carbon dynamics in a mixed deciduous forest following clear-cutting with and without residue removal. Soil Science Society of America Journal 47, 1014-1021.
- Epron, D., Farque, L., Lucot, E., Badot, P.M., 1999. Soil CO_2 efflux in a beech forest: dependence on soil temperature and soil water content. Annals of Forest Science 56, 221–226.

- Ewel, K.C., Cropper, W.P., Gholz, H.L., 1987. Soil CO_2 evolution in Florida slash pine plantations. II. Importance of root respiration. Canadian Journal of Forest Research 17, 330–333.
- Gasche, R., Papen, H. 1999. A 3-year continuous record of nitrogen trace gas fluxes from untreated and limed soil of a N-saturated spruce and beech forest ecosystem in Germany. 2. NO and NO_2 fluxes. Journal of Geophysical Research 104(D15), 18505–18520.
- Hanson, P.J., Wullschleger, S.D., Bohlman, S.A., Todd, D.E., 1993. Seasonal and topographic patterns of forest floor CO_2 efflux from an upland oak forest. Tree Physiology 13, 1–15.
- Hendricks, J.J., Nadelhoffer, K.J., Aber, J.D., 1993. Assessing the role of fine roots in carbon and nutrient cycling. Trends in Ecology and Evolution 8, 174–178.
- Högberg, A., Nordgren, N., Buchmann, A.F.S., Taylor, A., Ekblad, M.N., Högberg, G., Nyberg, M., Ottosson-Löfvenius, Read, D.J., 2001. Large-scale forest girdling shows that current photosynthesis drives soil respiration. Nature 411, 789–792.
- Houghton, R.A., Woodwell, G.M., 1989. Global climatic change. Scientific American 260(4), 36–44.
- Houghton, R.A., 2003. Revised estimates of the annual net flux of carbon to the atmosphere from changes in land use and land management 1850-2000. Tellus Series B-Chemical and Physical Meteorology 55, 378–390.
- IPCC, 2007. Climate Change, 2007. Synthesis Report. Contribution of Working Groups I, II and III to the Fourth Assessment Report of the Intergovernmental Panel on Climate Change. IPCC, Geneva, Switzerland, 104 pp.
- Jenkinson, D.S., Adams, D.E., Wild, A., 1991. Model estimates of CO_2 emissions from soil in response to global warming. Nature 351, 304–306.
- Kennedy, A.C., Gewin, V.I., 1997. Soil microbial diversity: present and future considerations. Soil Science 162, 607–617.
- Kimura, M., Murase, J., Lu, Y.H.,2004. Carbon cycling in rice field ecosystems in the context of input, decomposition and translocation of organic materials and the fates of their end products (CO_2 and CH_4): a review. Soil Biology and Biochemistry 36, 1399–1416.
- King, G.M., Schnell, S., 1998. Effects of ammonium and nonammonium salt additions on methane oxidation by Methylosinus trichosporium OB3b and Maine forest soils. Applied and Environmental Microbiology 64, 253–257.
- Kirschbaum, M.U.F., 2000. Will changes in soil organic carbon act as a positive or negative feedback on global warming? Biogeochemistry 48, 21–51.
- Law, B.E., Kelliher, F.M., Baldocchi, D.D., Anthoni, P.M., Irvine, J., Moore, D., Van Tuyl, S., 2001. Spatial and temporal variation in respiration in a young ponderosa pine forest during a summer drought. Agricultural and Forest Meteorology 110, 27–43.
- Lee, M.S., Mo, W.H., Koizumi, H., 2006. Soil respiration of forest ecosystems in Japan and global implications. Ecological Research 21, 828–839.
- Li, C.S., Frolking, S., Frolking, T.A., 1992. A model of nitrous oxide evolution from soil driven by rainfall events: I. Model structure and sensitivity. Journal of Geophysical Research 97, 9759–9776.
- Li, C., 2000. Modeling trace gas emissions from agricultural ecosystems. Nutrient Cycling in Agroecosystems 58, 259–276.

- Li, C., 2001. Biogeochemical concepts and methodologies: Development of the DNDC model (in Chinese with English abstract). Quaternary Sciences 21, 89–99.
- Li, C., Mosier, A., Wassmann, R., Cai, Z., Zheng, X., Huang, Y., Tsuruta, J., Boonjawat, J., Lantin, R., 2004. Modeling greenhouse gas emissions from rice-based production systems: Sensitivity and upscaling. Global Biogeochemical Cycles 18(1).
- Minami, K., 1994. Methane from rice production. Fertilizer Research 37, 167–180.
- Neue, H.U., Roger, P. A., 2000. Rice agriculture: Factors controlling emissions. In: Khalil M.A.K. (ed.), Atmospheric Methane. Its Role in the Global Environment. Springer, Berlin, pp. 134–169.
- Øvreas, L., 2000. Population and community level approaches for analyzing microbial diversity in natural environments. Ecology Letters 3, 236–251.
- Papen, H., Butterbach-Bahl, K. 1999. A 3-year continuous record of nitrogen trace gas fluxes from untreated and limed soil of a N-saturated spruce and beech forest ecosystem in Germany. 1. N_2O emissions. Journal of Geophysical Research 104(D15), 18487–18503.
- Papen, H., Daum, M., Steinkamp, R., Butterbach-Bahl, K., 2001. N_2O and CH_4-fluxes from soils of a N-limited and N-fertilized spruce forest ecosystem of the temperate zone. Journal of Applied Botany 75, 159–163.
- Parker L.W., Miller, J., Steinberger, Y., Whitford, W.G., 1983 Soil respiration in a Chihuahuan desert rangeland. Soil Biology and Biochemistry 15, 303–309.
- Raich, J.W., Bowden, R.D., Steudler, P.A.,1990. Comparison of two static chamber techniques for determining carbon dioxide effux from forest soil. Soil Science Society of America Journal 54, 1754-1757.
- Raich, J.W., Schlesinger, W.H., 1992. The global carbon dioxide flux in soil respiration and its relationship to vegetation and climate. Tellus 44B, 81–99.
- Raich, J.W., Potter, C.S., 1995. Global patterns of carbon dioxide emissions from soils. Global biogeochemical cycles 9(1), 23–36.
- Rodeghiero, M., Cescatti, A., 2006. Indirect partitioning of soil respiration in a series of evergreen forest ecosystems. Plant and Soil 284, 7–22.
- Russell, C.A., Voroney R.P., 1998. Carbon dioxide efflux from the floor of a boreal aspen forest. I. Relationship to environmental variables and estimates of C respired. Canadian Journal of Soil Science 78, 301-310.
- Ryan, M. G., Hubbard, R. M., Pongracic, S., Raison, R. J., and McMurtrie, R. E., 1996. Foliage,
- Sahrawat, K.L., Keeney, D.R., 1986. Nitrous oxide emission from soils. Advances in Soil Science 4, 103–148.
- Schiller, C.L., Hastie, D.R., 1996. Nitrous oxide and methane fluxes from perturbed and unperturbed boreal forest sites in northern Ontario. Journal of Geophysical Research 101, 22767–22774.
- Schlese, G.H., 1982. The response of CO_2 evolution from soils to global temperature changes. Zeitsschrift für Naturforschung 37, 287–291.
- Schlesinger, W.H., Andrews, J.A., 2000. Soil respiration and the global carbon cycle. Biogeochemistry 48, 7–20.
- Shibistova, O., Lloyd, J., Evgrafova, S., Savushkina, N., Zrazhevskaya, G., Arneth, A., Knohl, A., Kolle, O., Schulze, E.D., 2002. Seasonal and spatial variability in soil CO_2 efflux rates for a central Siberian Pinus sylvestris forest. Tellus 54B, 552–567.

- Simojoki, A., Jaakkola, A., 2000. Effect of nitrogen fertilization, cropping and irrigation on soil air composition and nitrous oxide emission in a loamy clay. European Journal of Soil Science 51, 413–424.
- Skiba, U., Fowler, D., Smith, K.A., 1994. Emissions of NO and N_2O from soils, Environmental Monitoring and Assessment 31, 153–158.
- Smith, C.J., Brandon, M., Patrick Jr., W.H., 1982. Nitrous oxide emission following urea-N fertilization of wetland rice. Soil Science and Plant Nutrition 28(2), 161–171.
- Steinkamp, R., Butterbach-Bahl, K., Papen, H., 2001. Methane oxidation by soils of an N limited and N fertilized spruce forest in the Black Forest, Germany. Soil Biology & Biochemistry 33, 145–153.
- Stoyan, H., De-Polli, H., Bhom, S., Robertson, G.P., Paul, E.A., 2000. Spatial heterogeneity of soil respiration and related properties at the plant scale. Plant and Soil 222, 203–214.
- Taylor, B.R., Parkinson D., Parsons, W.F.J., 1989. Nitrogen and lignin content as predictors of litter decay rates. A microcosm test. Ecology 70, 97–104.
- Thierron, V., Laudelout, H., 1996. Contribution of root respiration to total CO_2 efflux from the soil of a deciduous forest. Canadian Journal of Forest Research 26, 1142–1148.
- Toland, D.E., Zak, D.R., 1994. Seasonal patterns of soil respiration in intact and clear-cut northern hardwood forests. Canadian Journal of Forest Research 24, 1711-1716.
- Trumbore S.E., Chadwick, O.A., Amundson, R., 1996. Rapid exchange between soil carbon and atmospheric carbon dioxide driven by temperature change. Science 272, 393–396.
- Valentini, R., Matteucci, G., Dolman, A.J., Schulze, E.D., Rebmann, C., Moors, E.J., Granier, A., Gross, P., Jensen, N.O., Pilegaard, K., Lindroth, A., Grelle, A., Bernhofer, C., Grünwald, T., Aubinet, M., Ceulemans, R., Kowalski, A.S., Vesala, T., Rannik, U., Berbigier, P., Loustau, D., Guomundsson, J., Thorgeirsson, H., Ibrom, A., Morgenstern, K., Clement, R., Moncrieff, J., Montagnani, L., Minerbi, S., Jarvis, P.G., 2000. Respiration as the main determinant of carbon balance in European forests. Nature 404, 861–865.
- Vose, J.M., Elliott, K.J., Johnson, D.W., Walker, R.F., Johnson, M.G., Tingey, D.T., 1995. Effects of elevated CO_2 and N fertilization on soil respiration from ponderosa pine (Pinus ponderosa) in open-top chambers. Canadian Journal of Forest Research 25, 1243-1251.
- Wassmann, R., Lantin, R.S., Neue, H.U. (eds.), 2000b. Methane Emissions from Major Rice Ecosystems in Asia, Vol. 91. Kluwer, Dordrecht, the Netherlands.
- Yan, X.Y., Yagi, K., Akiyama, H., Akimoto, H., 2005. Statistical analysis of the major variables controlling methane emission from rice fields. Global Change Biology 11, 1131–1141.

CHAPTER 1

SPATIAL VARIABILITY STUDY OF SOIL CHEMICAL AND PHYSICAL PROPERTIES FOR THE IDENTIFICATION OF GAS MONITORING POINTS

1.1 INTRODUCTION

Soil is spatially heterogeneous, with most chemical and physical properties varying significantly as a consequence of the influence of geological and pedological processes. Soil forming factors, such as parent materials, biota, climate, and topography, explain most of general characteristic variability; however, not only natural but also anthropic factors may significantly affect soil variability.

Spatial heterogeneity is a substantial problem in monitoring and modeling nutrient transformations and gas emissions in terrestrial ecosystems. Soil CO_2, CH_4 and N_2O fluxes are highly variable in space and time, affected by soil environmental factors like temperature, moisture, pH, redox potential, substrate concentration gradients (Raich and Schlesinger, 1992; Coûteau et al., 1995; Aulakh et al., 2001), by biochemical reactions (Li, 2000, 2001; Li et al., 2004), and so as by climate and vegetation (Sahrawat and Keeney, 1986; Hanson et al. 1993; Toland and Zak 1994; Simojoki and Jaakkola, 2000).

At soil ecosystem level, the investigation of spatial variability of soil gas emissions at a detailed scale is difficult to carry out; to get a representative value of gas efflux within the ecosystem, a large number of "chambers" would be necessary. Consequently, monitoring of soil gas spatial variability would required elevated costs for technical equipment and for their checking and maintenance as well.

Thus, the existence and the knowledge of spatial pattern for the major soil properties affecting emissions of greenhouse gas from soils, can be used to predict the spatial pattern for efflux rates of such gases; information about the spatial distribution of soil properties as well as vegetation types can be useful for understanding ecosystems dynamics, assessing the contribution of gaseous emissions and identifying the appropriate sampling design.

Classic statistical methods have generally been used in the past to study soil variability in the field, assuming that all variability is random. On the contrary, soil characteristics generally show spatial dependence (Webster and Oliver, 2001), which means that samples close to each other are more similar than samples farther from each other.

Actually, spatial variability of soil properties is mostly studied by using geostatistical methods, which take into account spatial autocorrelation of a variable in predicting its value in an unsampled location. Geostatistics can therefore be used to detect model and estimate spatial pattern; it is then possible to interpolate any soil property and to map the estimated values.
Geostatistics was developed originally for mining and geology, but has also been used in the plant and soil sciences (Castrignanò et al., 1992; Bourgault et al., 1997; Castrignanò et al., 2000 a; Castrignanò et al., 2000 b).
The objective of this work was to study the spatial variability of some physical and chemical properties in a forest and in an agricultural ecosystem; the soil spatial variability was investigated using univariate and multivariate geostatistical techniques with the aim to identify the most suitable positions for gas emission monitoring.

1.2 PEDOLOGICAL STUDY

Within Nitroeurope and Carboeurope projects, two experimental site were chosen for monitoring of soil greenhouse gas emissions (CO_2, CH_4 and N_2O). The forest site is set on the morainic hills (Ispra, Lombardy), while the cropland site is located in the Po plain (Castellaro de' Giorgi, Lombardy) and is characterized by the presence of rice crop, in rotation with maize (fig. 1.1).

Fig. 1.1 Location of the experimental sites; red square represents the EMEP forest site of Ispra and black square represents the Castellaro cropland site.

1.2.1 THE FOREST SITE

The site is located in the Joint Research Center of Ispra (JRC-Directorate General of the European Commission), close to Varese; Ispra is on the eastern side of Maggiore lake, in the morainic hill area, between Po valley and Prealps. Its geographic position contributes to its characteristic climate: the thermal excursions are lower than those of the Po valley due to both the protective effect of mountains from cold north wind and to the mitigating action of the lake.

The annual mean temperature is 12.0 °C, with a minimum of 2.3 °C during January and a maximum of 22.1 °C during July (1973-2002 data – Brebbia and JRC station). Rainfall are abundant, higher than those of the plain, but lower than those of the Prealps. The annual average rainfall is 1580 mm, with two peaks in spring (May: 199 mm) and autumn (October: 200 mm).

The experimental site (4 hectares) is a mixed forest area that before 1960 was a stable grassland with conditions of high water content; probably before forest conversion, surface drainage was carried out, by a ditching system still visible in the area. This anthropic intervention led in some cases to bury surface horizons with new transported material.

The area is crossed along the E-W axis by an artificial concrete pipe, built about 1960, placed partially above ground but covered with soil and vegetation.

The forest is mainly composed by *Quercus robur*, *Robinia pseudoacacia*, *Alnus glutinosa* and *Pinus rigida* (fig. 1.2); *Quercus robur* is dominant, while *Alnus glutinosa* prevails in the south-east side were the groundwater level is higher; *Robinia pseudoacacia* (false acacia) mostly extends along the artificial pipe and *Pinus rigida*, artificially planted, is mainly present in the northern and north-eastern edge of the study site. The forest is also characterized by other minor tree species, such as *Corylus avellana* (hazel) and *Prunus serotina* (black cherry).

In order to study soil types, four pedological profiles were opened, described and sampled. Soil samples were taken from each horizon and analyzed: organic C and total nitrogen (Thermo Fisher Scientific CN elemental analyzer), pH_{H2O}, pH_{KCl}, soil texture (sieving and sedimentation), cation exchange capacity and exchangeable ions (Ca^{2+}, Mg^{2+}, K^{+}, Na^{+}) (NRCS, 2004) and base saturation were determined. According to the taxonomic system World Reference Base for Soil Resources (IUSS/ISRIC/FAO, 2006), all the soils are Umbrisols; they are weakly-developed soils, without thick diagnostic horizons, have a low base saturation and, in the lower part of the profile, gleyic properties (fig.1.3). The profiles P3 and P4, located in the wetter area characterized by the presence of alder, are different from the remaining two (P1 and P2), for the organic carbon content (over 1% up to depth of 50 cm from the surface soil) and for high water level (gleyic properties) by distinctive blue-grey color (fig. 1.3 c and d).

Nearby the concrete pipe, soils are thin and have been classified as Haplic Regosol (Dystric, Arenic, Transportic).

Figure 1.2 Map of vegetation types at Ispra forest experimental site. Areas represent forest with dominance of: P - *Pinus rigida*; Q - *Quercus robur*; A - *Alnus glutinosa*; R-Ps - *Robinia pseudoacacia* and *Prunus serotina*.
(image from Google Earth)

Following the characteristics of sampled soils (P1-P4) are described.

P1: Hypoendogleyic Umbrisol (Hyperdystric, Arenic)

Date	31/10/2007
Site	EMEP forest site-Ispra
Land cover/Vegetation	Forest / Oak, pine, false acacia
Groundwater depth	Not reached

Organic layers thicknesses:
OL 3 cm
OF 1 cm

A1	0- 7 cm	Moist; matrix colour 10YR 2/1; no rock fragments; many, very fine-coarse roots; granular structure; abrupt, wavy horizon lower boundary.
A2	7 – 24 cm	Moist; matrix colour 10YR 2/2; no rock fragments; common, very fine-coarse roots; subangular blocky structure; gradual, wavy horizon lower boundary.
AC	24 – 38 cm	Moist; matrix colour 10 YR 3/2; no rock fragments; few, very fine-medium roots; subangular blocky structure; clear, wavy horizon lower boundary.
C	38 – 70 cm	Moist; matrix colour 5Y 6,5/2; no rock fragments; few, very fine-medium roots; structureless; abrupt, wavy horizon lower boundary.
Cg1	70 – 168 cm	Very moist; matrix colour 5Y 7/1; redox concentration colour 10 YR 5/ 8; few, very fine-fine roots; structureless; clear, linear horizon lower boundary.
Cg2	168 – 200 cm	Wet; matrix colour 5Y 5,5/3; redox concentration colour 2,5 Y 5/6

diagnostic horizon: umbric 0 - 38 cm
diagnostic properties:
gleyic proprties 70 - 200 cm
redox conditions 70 - 200 cm

Horizon	cm	Texture g kg^{-1}							Textural class USDA
		Coarse sand 2-0.1 mm	Fine sand 0.1-0.05 mm	Total sand 2-0.05 mm	Coarse silt 50-20 µm	Fine silt 20-2 µm	Total silt 50-2 µm	Clay <2 µm	
A1	0-7	432	148	580	80	165	245	175	SL
A2	7-24	471	209	680	85	145	230	90	SL
AC	24-38	658	172	830	25	75	100	70	LS
C	38-70	905	76	981	4	5	9	10	S
Cg1	70-168	907	73	980	10	5	15	5	S
Cg2	168-200	738	177	915	45	30	75	10	S

Horizon	pH H_2O	pH KCl	OC g Kg^{-1}	Exchange complex (cmol(+) kg^{-1})					BS %
				CEC	Ca	Mg	Na	K	
A1	3.8	2.8	94.1	48.4	8.64	1.31	0.21	0.17	21.4
A2	4.5	3.6	62.6	21.9	0.76	0.33	0.26	0.04	6.3
AC	4.7	3.9	27.5	12.6	0.97	0.32	0.27	0.03	12.6
C	4.8	4.1	1.9	3.7	1.12	0.4	0.37	0.03	51.5
Cg1	4.1	3.5	0.6	2.7	1.01	0.55	0.25	0.02	66.8
Cg2	4.7	4.2	0.5	3.9	0.96	0.52	0.29	0.07	46.2

P2: Hypoendogleyic Umbrisol (Hyperdystric, Arenic)

Date	31/10/2007
Site	EMEP forest site-Ispra
Land cover/Vegetation	Forest / Oak, pine, false acacia
Groundwater depth	Not reached

Organic layers thicknesses:
OL 2 cm; OF 2 cm

A1	0 – 9 cm	Moist; matrix colour 10YR 2/1; no rock fragments; many, very fine-very coarse roots; granular structure; clear, wavy horizon boundary.
A2	9 – 31 cm	Moist; matrix colour 10YR 3/2; no rock fragments; common, very fine-very coarse roots; subangular blocky structure; gradual, wavy horizon boundary.
C1	31 – 50 cm	Moist; matrix colour 2,5Y 6/2; no rock fragments; few, very fine-coarse roots; structureless; abrupt, wavy horizon boundary; small iron-manganese concretions.

C2	50 – 88 cm	Moist; matrix colour 2,5Y 6/2; no rock fragments; few, very fine-fine roots; structureless; gradual, linear horizon boundary; small iron-manganese concretions.
Cg1	88 – 146 cm	moist; matrix colour 2,5Y 6/2; few, very fine roots; structureless; gradual, linear horizon boundary.
Cg2	146 – 180 cm	Very moist; matrix colour 5Y 5,5/2; few, very fine roots; structureless; diffuse horizon boundary.

diagnostic horizon: umbric 0 - 31 cm
diagnostic properties:
gleyic proprties 88 - 180 cm
redox conditions 88 - 180 cm

Horizon	cm	Texture g kg^{-1}							Textural class USDA
		Coarse sand 2-0.1 mm	Fine sand 0.1-0.05 mm	Total sand 2-0.05 mm	Coarse silt 50-20 µm	Fine silt 20-2 µm	Total silt 50-2 µm	Clay <2 µm	
A1	0-9	342	223	565	95	170	265	170	SL
A2	9-31	341	294	635	115	130	245	120	SL
C1	31-50	844	91	935	50	10	60	5	S
C2	50-88	861	124	985	5	5	10	5	S
Cg1	88-146	538	207	745	175	50	225	30	LS
Cg2	146-180	576	174	750	50	160	210	40	LS

Horizon	pH H_2O	pH KCl	OC g Kg^{-1}	Exchange complex (cmol(+) kg^{-1})					BS %
				CEC	Ca	Mg	Na	K	
A1	3.4	2.7	90.5	50.2	5.2	1.26	0.22	0.2	13.7
A2	4	3.4	20.9	17.4	1.37	0.42	0.26	0.13	12.5
C	4.4	3.6	1.2	5.8	1.25	0.62	0.42	0.11	41.3
C2	4.5	2.9	0.0	4.5	1.14	0.45	0.36	0.22	48.2
Cg1	4.4	2.8	0.1	2.8	1.02	0.5	0.32	0.04	66.9
Cg2	4.8	3.2	0.7	2.0	1.29	0.42	0.18	0.03	94.1

P3: Endogleyic Umbrisol (Humic, Hyperdystric, Siltic, Transportic)

Date	31/10/2007
Site	EMEP forest site-Ispra
Land cover/Vegetation	Forest / Oak, alder
Groundwater depth	190 cm

Organic layers thicknesses:
OL 2 cm; OF 2 cm

A1	0 – 15 cm	Moist; matrix colour 10YR 2/1; many, very fine-very coarse roots; granular structure; clear, wavy horizon boundary.
A2	15 –38 cm	Moist; matrix colour 10YR 3/2; common, very fine-coarse roots; subangular blocky structure; gradual, wavy horizon boundary.
Ab	38 – 50 cm	Moist; matrix colour 10YR 3/1; common, small-very small rock fragments; few, fine roots; subangular blocky structure; clear, irregular horizon boundary
C	50 – 88 cm	Very moist; matrix colour 5Y5,5/2 ; common, small rock fragments; few, medium-coarse roots; structureless; abrupt, linear horizon boundary.
Cg1	88 –160 cm	Very moist; matrix colour 5Y 5/2; redox concentration colour 2,5Y 5/6; few, medium-coarse roots; structureless; gradual, linear horizon boundary.
Cg2	160 – 190 cm	Wet; matrix colour 10Y 5/1; structureless.

diagnostic horizon: umbric 0 - 50 cm
diagnostic properties:
gleyic proprties 88 - 190 cm
redox conditions 88 - 190 cm

Horizon	cm	Texture g kg^{-1}							Textural class USDA
		Coarse sand 2-0.1 mm	Fine s and 0.1-0.05 mm	Total sand 2-0.05 mm	Coarse silt 50-20 µm	Fine silt 20-2 µm	Total silt 50-2 µm	Clay <2 µm	
A1	0-15	559	136	695	105	160	265	40	SL
A2	15-38	650	115	765	80	105	185	50	LS
Ab	38-50	280	175	455	195	275	470	75	L
C	50-88	137	93	230	150	520	670	100	SiL
Cg1	88-160	896	59	955	5	30	35	10	S
Cg2	160-190	917	68	985	35	25	60	5	S

Horizon	pH H2O	pH KCl	OC g Kg^{-1}	Exchange complex (cmol(+) kg^{-1})					BS %
				CEC	Ca	Mg	Na	K	
A1	3.7	2.9	82.7	41.5	6.18	1.15	0.26	0.38	19.2
A2	4.0	3.8	27.3	20.8	1.29	0.55	0.26	0.06	10.4
Ab	4.3	4.0	15.8	11.8	1.23	0.41	0.79	0.06	21
C	4.7	4.0	0.7	1.8	0.54	0.3	0.2	0.04	60
Cg1	4.8	4.1	1.1	2.8	3.52	0.94	0.29	0.14	100
Cg2	5.0	4.9	1.3	2.7	3.64	1.23	0.4	0.15	100

P4: Endogleyic Mollic Umbrisol (Arenic, Transportic)

Date	31/10/2007
Site	EMEP forest site-Ispra
Land cover/Vegetation	Forest / Oak, alder
Groundwater depth	170 cm

Organic layers thicknesses:
OL 2 cm

A1	0 – 17 cm	Moist; matrix colour 10YR 2/1; no rock fragments; many, very fine-very coarse roots; granular structure; clear, wavy horizon boundary.
A2	17 – 48 cm	Moist; matrix colour 10YR 3/2; very few, very small-small rock fragments; few, very fine-fine roots; subangular blocky structure; gradual, wavy horizon boundary.
Ab	48 – 65 cm	Moist; matrix colour 10YR 3/1; many, small-medium rock fragments; few, very fine-fine roots; subangular blocky structure; clear, irregular horizon boundary.

Cg1	65 – 110 cm	Very moist; matrix colour 5Y 5/2; redox concentration colour 2,5Y 5/6; many, small-coarse rock fragments; few, very fine-fine roots; structureless; gradual, linear horizon boundary.
Cg2	110 – 180 cm	Wet; matrix colour 10Y 5/1; redox concentration colour 2,5Y 5/6; very few, small rock fragments; structureless.

diagnostic horizon: mollic 0 - 65 cm
diagnostic properties:
gleyic proprties 65 - 180 cm
redox conditions 65 - 180 cm

Horizon	cm	Texture g kg^{-1}							Textural class USDA
		Coarse sand 2-0.1 mm	Fine sand 0.1-0.05 mm	Total sand 2-0.05 mm	Coarse silt 50-20 µm	Fine silt 20-2 µm	Total silt 50-2 µm	Clay <2 µm	
A1	0-17	622	118	740	95	135	230	30	LS
A2	17-78	537	183	720	65	180	245	35	SL
Ab	48-65	589	166	755	80	125	205	40	LS
Cg1	65-110	486	174	660	95	190	285	55	SL
Cg2	110-180	589	186	775	45	140	185	40	LS

Horizon	pH H2O	pH KCl	OC g Kg^{-1}	Exchange complex (cmol(+) kg^{-1})					BS %
				CEC	Ca	Mg	Na	K	
A1	5.1	4.2	40.6	16.3	7.09	1.32	0.35	0.09	54.3
A2	5.1	4.3	29.5	15.9	8.56	1.2	0.32	0.02	63.4
Ab	5.4	4.6	29.1	18.2	6.23	1.17	0.35	0.16	43.5
Cg1	5.7	4.7	1.4	2.6	2.82	1.27	0.33	0.16	100
Cg2	5.9	4.1	1.1	2.7	4.56	1.34	0.34	0.09	100

a)

b)

c)

d)

Figure 1.3. Soil profiles. P1: Hypoendogleyic Umbrisol (Hyperdystric, Arenic**)**; P2: Hypoendogleyic Umbrisol (Hyperdystric, Arenic) (b); P3: Endogleyic Umbrisol (Humic, Hyperdystric, Siltic, Transportic); P4: Endogleyic Mollic Umbrisol (Arenic, Transportic) (d).

1.2.2 THE CROPLAND SITE

The site is located in the Po valley, in the southern part of Lombardy, near Castellaro de' Giorgi (PV). The climate is characterized by the long term meteorological station at Pavia as temperate continental with average rainfall of 782 mm and temperature of 12.6 °C. About rainfall, the maximum and the minimum are registered in November and February, respectively; air temperatures ranges between 0.6 °C in January and 23.4 °C in July. The general soil moisture regime is Udic and the soil temperature regime is Mesic.

Agriculture is the main land use and rice cultivation is here particularly widespread; the study site (about 3 hectares) is in fact characterized by the presence of rice crops, in rotation with maize (3-4 years rice, 1-2 years maize).

An old woody meander surrounds the experimental field, which in the past was a marshy area, reclaimed shortly after the year one thousand and then used for agricultural purposes. The cultivation tillage and agricultural practices for rice lead to reduce soil permeability and cause poorly drainage resulting in surface water excesses also during no rice cultivation time.

In order to characterize soil properties, two pedological profiles were opened and described.

The organic C and total nitrogen content (Thermo Fisher CN elemental analyzer), pH_{H2O}, pH_{KCl}, soil texture (sieving and sedimentation), cation exchange capacity, exchangeable ions (Ca^{2+}, Mg^{2+}, K^{+}, Na^{+}) (NRCS, 2004) and base saturation were determined.

According to the taxonomic system World Reference Base for Soil Resources (IUSS/ISRIC/FAO, 2006), the soils are Gleysols; they are wetland soils that, unless drained, are saturated with groundwater for long periods that allows reducing conditions to occur and to develop a gleyic color pattern (fig. 4).

Following the characteristics of sampled soils are showed.

P1: Haplic Gleysol (Calcaric, Endoarenic)

Date	26/5/06
Site	Torre Beretti e Castellaro
elevation	89 m a.s.l.
crop cover	maize and rice rotation (2006 maize)
parent material	fluvial deposits
groundwater depth	25 cm
drainage	poorly drained

Apg	0 - 25 cm	moist; matrix colour 2,5Y 4/1,5; very few, rounded, gravelly rock fragments; cloddy structure; abrupt, wavy horizon lower boundary; presence of rice stubble.

Cg1	25 - 43 cm	very moist; matrix colour N 4/; redox concentration colour 10YR 4/6; no rock fragments; massive; abrupt, wavy horizon lower boundary; presence of organic material.
Cg2	43 - 66 cm	wet; matrix colour 10 GY 4/1; no rock fragments; massive; abrupt, wavy horizon lower boundary.
Cg3	66 - 110 cm	wet; structereless; unknown horizon lower boundary.

diagnostic horizon: ochric 0 - 25 cm
diagnostic properties:
gleyic properties 0 - 110 cm
redox conditions 0 - 110 cm
calcaric materials 0 - 43; 66 - 110 cm

Horizon	pH H_2O	pH KCl	OC g Kg^{-1}	OM g Kg-1	total carbonate g Kg-1	Texture g kg-1			Textural class USDA
						Sand 2-0.05 mm	Silt 50-2 µm	Clay <2 µm	
Apg	6.7	6.6	16	27	74	300	393	307	SiL
Cg1	6.8	6.5	8	14	84	223	467	310	CL
Cg2	7.1	7	2	4	0	567	374	59	SL
Cg3	7	6.9	2	4	16	976	20	4	S

Horizon	Exchange complex (cmol(+) kg^{-1})					BS %
	CEC	Ca	Mg	Na	K	
Apg	21.04	19.92	2.76	0.44	0.37	100
Cg1	24.21	22.25	2.99	0.39	0.28	100
Cg2	3.55	4.48	0.8	0.63	0.37	100
Cg3	1.66	0.96	0.37	2.29	3.09	100

P2: Calcic Gleysol (Hypercalcaric, Humic)

Date	26/5/06
Site	Torre Beretti e Castellaro
elevation	89 m a.s.l.
crop cover	maize and rice rotation (2006 maize)
parent material	fluvial deposits
drainage	poorly drained

Ap	0 -28 cm	moist; matrix colour 10YR 3,5/1; common, coarse gravelly and cobbly, subrounded rock fragments; cloddy structure; abrupt horizon lower boundary; presence of rice stubble.
Apg	28 -40 cm	very moist; matrix colour 10YR 3/1; redox concentrations colour 10YR 3/6; very few, gravelly rock fragments; few, fine roots; gradual, wavy horizon lower boundary; presence of old rice stubble (about 2 years).
ACg	40 - 57 cm	moist; matrix colour 10YR 4/2; redox concentrations colour 2,5Y 3/6; very few, gravelly rock fragments; massive; few, very fine roots; gradual, wavy horizon lower boundary.
Cg1	57 - 70 cm	moist; matrix colour N4/; common, gravelly rock fragments; massive few, very fine roots; CaCO3 concentrations (2-20); gradual, wavy horizon lower boundary.
Cg2	70 - 95 cm	very moist; matrix colour N4,5/; massive; clear, wavy horizon lower boundary.
Cg3	95 - 120 cm	wet; N4/; structureless; abrupt, wavy horizon lower boundary.
Ab	120 - 130 cm	wet; structureless dark material that rises in the fifth and sixth horizons; unknown horizon lower boundary.

diagnostic horizon: ochric 0 - 28 cm
diagnostic properties:
gleyic proprties 28 - 120 cm
redox conditions 28 - 120 cm

calcaric materials: 0 - 130 cm

Horizon	pH H_2O	pH KCl	OC g Kg^{-1}	OM g Kg-1	total carbonate g Kg-1	Texture g kg-1			Textural class USDA
						Sand 2-0.05 mm	Silt 50-2 µm	Clay <2 µm	
Ap	7	6.5	15	25	32	440	307	253	SiL
Apg	7	6.5	19	32	20	315	414	271	L
ACg	7.2	6.7	16	28	128	398	323	279	L
Cg1	7.1	6.8	8	14	891	463	339	198	L
Cg2	7.2	7	2	4	395	605	298	97	SL
Cg3	7.1	7	2	3	477	881	96	23	SiL

horizon	Horizon	Exchange complex (cmol(+) kg^{-1})				BS %
		Ca	Mg	Na	K	
Ap	18.88	19.47	0.97	0.51	0.52	100
Apg	20.44	14.39	2.53	0.23	0.28	85.3
ACg	21.47	17.43	2.35	0.28	0.26	94.6
Cg1	12.07	3.88	0.64	0.17	0.22	40.7
Cg2	1.06	11.01	1.82	0.44	0.34	100

a)

b)

Figure 1.4. Soil profiles. P1: Haplic Gleysol (Calcaric, Endoarenic) (a); P2: Calcic Gleysol (Hypercalcaric, Humic) (b).

1.3 STUDY OF SPATIAL VARIABILITY

On the basis of the profile descriptions, physical and chemical soil variability was analyzed in both sites according to regular grids.
Geostatistical analysis was applied to estimate the spatial distribution of soil properties; the semivariogram was estimated by the equation (Journel and Huijbregts, 1978) :

$$g(\mathrm{h}) = \frac{1}{2N(\mathrm{h})} \sum_{i=1}^{N(\mathrm{h})} [z(\mathrm{x}_i) - z(\mathrm{x}_i + h)]^2 \qquad i = 1,\ldots,N(\mathrm{h})$$

where n(h) is the number of lag pairs at distance interval h, and z is the value of the parameter at location x and x+h.
Semivariograms for all variables were fitted to a spherical, exponential, gaussian or nugget model and mapping was performed using the kriging method. When necessary data were normalized.
On the basis of cross validation and statistics on the kriging prediction errors (mean error, root-mean-square error, average standard error and root-mean square standardized error) the quality of the modeled surfaces was assessed.
In the forest site, spatial distribution of N, C, pH_{H2O} and pH_{KCl} of the surface horizons (A1) was investigated; additionally, since the thicknesses of such horizons were variable, ranging between 5 and 21 cm (average thickness 9 cm), we compared the obtained maps with those relative to 0-15 cm layer (obtained by adding the contributions of the first two horizons, weighted to their thicknesses).
Then, aiming at localizing measurement points for gaseous emissions, a multivariate geostatistical approach was applied; the Factorial Kriging Analysis (FKA), combines classical factor analysis, for describing the correlation structure of multivariate data sets, with geostatistics, to take into account the regionalized nature of the variables.
Factorial Kriging Analysis is a relatively recent geostatistical method developed by Matheron (1982) and well suited for analysing multivariate spatial data set. The approach consists in decomposing the set of original second-order random stationary variables into a set of reciprocally orthogonal regionalized factors, through transformation coefficients, combining the spatial with the multivariate decomposition (Goovaerts and Webster, 1994; Castrignanò et al., 2000 a). The first step consisted in modelling the coregionalization of the set of variables, using the Linear Model of Coregionalization (LMC); then, the correlation structure between the variables was analyzed by applying Principal Component Analysis (PCA); finally, specific factors were mapped using cokriging (Wackernagel, 1988).
With regard to cropland site, on the basis of spatial distribution obtained for each soil variable and considering correlation matrix results, a smaller number of soil parameters were used for the analysis: organic carbon, pH_{H2O} and sand content (relative to Ap horizon).

It was possible to illustrate the behavior and relationships among variables by mapping the first regionalized factor.
All the geostatistical analysis were performed using Arcgis (ESRI, 2006) and Isatis (Geovariances, 2003) software.

1.3.1 THE FOREST SITE

In order to analyze soil variability, a total of 79 soil observations (fig. 1.5) were opened, up to C horizon, described and sampled (usually A1-A2-C, sometimes A1-AC-C horizons); of the overall 79 points, 63 observations were placed according a regular grid (25 x 25 m) and 16 additional soil minipits were done in four locations, at a distance of about 3-6 m from each sampling point.

Figure 1.5 EMEP forest site (Ispra, Va): soil sampling points. Red dots represent individual soil observations for the spatial variability survey; yellow dots represent pedological profiles. The broken line represents the concrete pipe.
(image from Google Earth)

The soil samples were air-dried and sieved (2 mm mesh). Soil pH was determined potentiometrically in a soil-to-solution (water and KCl 1N) ratio of 1:2,5. Organic carbon and total nitrogen were measured using Thermo Fisher Scientific CN elemental analyzer. In ta-

ble 1.1 mean, standard error, standard deviation, minimum and maximum values of investigated soil parameters are showed.

Table 1.1 Main statistics (mean, standard error, standard deviation, minimum and maximum values) of soil parameters at forest site (OC: organic carbon; N: total nitrogen; pHw: pH_{H2O} in water; pH_{KCl}: pH in KCl).

	Horizon	n.	Mean	St.Err.	St.Dev.	Min	Max
OC (%)	A1	79	11.4	0.5	4.1	4.1	23.7
	A2 or AC	79	4.9	0.3	2.3	0.8	14.3
	C or CA	29	1.0	0.1	0.6	0.1	2.9
N (%)	A1	79	0.8	0.04	0.3	0.4	2.1
	A2 or AC	79	0.3	0.01	0.1	0.1	0.7
	C or CA	29	0.1	0.02	0.1	0.01	0.2
pH_{H2O}	A1	79	4.1	0.07	0.6	3.5	6.6
	A2 or AC	79	4.6	0.06	0.6	3.6	7.0
	C or CA	29	5.0	0.04	0.5	4.4	6.6
pH_{KCl}	A1	79	3.6	0.07	0.5	3.0	6.2
	A2 or AC	79	4.1	0.05	0.4	3.1	6.3
	C or CA	29	4.4	0.10	0.2	4.0	4.9

The average organic carbon content in the surface horizon (A1) was very high, 11.4±4.1% (mean±SD) with a coefficient of variation (CV) of 36%. The second horizon (A2) showed an average organic carbon content of 4.9±2.3% and an higher CV (46%). With the increasing of depth the organic carbon decreased to 1±0.6% (C or CA horizons). Additionally, the organic carbon content, relative to the whole thickness of soil (down the profile to C horizon, at about 50 cm) was calculated for all the grid points; the carbon values (expressed in kg m^{-2}) ranged between 3 (nearby the concrete pipe) and 43.4 kg m^{-2} with an average value of 22.1±10.2 kg m^{-2}.

The total nitrogen was between 0.4 and 2.1% and between 0.1 and 0.7% in the A1 and A2 horizons, respectively.

The surface pH_{H2O} showed an high variation, from very acid (3.5) to sub-acid values (6.6); the average value was 4.1±0.6 and increased to 4.6±0.6 with depth, up to C horizon.

The pH_{KCl} was 3.6, 4.1 and 4.4 in the A1, A2 and C horizons respectively.

The correlation matrix (table 1.2) exhibits significant relations (p value <0.05) between all the considered parameters. In particular, organic carbon and total nitrogen were directly correlated; on the contrary, they were inversely correlated with pH values.

All the investigated soil properties showed spatial autocorrelation down the profile to 15 cm. The goodness of fitting was tested by cross-validation, calculating mean error and root-mean square, which were close to 0 and 1, respectively. The nugget effect obtained by fitting the semivariogram of carbon content, relative to the upper 50 cm, revealed absence of spatial correlation. The kriging maps of organic carbon, total nitrogen, pH_{H2O},

and pH_{KCl} are reported in fig. 1.6, while in table 1.3 the fitted semivariogram parameters are showed.

Table1.2 Correlation matrix between investigated soil parameters in the A1 and A2 horizons (OC: organic carbon; N: total nitrogen; pH_{H2O}: pH in water; pH_{KCl}: pH in KCl); bold indicates significant correlation (p value < 0.05)

A1 horizon

	OC	N	pH_{H2O}	pH_{KCl}
OC	1.00	**0.79**	**-0.36**	**-0.38**
N	**0.79**	1.00	**-0.33**	**-0.35**
pH_{H2O}	**-0.36**	**-0.33**	1.00	**0.95**
pH_{KCl}	**-0.38**	**-0.35**	**0.95**	**1.00**

A2 horizon

	OC	N	pH_{H2O}	pH_{KCl}
OC	1.00	**0.9**	**0.69**	**0.71**
N	**0.9**	1.00	**0.74**	**0.74**
pH_{H2O}	**0.69**	**0.74**	1.00	**0.98**
pH_{KCl}	**0.71**	**0.74**	**0.98**	1.00

Table 1.3 Fitted semivariogram parameters for the forest site.
OC: organic carbon; N: total nitrogen; pHw: pH in water, pH in KCl
*normalized variable

Parameter	Model	Nugget variance	Sill variance	Range (m)	structured variance (%)
A1 horizon					
OC	exponential	8	21	188	62
N	exponential*	0.01	0.022	78	54
pH_{H2O}	spherical*	0.01	0.015	92	33
pH_{KCl}	spherical*	0.01	0.016	93	37
0-15 cm					
OC	Exponential	5	13	178	61
N	exponential*	0.08	0.12	37	33
pH_{H2O}	spherical*	0.002	0.003	83	33
pH_{KCl}	spherical*	0.002	0.0032	89	37
A1 horizon - with the exclusion of points near pipe					
OC	Exponential	9	18	197	50
N	exponential*	0.01	0.021	178	52
pH_{H2O}	spherical*	0.0009	0.002	178	55

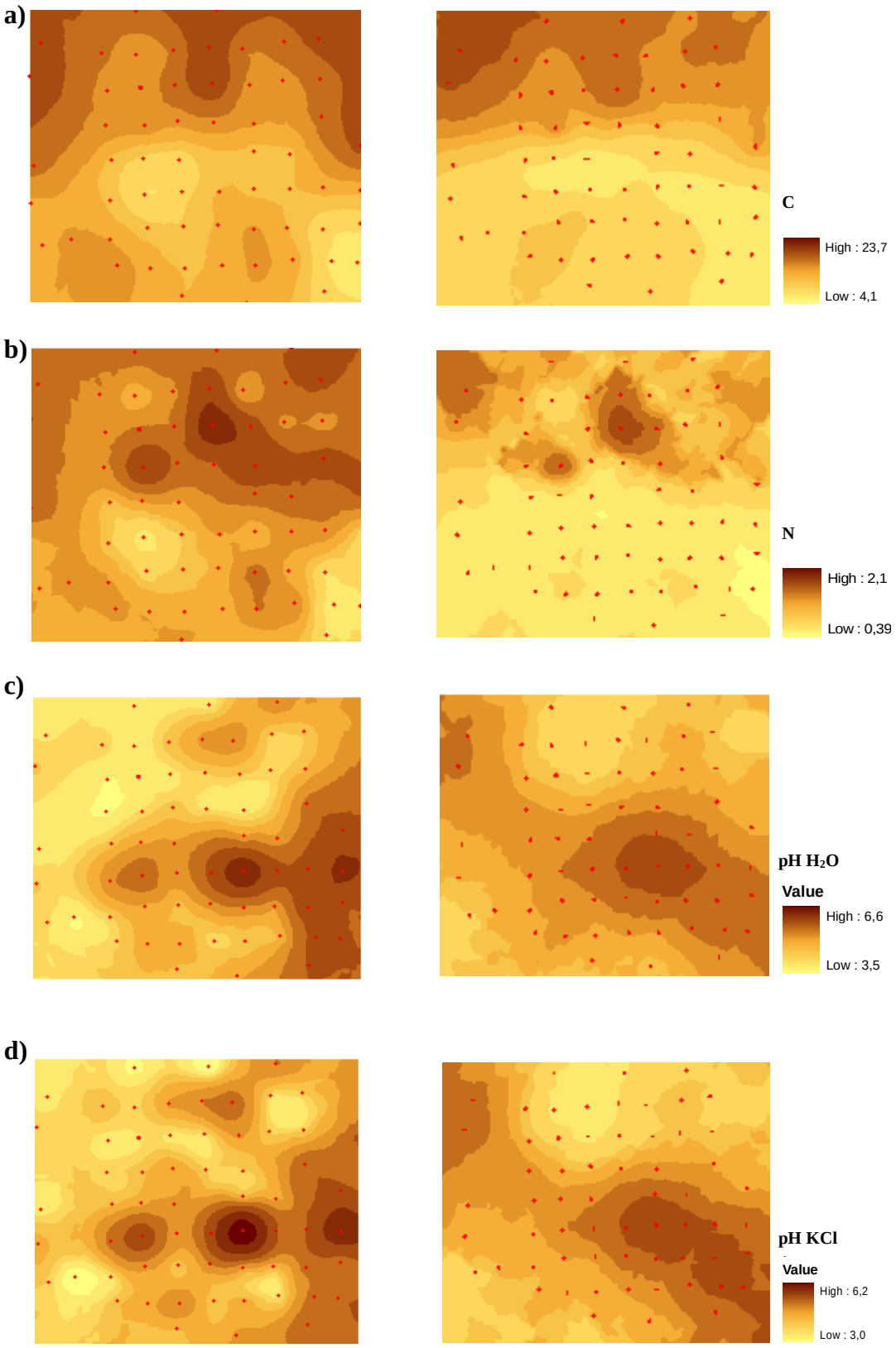

Figure 1.6 Kriking maps of forest site: organic carbon in A1 horizon and in 0-15 cm layer (a); total nitrogen in A1 horizon and in 0-15 cm layer (b); pH_{H2O} in A1 horizon and in 0-15 cm layer (c); pH_{KCl} in A1 horizon and in 0-15 cm layer d).

Semivariogram for organic carbon was fitted to an exponential model with range of 188 and 178 m for A1 horizon and 0-15 cm layer, respectively; the structured component counted for 62% of the total variance.
An exponential model with a range of 78 m was used to fit the semivariogram of total nitrogen in A1 horizon. Both the range and the structured variance strongly decreased considering the N content of the 15 cm thickness layer.
The range of autocorrelation was between 83 and 93 m for pH (water and KCl) values, considering both the A1 horizon and the 15 cm thickness layer. Less than 40% of the variance was structured.

1.3.1.1 Discussion

The organic carbon was particularly high (average value of 22.1±10.2 kg m^{-2}); it exceeds the mean carbon pools reported by Schlesinger (1984), of 13.4 kg m^{-2} and 18.9 kg m^{-2} for temperate forests and temperate grasslands, respectively.
Such organic carbon amount was probably accumulated in the past during meadow land use, promoted by soil water stagnation conditions that characterized this area.
All the semivariograms had a large nugget effect; this would suggest a common cause of micro-scale variability of all investigated parameters, probably connected with the excavation works for the drainage of soil.
Further soil translocations were done in concomitance of the concrete pipe construction. In fact, looking at maps, in the centre of the site there is an area with E-O orientation, characterized by lower organic carbon and nitrogen contents and higher pH_{H2O}, and pH_{KCl} values, probably related to the presence of the artificial pipe. Concerning pH values, the structured variance was substantially lower than those of other parameters; pH values were probably affected by both soil addition/removal and characteristic of building material.
Observing fig. 1.7, the spatial trends of C, N and pH_{H2O}, obtained after the exclusion of points near the pipe, were more clear: there is a growing gradient of carbon and nitrogen contents, in the N-S direction, while pH values increased along the axis SE-NW.
After removing the pipe disturbance, all the ranges of autocorrelation were similar, meaning a common source of variability.
The distribution of the investigated parameters can be compared with the distribution of vegetation types; higher soil organic carbon content was found under pine vegetation, where the mineralization of litter materials slowly proceeded, resulting in a succession of more acid organic layers characterized by low biological activity with the main presence of arthropods.
Going towards the southern part of the experimental site, the presence of false acacia and alder promoted a humus type with higher biological activity (largely earthworms), more rapid litter mineralization and lower soil organic carbon content (about humus layers see also chapter 4).
Vegetation conditioned pH values too; very acid values were mainly under pine while pH gradually increased towards southern direction in the alder zone.

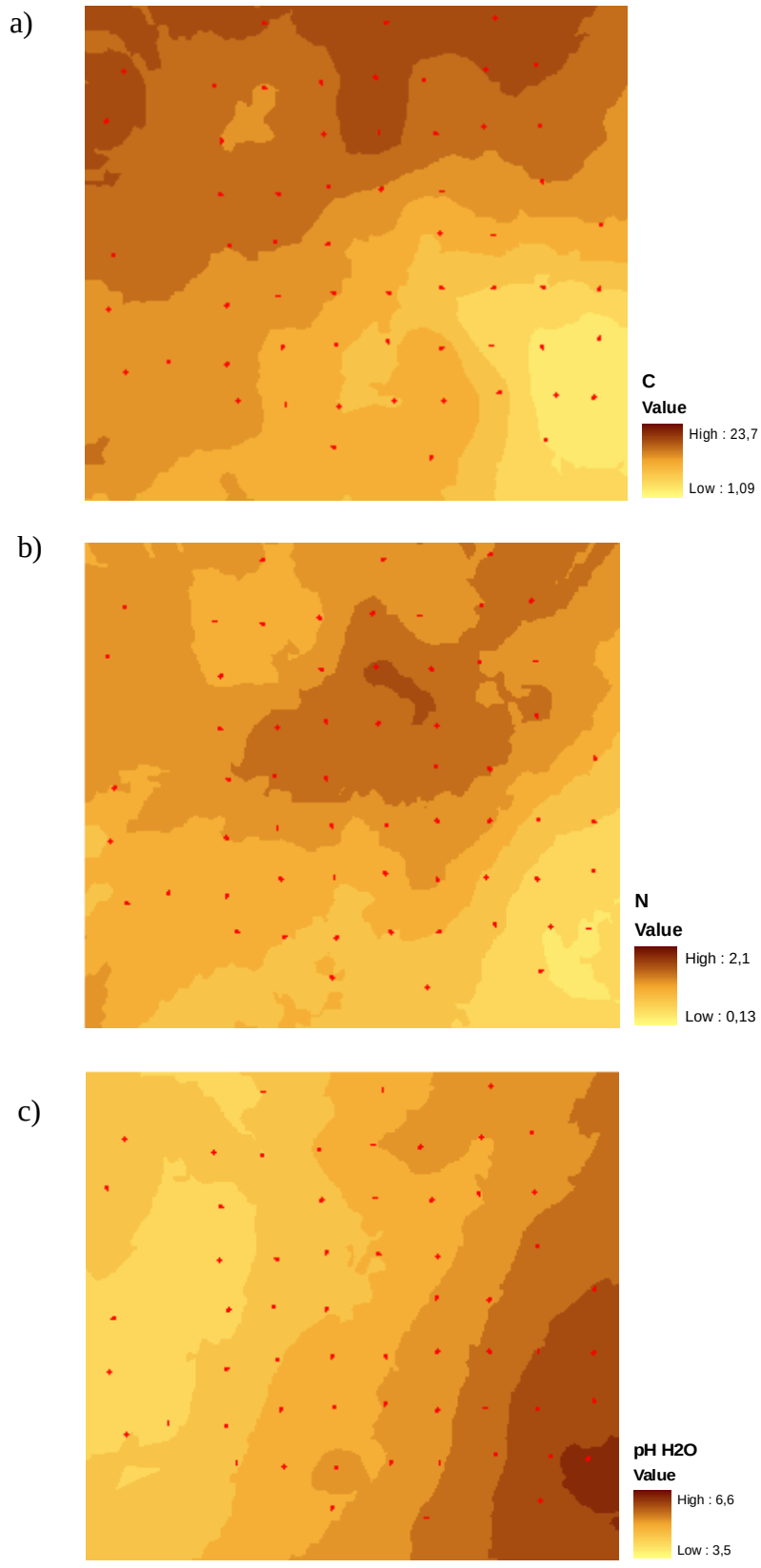

Figure 1.7 Kriking maps of forest site obtained after exclusion of the points near the concrete pipe: organic carbon in A1 horizon (a); total nitrogen in A1 horizon (b); pH_{H2O} in A1 horizon (c).

As a consequence of anthropic disturb, which in the past involved the investigated soil thickness (down the profile to C horizon, at about 50 cm depth), it was not possible to obtain the distribution maps of soil parameters relative to the whole soil thickness. On the contrary, with regard to the genetic A1 horizon, in a new equilibrium with the above vegetation, spatial autocorrelation of carbon and nitrogen contents was found.

1.3.2 THE CROPLAND SITE

On the basis of the soil profile description, chemical and physical soil variability were studied through coring. The sampling was done according to a regular grid (figure 1.8): 35 m x 35 m for a total of 59 coring. A more detailed survey was carried out at two points: at a distance of 3 m from each plot, 4 additional soil corings were done.

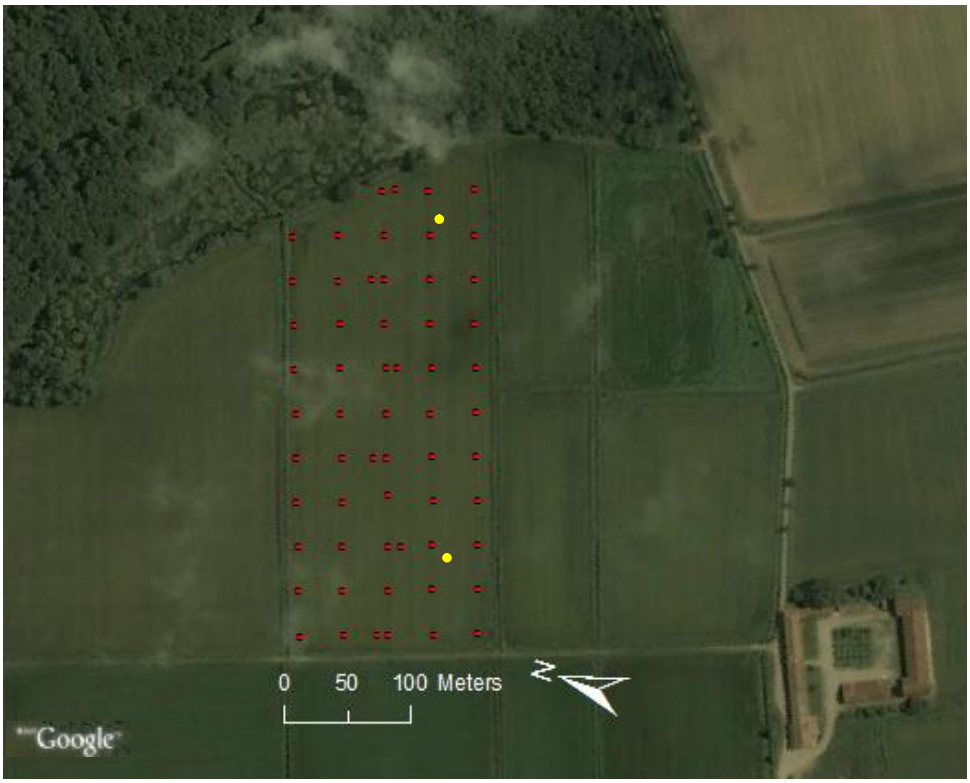

Figure 1.8 Cropland site (Castellaro dè Giorgi): soil sampling points. Red dots represent individual soil observations for the spatial variability survey; yellow dots represent pedological profiles.
(image from Google Earth)

The 67 corings were then described and for each point the Ap surface horizon (mean depth: 30 cm) was sampled and analyzed.
Soil pH_{H2O}, pH_{KCl}, organic carbon, total nitrogen, soil texture and total carbonates (gas-volumetric method - Scheibler calcimeter) were determined. Table 1.4 reports the main results of the considered soil characteristics.

Table 1.4 Main statistics (mean, standard error, standard deviation, minimum and maximum values) of soil parameters at cropland site (OC: organic carbon; N: total nitrogen; pH_{H2O}: pH in water; pH_{KCl}: pH in KCl).

	n.	Mean	St.Dev.	St.Err.	Min	Max
OC (%)	67	2.39	0.50	0.06	1.26	3.48
N (%)	67	0.26	0.50	0.01	0.15	0.38
pH_{H2O}	67	7.10	0.25	0.03	6.30	7.50
pH_{KCl}	67	6.80	0.45	0.06	5.50	7.30
$CaCO_3$ (%)	67	0.95	0.75	0.10	0.20	3.90
sand (%)	67	26.50	5.90	0.74	15.30	47.30
silt (%)	67	45.00	4.19	0.52	33.00	60.50
clay (%)	67	28.20	2.90	0.36	19.70	35.60

The surface organic carbon content was between 1.26 and 3.48% (mean value 2.39±0.50 while surface nitrogen content ranged between 0.15 and 0.38% with a mean value of 0.26±0.50%.

The mean pH_{H2O} value was 7.1, with a minimum of 6.3 and a maximum of 7.5. The total carbonates were quite low and ranged between 0.20 and 3.90%, with a mean value of 0.95±0.75%.

The soil texture (USDA class) was mainly clay loam, silty loam and silty clay loam. Sand content was included from 15 and 47%, with an average value of 26.5±6%. Silt content was included from 33 to 60%, with an average value of 45±4%. Clay content is included from 20 and 36%, with an average value of 28±3%.

The identified correlations (table 1.5) between soil characteristics (pH_{H2O} and pH_{KCl}, organic carbon, total nitrogen, total carbonates, sand, silt and clay contents) showed that the pH values were directly correlated to total carbonates contents and inversely correlated to organic carbon and total nitrogen contents; these last parameters were directly correlated to soil clay and silt content and inversely correlated to soil sand content. Map similarities (fig 1.9) of soil variables reflected these correlations. Table 1.6 reported the fitted semivariogram parameters for each considered variables.

The organic carbon and the total nitrogen content presented an high percentages of structured variance (85 and 97% respectively). Organic carbon and total nitrogen were reported to be auto-correlated at distances of 137 and 164 m respectively. The obtained maps highlight how carbon and nitrogen show similar spatial distribution with a general gradient of concentration along the NE-SW direction and intermediate values in the west zone, in proximity of the relict forest.

Table 1.5 Correlation matrix between investigated soil parameters in the Ap horizon of the cropland site (OC: organic carbon; N: total nitrogen; pH_{H2O}: pH in water; pH_{KCl}: pH in KCl; carbonate: $CaCO_3$; sand; silt; clay); bold indicates significant correlation (p value < 0.05)

	OC	N	pHw	pHKCl	$CaCO_3$	sand	silt	clay
OC	1.00	**0.91**	**-0.45**	**-0.36**	-0.01	**-0.72**	**0.71**	**0.51**
N	**0.91**	1.00	**-0.45**	**-0.39**	-0.19	**-0.61**	**0.61**	**0.43**
pH_{H2O}	**-0.45**	**-0.45**	1.00	0.75	**0.54**	0.19	-0.2	-0.1
pH_{KCl}	**-0.36**	**-0.39**	**0.75**	1.00	**0.51**	0.09	-0.16	-0.01
$CaCO_3$	-0.01	-0.19	**0.54**	**0.51**	1.00	-0.07	0.03	0.07
sand	**-0.72**	**-0.61**	0.19	0.09	-0.07	1.00	**-0.85**	**-0.73**
silt	**0.71**	**0.61**	-0.2	-0.16	0.03	**-0.85**	1.00	0.38
clay	**0.51**	**0.43**	-0.1	-0.01	0.07	**-0.73**	**0.38**	1.00

The range of autocorrelation for pH in water, pH in KCl and total carbonates was 117, 119, 122 m respectively, with a structural variance of 75%. Their spatial distribution presented a similar pattern (pH_{KCl} not showed) with lower values in the central area of the field.

The range of autocorrelation was 153, 165 and 128 m for sand, silt and clay contents respectively.

Table 1.6 Fitted semivariogram parameters for the cropland site (OC: organic carbon; N: total nitrogen; pH_{H2O}: pH in water; pH_{KCl}: pH in KCl; $CaCO_3$: total carbonates; sand; silt; clay - *normalized variable).

Parameter	Model	Nugget variance	Sill variance	Range (m)	structural variance (%)
OC	gaussian	0.04	0.27	137	85
N	spherical*	0.0001	0.0037	164	97
pH_{H2O}	spherical*	0.0004	0.0016	117	75
pH_{KCl}	spherical*	0.0015	0.006	119	75
$CaCO_3$	spherical	0.17	0.7	122	75
sand	spherical*	0.02	0.05	153	60
silt	spherical*	0.004	0.014	165	71
clay	exponential	0.008	0.015	128	46

1.3.2.1 Discussion

From the agronomic point of view, and taking into account the percentage of clay, organic carbon content was very high (mean value 2.39%) with large differences between minimum (1.38%) and maximum (3.52%). This high organic carbon value was probably related to the ancient history of the field (e.g.: reclamation of a marshy area; ditching for drainage; organic manuring; soil movements for agricultural purposes; leveling of the field for rice cultivation) and it was also a consequence of the present hydromorphic conditions, caused by the low paddy soil permeability, leading to a slow decomposition of crop residuals, incorporated into soil through ploughing. Additionally, soil texture exhibited considerable variations, resulting in the identification of different texture classes such as clay loam, silty loam and silty clay loam.

According to fluvial depositional scheme (Huggett, 2007) the distribution maps (1.9 c and f) showed the decreasing of particle size going away from the old course of the river; higher sand and lower clay contents were in fact observed in the area in proximity to the relict forest, near the old meander; going away from meander, along E-W direction, clay content increased, while the sand percentage was lower.

Fluvial processes probably affected spatial distribution of soil texture as of carbonate content. The characteristic spatial pattern observed for sand and clay and connected with fluvial depositional dynamics, was less evident for carbonate. The soil moving and leveling for agricultural intents, may have involved the subsurface soil horizons causing in certain cases, the transfer of $CaCO_3$ from the deeper layers into upper horizons and its non homogeneous superficial distribution. As a consequence, the spatial pattern of pH followed that of carbonates.

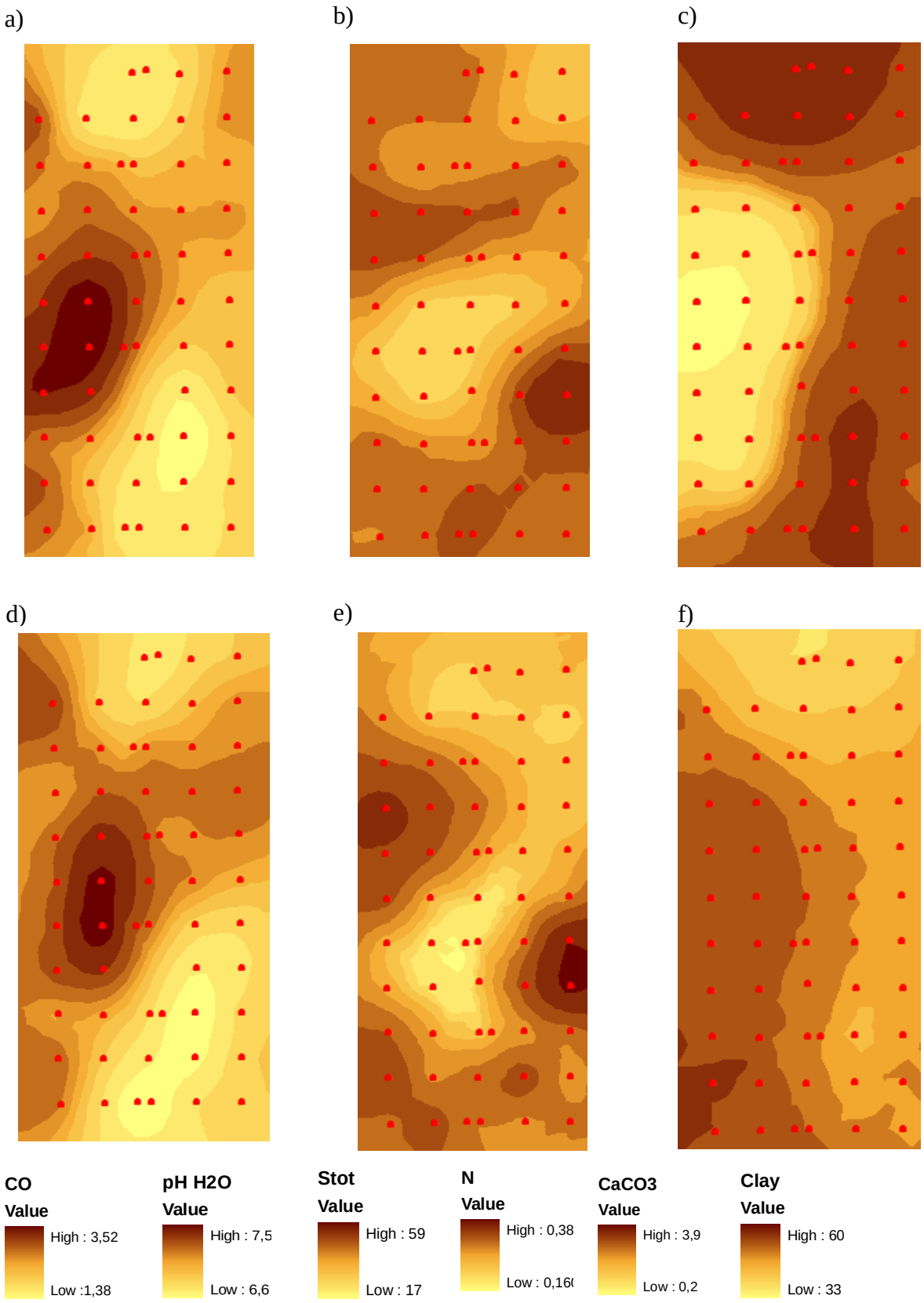

Figure 1.9 Spatial distribution maps of organic carbon (%) (a), pH_{H2O} (b), sand (%) (c), nitrogen (%) (d), carbonate (%) (e), clay (%) (f) at the cropland site (Ap horizon).

1.3.3 CHOOSE OF MONITORING POINTS

For each experimental site the spatial distribution map of the first regionalized factor obtained by multivariate analysis, was obtained aiming at identifying gas measurement points.

1.3.3.1 The forest site

A LMC was fitted to the set of the direct and cross-variograms, including 2 basic structures: a nugget effect and a spherical model with range of 65 m. The first observed structure was pure nugget effect, probably due to measurement errors and micro-variations within the smallest sampling interval (25 m). Therefore, passing over the nugget effect, the structure with range of 65 m was considered and, using the factorial kriging analysis, the regionalized factors were isolated (table 1.7) and the first component was mapped (fig. 1.10).

The first two factors explained 93% of variance and in particular the first factor (F1) explained the 67% of variance and was negatively correlated to organic carbon (-0.64) and total nitrogen (-0.63), and positively correlated to pH_{H2O} (0.43).

The map relative to the first factor confirmed the presence in the forest site of spatial distribution gradient along S-N direction, already revealed by the distribution map of each investigated variable; the northern part of forest was characterized by lower values of the first factor than the southern area, corresponding mainly to higher organic carbon and total nitrogen content, but also to lower pH values.

Based on the cokriging map the monitoring points for soil respiration were selected with the aim of capturing the site condition and the spatial variability of soil properties, a consequence of the spatial distribution of different vegetation. A sampling scheme according to two crossed transects along axes NW-SE and NE-SW was chosen (fig.1.10). Each transect was made by 8 measuring points for a total of 16 sampling points spaced at about 12.5 m one from each other. The SE-NW transect started from the area where *Alnus glutinosa* prevailed, characterized by 7.41 and 0.51% of organic carbon and total nitrogen content, respectively, and by a pH_{H2O} of 4.4 (15 cm layer) and reached the forest part characterized by the presence of *Quercus robur* and *Pinus rigida* (C 9.41%; N 0.61%; pH 3.6). The second transect started from the SW edge, where carbon and nitrogen content were 10.2 and 0.68%, respectively, and pH was 4.1, pointed to the NE pine zone (C 10.0%; N 0.54%; pH 3.7).

1.3.3.2 The cropland site

The variogram function used for the best coregionalization model was the Gaussian model with range of 126 m, comparable with the range found for individual variables, using univariate geostatistical approach (paragraph 1.3.2).

The Gaussian model is continuous and infinitively differentiable at the origin, meaning high spatial correlation of processes which act at short range. This characteristic permits to extend it at distance higher than the range. This is realistic when different processes operate at different spatial scale: in this site the spatial distribution of investigated parameters

revealed in fact a consequence of both antrophic processes, acting at short distances, and pedological and fluvial processes acting at long scale.
With the factorial kriging analysis, the regionalized factors were isolated (table 1.7). The first two factors explained 92.5% of variance; the first factor (F1) explains the 65% of variance and was positively correlated to organic carbon (0.67) and negatively correlated to sand (-0.60) and pH_{H2O} (-0.44).
The distribution of the first component (fig. 1.10) points out the presence in the site of an area characterized by high organic carbon contents but low sand amounts and pH values (high values of factor1), and two zones with opposite features (low values of factor 1). The remaining part of the field was represented by mean values of factor 1 and therefore by intermediate soil properties. Just this area was chosen for gas monitoring; the necessity to place in a unique area the needed equipment for the flux measurements, due to logistic and economic reasons and to avoid disturb to the rice cultivation during cropping season, led to prefer such a position, excluding the field locations characterized by extreme soil properties, therefore less representative of site soil.
In figures 1.10 the selected area for soil and ecosystem gas flux measurements is shown.

Table 1.7 The eigenvector matrix, the corresponding eigenvalues and the percentage of variance explained by them for forest site and cropland site.

Forest site

	C	pH	N	Eigen value	Var. %
F1	-0.641990	0.431269	-0.633922	2.024561	67.48537
F2	-0.277412	-0.901444	-0.332327	0.766862	25.56207
F3	-0.714767	-0.037493	0.698357	0.208577	6.95256

Cropland site

	C	pH	S	Eigen value	Var. %
F1	0.669473	-0.43981	-0.59864	1.941127	64.70424
F2	-0.10155	-0.85251	0.512758	0.834695	27.82316
F3	0.735863	0.282485	0.615393	0.224178	7.4726

a)

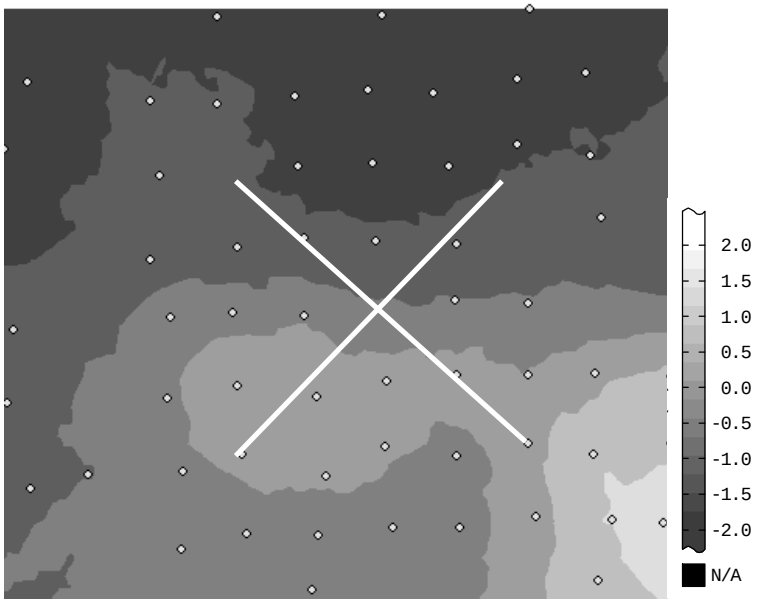

b)

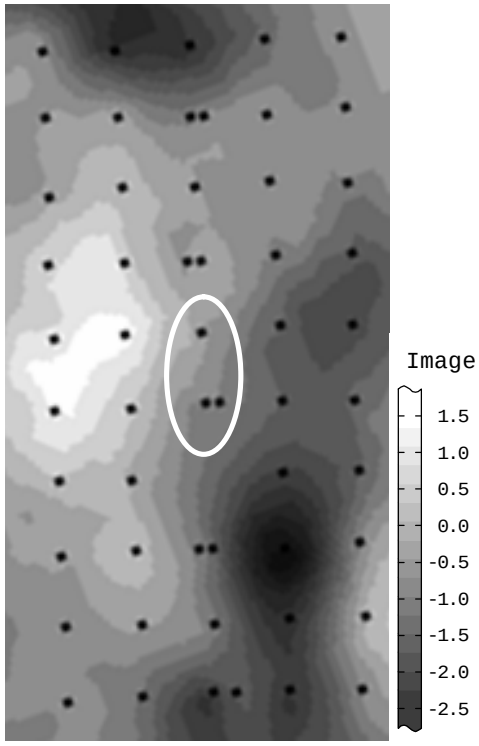

Figure 1.10 Spatial distribution maps of first factor (F1) for the forest site (a) and cropland site (b). White lines in the map of Ispra site represent transects for soil respiration measurements; in the map of the cropland site white circle represents monitoring area for CH_4, N_2O, CO_2.

1.4 CONCLUSION

In terms of soil gas emissions, the large heterogeneity of investigated soil properties is of great importance, since it can directly and indirectly affect flux rates.
The study of the soil spatial variability showed the presence of significant differences in the main physical and chemical soil properties, not only in the forest site, where the variability in vegetation type may give an indication about this, but also in cropland site where at a rapid observation, the soil can erroneously appear homogeneous.
The study revealed to be essential for selecting and assessing representative plots for flux measurements: for the forest site we selected a sampling scheme aimed at capturing the observed spatial variability, while for the agricultural site, where logistic and economic reasons forced to select only one location, the knowledge of the spatial trend of soil characteristics demonstrated to be crucial for the plots choice, leading to the exclusion of unsuitable areas as characterized by extreme values of soil properties.

REFERENCES

- Aulakh, M.S., Wassmann, R., Rennenberg, H., 2001. Methane transport capacity of twenty-two rice cultivars from five major Asian rice-growing countries. Agriculture, Ecosystems and Environment.
- Bourgault, G., Journel, A.G., Rhoades, J.D., Corwin, D.L., Lesch, S.M., 1997. Geostatistical analysis of a soil salinity data set. Advances in Agronomy 58, 241–292.
- Castrignanò, A., Giugliarini, L., Martinelli, N., Risaliti, R., 2000a. Study of spatial relationships among soil physical-chemical properties using Multivariate Geostatistics. Geoderma 97, 39–60.
- Castrignanò, A., Goovaerts, P., Lulli, L., Bragato, G., Gardin, L., 2000b. A geostatistical approach to estimate probability of occurrence of Tuber melanosporum in relation to some soil properties. Geoderma 98, 95–113.
- Castrignanò, A., Mazzoncini, M., Giugliarini, L., 1998. Spatial characterization of soil properties. Advances in GeoEcology 31, 105–111.
- Coûteau, M.M., Bottner, P., Berg, B., 1995. Litter decomposition, climate and litter quality. Trends in Ecology and Evolution 10, 63-66.
- ESRI, 2006. Arcgis 9.2.
- Geovariances, 2003. ISATIS, release 4.02.
- Goovaerts, P., Webster, R., 1994. Scale-dependent correlation between topsoil copper and cobalt concentrations in Scotland. European Journal of Soil Science 45, 79–95.

- Hanson, P.J., Wullschleger, S.D., Bohlman, S.A., Todd, D.E., 1993. Seasonal and topographic patterns of forest floor CO_2 efflux from an upland oak forest. Tree Physiology 13, 1–15.
- Huggett, R. J., 2007. Fundamentals of geomorphology - Second Edition. Routledge, London and New York, pp. 483.
- IUSS/ISRIC/FAO, 2006. World Reference Base for Soil Resources. World Soil Resources Reports 103, FAO, Rome, pp. 128.
- Journel, A.G., Huijbregts, C.J., 1978. Mining Geostatistics. Academic Press Inc, London, UK, pp. 600.
- Li, C., 2000. Modeling trace gas emissions from agricultural ecosystems. Nutrient Cycling in Agroecosystems 58, 259–276.
- Li, C., 2001. Biogeochemical concepts and methodologies: Development of the DNDC model (in Chinese with English abstract). Quaternary Sciences 21, 89–99.
- Li, C., Mosier, A., Wassmann, R., Cai, Z., Zheng, X., Huang, Y., Tsuruta, J., Boonjawat, J., Lantin, R., 2004. Modeling greenhouse gas emissions from rice-based production systems: Sensitivity and upscaling. Global biogeochemical cycles 18(1).
- Matheron, G., 1982. Pour une analyse Krigeante des données regionalisées. Report 732. Centre de Geostatistique, Fontainebleau, France.
- NRCS, 2004. Soil Survey Laboratory Methods Manual. Soil Survey Investigations Report 42. USDA-NRCS, pp. 700.
- Raich, J.W., Schlesinger, W.H., 1992. The global carbon dioxide flux in soil respiration and its relationship to vegetation and climate. Tellus 44B, 81–99.
- Sahrawat, K.L., Keeney, D.R., 1986. Nitrous oxide emission from soils. Advances in Soil Science 4, 103–148.
- Schlesinger, W.H., 1984. Soil organic matter: a source of atmospheric CO_2. In: Woodwell G.M. (ed.), Role of terrestrial vegetation in the global carbon cycle: Measurement by remote sensing. John Wiley & Sons, Chichester, UK , pp. 111–127.
- Simojoki, A., Jaakkola, A., 2000. Effect of nitrogen fertilization, cropping and irrigation on soil air composition and nitrous oxide emission in a loamy clay. European Journal of Soil Science 51, 413–424.
- Toland, D.E., Zak, D.R., 1994. Seasonal patterns of soil respiration in intact and clear-cut northern hardwood forests. Canadian Journal of Forest Research 24, 1711-1716.
- Wackernagel, H., 1988. Geostatistical techniques for interpreting multivariate spatial information. In: Chung, C.F. (ed.), Quantitative Analysis of Mineral and Energy Resources. Reidel, Dordrecht, NL, pp. 393–409.
- Webster, R., Oliver, M.A., 2001. Geostatistics for environmental scientists. John Wiley & Sons, John Wiley & Sons, pp. 271.

CHAPTER 2

MEASUREMENTS OF METHANE, NITROUS OXIDE AND CARBON DIOXIDE EMISSIONS FROM A RICE PADDY AND VALIDATION OF DNDC MODEL

2.1 INTRODUCTION

Rice paddies have been identified as one of the major sources of atmospheric CH_4, contributing about 10-15% to global CH_4 emission (Neue, 1993), of which 70% is of anthropogenic origin. Rice paddies are also known to emit high N_2O fluxes under certain water management regimes (Bronson et al., 1997; Zheng et al., 1997; Cai et al., 1999; Abao et al., 2000). These gases are important to atmospheric chemistry and earth's radiative balance because of their long atmospheric life times (10 yr for CH_4 and 120 yr for N_2O). Both species absorb terrestrial thermal radiation: N_2O is the strongest climate gas with a global warming potential (GWP) of 310 compared to the GWPs of CH_4 and CO_2 of 21 and 1, respectively.

Agricultural soils are subjected to management practices including tillage, fertilization, irrigation, weeding and manure amendments which affect trace gas emissions playing an important role in the atmospheric balance of the trace gases. Many of the factors controlling gas exchange between rice paddies and the atmosphere are different from those in dry agriculture soils and other ecosystems because rice is flooded during most of its cultivation period. Depending on the water management, paddy soils are characterized by frequent changes between saturated and unsaturated conditions. During these changes in soil water content, the soil redox potential, which is one of the key processes controlling production and consumption of CH_4, N_2O and CO_2, is subjected to substantial changes between +600 and -300 mV.

There are only few studies that include N_2O emissions and net CO_2 exchange in flooded ecosystems, while for CH_4 fluxes there are available data usually only referred to the rice growing season.

The mechanism of CO_2 efflux is not fully understood and the budget of CO_2 between the atmosphere and the rice paddies has not been documented well; the presence of floodwater and the existence of anaerobic soil conditions influence root activity, photosynthesis and respiration of rice plants. Additionally, the activity of aquatic plants such as algae, may also affect CO_2 exchange between rice paddies and the atmosphere (Koizumi et al., 2001).

One of the principal causes which affects the estimates of gases is the large spatial and temporal variability in their emissions. Moreover, the estimates of GHG emissions from rice paddies differ largely, depending on the techniques and approaches.
Therefore, more site-specific information is necessary and of great importance for understanding such a variability, for reducing uncertainties of estimates and for model validating.
The objective of this study was to measure soil CO_2, N_2O, and CH_4 exchange between a paddy soil and the atmosphere including both growing and fallow season.
The DNDC (DeNitrification and DeComposition) model (Li et al., 1992), which has already been used to estimate emissions in major rice producing countries such as China and India (Li et al., 2005; Jagadeesh Babu et al., 2006), was tested against experimental data.

2.2 MATERIALS AND METHODS

2.2.1 STUDY SITE

The study area (about 3 hectares) is located in the Po plain (Castellaro de' Giorgi, Lombardy) and is characterized by the presence of rice crop, in rotation with maize (3-4 years rice and 1 year maize).
According to the classification system of the World Reference Base (IUSS/ISRIC/FAO, 2006), soils are Gleysols: Haplic Gleysol (Calcaric, Endoarenic) and Calcic Gleysol (Hypercalcaric, Humic).
The soil texture (USDA class) is mainly clay loam, silty loam and silty clay loam; the soil reaction may be defined neutral (the water pH mean value is 7.1). The surface (0-30 cm) nitrogen content is between 0.15 and 0.38% with the mean value of 0.26%, while surface organic carbon content ranges between 1.26 and 3.48%. The high carbon content is the consequence of the low decomposition rate of organic material due to surface water excesses; the groundwater level is often high and moreover the reduced soil permeability, due to tillage and agricultural practices for rice, causes anthraquic conditions and poorly drainage also during no rice cultivation time.
The soil was prepared for the sowing through a 30 cm-depth ploughing, carried out on February 28th. On May 7th, the manure amendment (16 t ha^{-1} of sugar-beet industrial slops) was distributed on the soil surface and, a few days after, incorporated into the soil through a seed-bed harrow (10 cm depth). The field was leveled and then submerged to prepare sowing which was carried out in water on May 12th.
The flooding conditions (water level about 12 cm) were maintained until the distribution of herbicide for weed control, which was carried out on saturated and partially submerged (3-4 cm) soil on June 11th. The flooding was established again 2-3 days after the distribution and continuously maintained until September 5th. On July 1st, at panicle initiation stage, N fertilization was top-dressed (15 kg ha^{-1} N-NH_3 and 24 kg ha^{-1} N_{ureic}). The crop was harvested on October 17th.
Details about study site and soil characteristics can be found in chapter 1.

2.2.2 FLUXES AND ANCILLARY MEASUREMENTS

Based on detailed mapping of soils (see chapter 1), a set of static and dynamic manual chambers were installed in the centre of the field (fig. 2.1).

A small bank halved the field in NE-SO direction, reaching the two areas for gas measurements (A and B). Each soil measurement area was made by two plots, spaced at about 4 m, each composed by two points for N_2O and CH_4 emission measures and three points for CO_2 measures, for an overall of 8 chambers for N_2O and CH_4 and 12 chambers for CO_2.

Figure 2.1 Monitoring areas of CH_4, N_2O and CO_2 fluxes (A and B). The eddy tower for ecosystem flux is represented by black rectangle.
(image from Google Earth)

Fluxes were measured using the static (N_2O and CH_4) and dynamic (CO_2) chamber techniques.

After the insertion, the collars remained in place for all the duration of the experiment; they were temporarily removed only in concomitance of management practices such as ploughing or sowing. Soil fluxes were biweekly measured during winter period, while weekly samples were collected during vegetation period; a flexible sampling scheme was instead adopted before and after management interventions in order to get the high variability of emissions.

During flooding period, chambers were reached using steel catwalks to avoid soil disturbance and modification in gas rates, due to the crossing in the field.
During the no-flooding period, the total soil emissions flux of CO_2 (kg C ha^{-1}) was computed as the sum of half-hourly fluxes estimated using the dependence of measured rates from the soil temperature registered by the meteorological station placed at the site; annual emission of CH_4 and N_2O and emissions of CO_2 relative to the flooding period, were determined by integrating the curve obtained by interpolation of the flux rates.

2.2.2.1 N_2O and CH_4 soil fluxes

Fluxes were measured using the static chamber technique. The chambers were placed open-top on stainless steel frames in the field and their height was adjusted during the growing season to follow the growth of the rice plants.
For the sampling, chambers were left closed for 1 hour taking a gas sample every 20 minutes; during the flooding period, as the observed flux rates were high for CH_4 and low for N_2O, we left the chambers closed for 1.5 hours, taking a gas sample immediately after closing the chamber and after 15, 30, and 90 minutes.
The air mixing into the chambers was ensured by large slowly rotating impellers. Turbulent flow conditions were established in the chambers with four baffles inside the chamber walls.
Sampling was done by using previously flushed and evacuated glass vials connected to the chamber air with the help of a needle inserted through a rubber stopper in the chamber lid.
Gas samples analyses were done with a Shimadzu GC 14B gas chromatograph provided with a 6-port valve to interface with the injection system and a Porapak Q column (2 m x 1/8" x 2 mm SS, 80/100 mesh, Chrompack). Gases were detected with an ECD (N_2O) and an FID (CH_4) (both Shimadzu), mounted in series. The gas chromatographic peaks were evaluated with the software Chrom-Card (CE Instruments, UK). Calibration was done by means of a standard mixture of N_2O and CH_4 in nitrogen, which has been calibrated with a standard mixture (Scott Speciality Gases) using a second gas chromatograph.
For injection of the gas samples, a self-built system for automatic injection up to 163 gas samples, was used; pressure close to the sample loop was measured prior to transfer the sample on the gas chromatographic column. A calibration was done with each set of samples, to compensate for daily changes in temperature or pressure. During the closure time of a flux chamber, changes in temperature or air humidity led to an additional, 'artificial', change in the mixing ratio of the gases; measured changes in the observed mixing ratio must be corrected for this effect (e.g., Schmidt et al., 1988). By ensuring that the equilibrium between the conditions in the chamber and vial was established during field sampling, we were able to correct this effect using the information obtained during the analyses (for details see Leip, 2000).
Unless we observed a zero flux rate, only the measurements with linearity were used.

2.2.2.2 CO_2 soil fluxes

CO_2 soil fluxes were measured with a portable infrared gas analyzer (LI-6400) equipped with a chamber based on the principle of closed dynamic systems.

The Li-6400 is a portable system connected to the Li-6400 soil flux chamber; the chamber is cylindrical with a diameter of 9.5 cm, a base area of 76.1 cm^2, and a volume of 991 cm^3. The chamber concentration is automatically scrubbed to just below an ambient target, and then measured as it rises slightly above the ambient target. This maintains the CO_2 concentration gradient within a few ppm of the natural, undisturbed value. The mixing fan in the sensor head is used to move air through a perforated manifold thoroughly mixing the air in the chamber; a pressure equilibration tube is used to eliminate pressure differentials and avoid chamber leaks.
The permanent installed collars were custom-made from stainless-steel, with four rods helping to fix the collar tightly into the soil. The factory made chamber was slightly modified and an O-ring was added to the base in order to improve its sealing with the collars.
After the insertion, the collars remained in place for all the duration of the experiment. CO_2 soil fluxes were measured every 15-30 days, depending on the season.
The site was also equipped with an eddy flux tower for monitoring fluxes of water vapour and fluxes and CO_2 at ecosystem level. The turbulent vertical fluxes of CO_2, water vapour, latent and sensible heat were measured using the eddy covariance technique (Baldocchi et al., 1988).

2.2.2.3 Temperature and soil water content measurements

Simultaneously with soil fluxes, soil temperature and soil water content were measured at all sites. Soil temperature was determined with the built-in temperature probe of the CO_2 analyzer, usually at a depth of 5 cm, while soil water content was measured with a portable TDR system (IMKO Micromodultechnik, GmbH, Ettlingen, Germany) using a 12 cm long trifurcated probe. Together with other parameters, a weather station measured continuously (30 minutes averages) soil and air temperature.

2.2.3 THE DNDC MODEL

The Denitrification–Decomposition (DNDC) model was originally developed for predicting C sequestration and trace gas emissions for non-flooded agricultural lands, simulating the fundamental processes and controlling the interactions among various ecological drivers, soil environmental factors and relevant biochemical or geochemical reactions, which collectively determine the rates of trace gas production and consumption in agricultural ecosystems (Li et al., 1992, 1994, 1996). To enable DNDC to simulate C and N biogeochemical cycling in paddy rice ecosystems, the model was modified by adding a series of anaerobic processes (Li, 2003, 2004; Cai et al., 2003).
Paddy soil is characterized by the frequent changes between saturated and unsaturated conditions, depending on the water management. During these changes in soil water content, the soil redox potential is subject to substantial variations between +600 and -300 mV. One of the key processes controlling CH_4 and N_2O production/consumption in paddy soils is soil Eh dynamics (Yu and Patrick, 2004). CH_4 or N_2O are produced or consumed under certain Eh conditions (-300 to -150 mV for CH_4, and 200–500 mV for N_2O), so the two gases are produced during different stages of the varying soil redox potential. DNDC allocates substrates (e.g., DOC, NO_3, NH_4^+, CH_4 etc.) to reductive reactions (e.g., denitri-

fication, methanogenesis) and oxidative reactions (e.g., respiration, nitrification, methanotrophy) based on relative fractional volumes of the oxidizing and reducing zones, and the potential oxidation and reduction reactions are determined by Eh and pH (Yu et al., 2001).
The model consists of two components. The first, consisting of the soil climate, crop growth and decomposition sub-models, predicts soil temperature, moisture, pH, redox potential (Eh) and substrate concentration profiles driven by ecological variables (e.g., climate, soil, vegetation and anthropogenic activity). The second component, consisting of the nitrification, denitrification and fermentation sub-models, predicts NO, N_2O, N_2, CH_4 and NH_3 fluxes based on the modeled soil environmental factors. Classical laws of physics, chemistry and biology, as well as empirical equations generated from laboratory studies have been employed in the model to parameterize each specific geochemical or biochemical reaction.
For the present study we used DNDC version 9.3.

2.2.4 STATISTICAL ANALYSES

Statistical analyses were performed using the Statistica software (version 7). Flux results were subjected to the analyses of variance (ANOVA).
The model was evaluated using the modeling efficiency (EF) and the regression coefficient (R^2) (Mayer and Butler, 1993).

2.3 RESULTS AND DISCUSSION

2.3.1 ANALYSIS OF VARIANCE

The ANOVA (table 2.1) revealed significant differences in gas fluxes between sampling dates, while chambers positions resulted not affect gases emissions, with the exception for CH_4 in position 4, which showed different fluxes, lower than the other sampling points.

Table 2.1 Analysis of variance; bold indicates significant correlation (p value < 0.05).

		N_2O	CH_4	CO_2
date	df	19	19	18
	F	4.5	15.3	29
	p value	**0.000**	**0.000**	**0.000**
position	df	3	3	3
	p value	0.458	**0.000**	0.777
	F	0.9	7.1	0.29
date x posit.	df	57	57	54
	p value	0.106	0.214	**0.000**
	F	1.3	1.2	1.8

The reasons of such result could be explained by a different height of water table above soil surface or by lower plant density inside these chambers; some studies documented how transport and emissions of CH_4 were affected by water level and rice plants (Raimbault et al., 1977; Cicerone and Shetter, 1981; Aulakh et al., 2000a, 2000b, 2002).
The analysis showed an interaction effect between sampling dates and positions for CO_2 fluxes; the application of a post hoc test discovered dissimilarities between chambers in position 2, 3, 4 on May 8th and between chambers in position 1, 3, 4 on September 11th. At the former date the manure amendment with sugar beet slops was applied, while the latter date was at the end of flooding period, immediately after water removing; therefore, the heterogeneity of manure application and soil saturation conditions could have caused heterogeneity of CO_2 emissions.

2.3.2 OVERVIEW OF SOIL FLUXES

Fig. 2.2 shows an overview of fluxes of CH_4, N_2O and CO_2, while fig. 2.3 presents ecosystem respiration (Re) and net ecosystem exchange (NEE) data, relative to January-October period.
Soil gaseous emissions are reported as daily mean rates (±SE) of all site chambers; only for CH_4 trends, fluxes emitted by soil at sampling area B, position 4, were taken and showed separately.

2.3.2.1 Methane fluxes

Throughout the rice-growing season, CH_4 emissions between 36±10 and 22991±681 µg C-CH_4 $m^{-2}h^{-1}$ were measured (fig. 2.2 a). Smaller fluxes ranging between 0–26 µg C-CH_4 $m^{-2}h^{-1}$, mainly occurred in the fallow season, in winter and autumn time, when, as reported in chapter 1, the site was often characterized by water excess following rainy events. Only on 7th April at the sampling area B, position 4, CH_4 oxidation (-66 µg CH_4 $m^{-2}h^{-1}$) occurred.
During flooding, fluxes showed an initial period of moderate values ranging between 6424±1300 and 9461±2720 µg C-CH_4 $m^{-2}h^{-1}$, increased to the high rate of 18455±1621 µg C-CH_4 $m^{-2}h^{-1}$ on 11th July and then decreased to the lowest value of 4020±499 on 16th July. Afterwards, emissions progressively increased again with crop growing, with an emission peak at flowering (6th August). This relative maximum was followed by the lower value of 5937±926 µg C-CH_4 $m^{-2}h^{-1}$ and the highest value of 22991±681 (absolute maximum), only 2 and 8 days after flowering, respectively. Then fluxes maintained at a mean value of 10935±518 µg C-CH_4 $m^{-2}h^{-1}$ as the crop ripened till the definitive water removing, afterwards they substantially decreased.
The first emission maximum, observed after flooding, could be attributed to the degradation of organic matter present in the soil (Rennenberg et al., 1992) and it was probably accentuated by the application of manure amendment occurred on 7th May; Neue et al. (1994) observed that the early maximum was pronounced in soils that received organic manure, whereas soils with low organic inputs showed gradual increases of CH_4 emissions. The maximum measured at flowering stage may have been caused by the availabil-

ity of root exudates as substrate for methanogenesis (Minoda and Kimura, 1994; Wang et al, 1997; Lu et al., 2000).

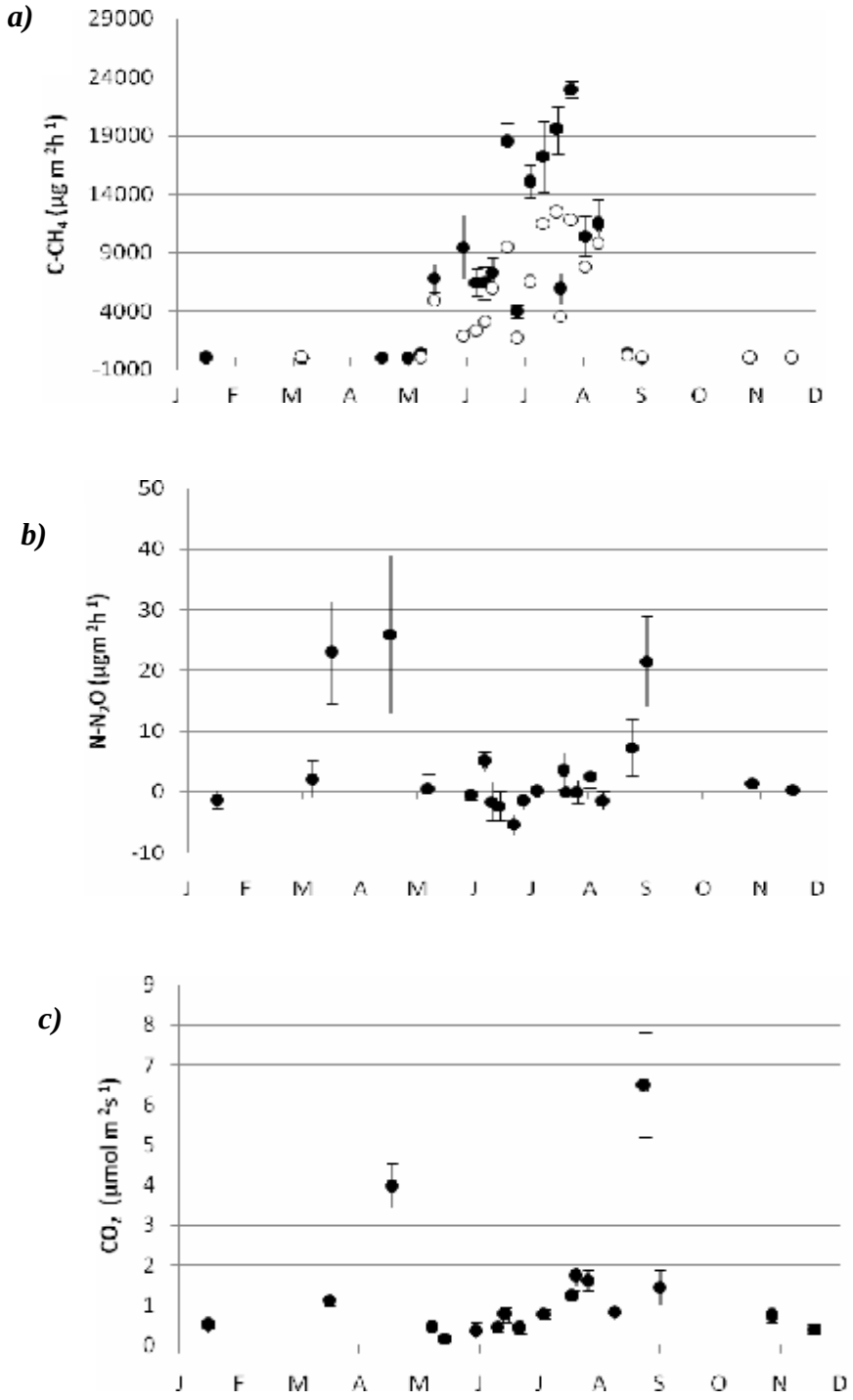

Figure 2.2 Fluxes of CH_4 (a), N_2O (b) and CO_2 (c) (daily mean of chamber rates ± SE) in cropland site during rice cultivation. In CH_4 graph, black dots represent daily mean rates of all site chambers with the exclusion of chambers in position 4, represented by white dots.

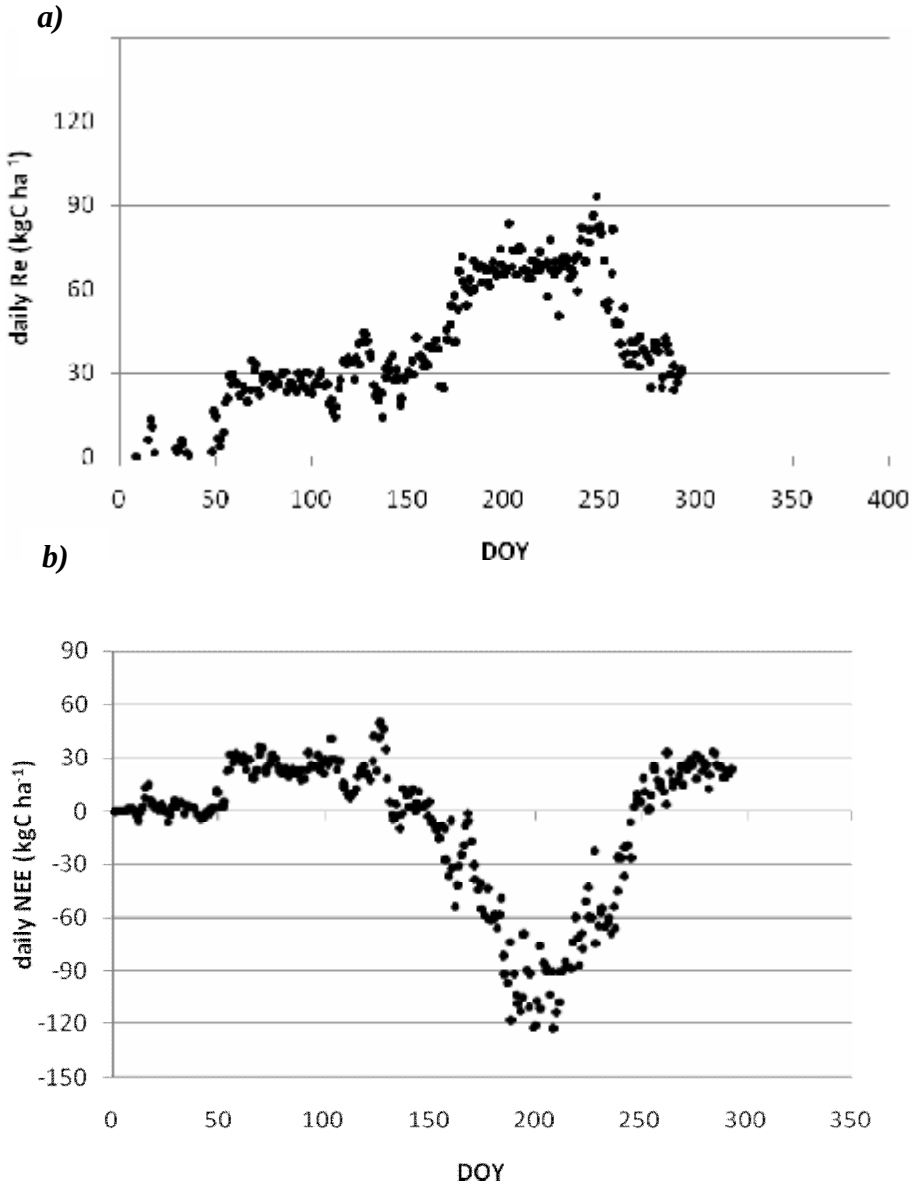

Figure 2.3 Ecosystem respiration-Re (a) and net ecosystem exchange-NEE (b) (eddy tower fluxes) relative to January-October period.

At position 4, during flooding we observed lower CH_4 emissions ranging between 20 and 11486 µg C-CH_4 $m^{-2}h^{-1}$, but the seasonal trend is the same of that considered as representative of the site and just expounded.
Annually integrated fluxes were 268 kg C-CH_4 ha^{-1}. Leip et al. (2007) reported seasonally fluxes of 375-450 kg C-CH_4 ha^{-1} in a rice paddy in Italy (Piedmont), with large reduction of the emissions for the late-flooding field, with only 90-127 kg C-CH_4 ha^{-1}.
At position 4, annual emission rate was significantly lower, amounting to 158 kg C-CH_4 ha^{-1}.

2.3.2.2 Nitrous oxide fluxes

Mean nitrous oxide emissions were 3.8±0.5 µg N-N_2O $m^{-2}h^{-1}$(fig 2.2 b). The highest N_2O emissions were measured during fallow period on 7th April (23.0 µg N-N_2O $m^{-2}h^{-1}$) and on 8th May (26.0 µg N-N_2O $m^{-2}h^{-1}$), respectively. During monitoring year, the mean soil water content (v/v) was 59%, ranging between 24% and 70% (fig. 2.4). As demonstrated by controlled laboratory experiment, proposed by Schaufler et al. (submitted), for Castellaro site the N_2O emission starts at water filled pore space (WFPS) between 30 and 40% and increases with the soil moisture increasing, reaching its maximum at about 50-60% WFPS; after that, it decreases. In particular for April and May sampling dates, the estimated WFPS was 48 and 44%, respectively. The higher N_2O emission obtained for the sampling date characterized by 44% WFPS was probably justified by stimulation of N_2O production as consequence of the manure amendment application.

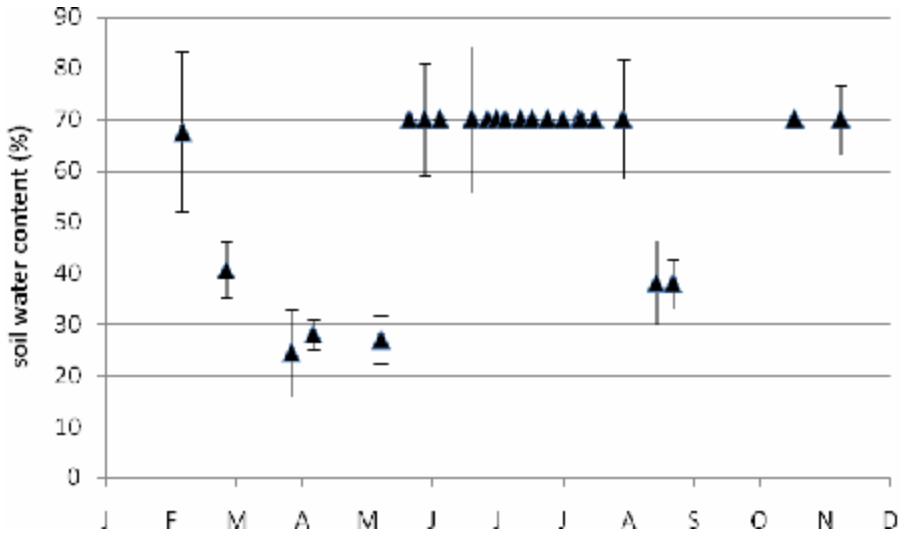

Figure 2.4 Soil water content (%).

During flooding period, a consumption of N_2O inside chambers was detected. Denitrification is one of the major sources for nitrous oxides and molecular nitrogen; it is a form of anaerobic respiration in bacteria which couples the stepwise reduction of nitrate oxides to electron transport with the intermediate products nitrite, nitric oxide, and nitrous oxide (Firestone and Davidson, 1989). Through flooding, conditions are sufficiently reducing and the availability of organic substances is sufficiently large so that denitrification proceeds to N_2. The soil moisture in the study site was 100% WFPS, so that N_2O was reduced by denitrifying bacteria to molecular nitrogen. After application of fertilizer into the flooded soil, the highest N_2O consumptions were measured, 4 and 11 days after N-fertilization.

During the submerged period, non-zero N_2O emissions were also observed. Some studies report that under field conditions, rhizospheric zone can significantly influence C and N dynamics in rice soils through influence of soil Eh, pH and substrate availability (NH_4, NO_3 and DOC) (Reddy and Patrick, 1984; Flessa and Fischer, 1992). Nitrification followed by denitrification takes place at the vicinity of rice roots producing N_2O, which may escape into the atmosphere through rice plants (Wang et al., 1999).
After water drainage from the paddy soil, the shift of the soil aeration stimulated decomposition, nitrification and denitrification to emit fluxes of N_2O (emissions of 21.5 µg N-N_2O $m^{-2}h^{-1}$ on 19th September).
The annual site N_2O emissions amounted to 0.4 kg N-N_2O $ha^{-1}yr^{-1}$, while during crop season the soil emitted 0.2 kg N-N_2O $ha^{-1}yr^{-1}$; these flux rates are lower but comparable with the data published, which reported mean N_2O emissions from rice paddy fields of 0.7 g N-N_2O $ha^{-1}yr^{-1}$ (Bouwman et al., 2002).
Akiyama and Yagi (2005) gives mean rate±standard deviation of 0.3±0.4 g N $ha^{-1}season^{-1}$, on the basis of data published before 2004, comprising 147 field measurements for fertilized fields continuously flooded.

2.3.2.3 Carbon dioxide fluxes

Soil CO_2 emissions ranged between 0.4±0.1 and 6.5±1.3 µmol $m^{-2}s^{-1}$ with an average value of 1.3±0.4 8 (fig. 2.2 c). Two emission peaks were observed, on 8th May and 11th September; the former was the consequence of manure amendment; the latter happened 6 days after the definitive water removing, at the start of dry period for rice ripening. During flooding we observed a growing trend with the proceeding of vegetative season and consequently with the development of plant roots, till a maximum, measured at flowering stage (1.7 µmol $m^{-2}s^{-1}$); after that, CO_2 emissions slowly decreased.
The total measured CO_2 soil emissions were 1.13 kg CO_2 $m^{-2}y^{-1}$. These emissions were consistent with soil CO_2 fluxes estimated from data obtained by eddy covariance method, in a Chinese paddy ecosystem, ranging between 1.56 and 2.28 kg CO_2 $m^{-2}h^{-1}y^{-1}$ (Ren et al., 2007). Lack of bibliographic data concerning soil CO_2 rates, makes a difficult interpretation of our results. During the flooding period, daily flux could be slightly underestimated for exclusion of nighttime contribution of weed respiration to the daily CO_2 rate; biological processes of photosynthesis and respiration of aquatic plants and soil microbes are known to exert an important influence on CO_2 flux between the atmosphere and the water surface in paddy fields during submerged period (Koizumi et al., 2001).
Within the project, measurements at ecosystem level were simultaneously carried out. Before flooding period, ecosystem respiration occurred till May, then carbon uptake started, reaching the highest value in July (-121 kg C $ha^{-1}d^{-1}$) and stopped at the start of September (fig. 2.3).
Considering the entire period January-October, Re and NEE were 10603 and -2847 kg C ha^{-1}, respectively (table 2.2).

2.3.3 DNDC MODEL

Simulated CO_2 and CH_4 soil gas emissions at the experimental site were in good agreement with the observed rates (fig. 2.5); for CO_2 data the coefficients of regression and the model efficiency were 0.68 and 0.60, respectively, while for CH_4 the coefficient of regression was 0.52 and the model efficiency was 0.75 (table 2.2).

Model was capable of describing ecosystem respiration and net CO_2 exchanges too (fig. 2.6); the models efficiencies were 0.52 and 0.87 for Re and NEE, respectively. A lower model efficiency was observed in N_2O simulation (0.01).

Table 2.2 Modeled and measured annual gas emissions, model efficiency (EF) and R^2. Soil CO_2: heterotrophic and root respiration. All ecosystem emission data refer to the January – October period.

		soil			ecosystem	
		CH_4	N_2O	CO_2	Re	NEE
EF		0.7	0.01	0.6	0.5	0.9
R^2		0.5	0.2	0.7	0.7	0.7
measured	kg N or C ha^{-1} yr^{-1}	268	0.417	4250	10603	-2847
DNDC	kg N or C ha^{-1} yr^{-1}	197	0.888	4866	8085	-2548

The seasonal pattern of soil CO_2 emissions agreed closely with field observations (fig. 2.5 c). Model was capable of simulating the changes of emissions connected with manure amendment and definitive water removal. A comparison of measured and modeled CO_2 rates showed that DNDC well simulated the magnitude of emissions during fallow period, while it generally overestimated daily fluxes in presence of the crop, mainly during flooding time along the growing crop season.

Only when water was drained from field, measured flux surpassed model estimate; model simulates the increase of CO_2 emissions connected to the renewal of aerobic decomposition but it could not predict the emission increases which could be caused by rapid mineralization of weed and aquatic plant residues.

Throughout the growing season the pattern of simulated CH_4 emissions was similar to field observations even if a delay in emission times of estimated values, compared with those measured, was revealed (fig. 2.5 a).

Model simulation capacity for N_2O emissions was poor; DNDC simulated zero N_2O emissions during the flooding period, while we observed values ranging between 0 and 0.8 g $N\text{-}N_2O$ $ha^{-1}d^{-1}$ (fig. 2.5 b). The influence of the rhizosphere on the ecological drivers is not yet incorporated in DNDC, so the model simulates flooded anoxic soil with very suppressed rates of nitrification, leading to zero N_2O emissions in continuously flooded rice fields.

Model was capable of simulating the increase of emissions connected with manure amendment, but not of predicting the enhance of N_2O connected with water removing.

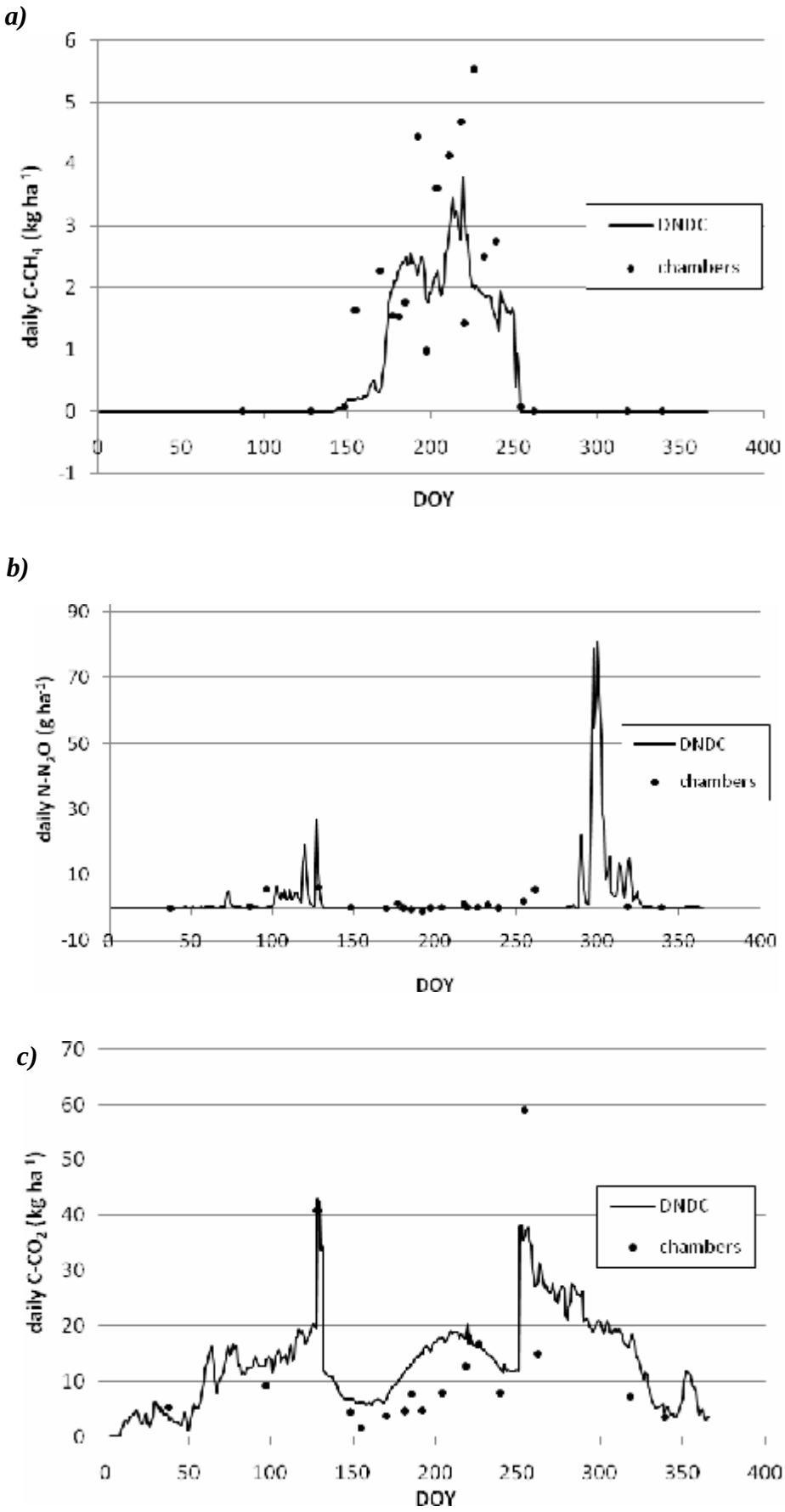

Figure 2.5 Modelled and measured CH_4 (a), N_2O (b) and CO_2 (c) emissions.

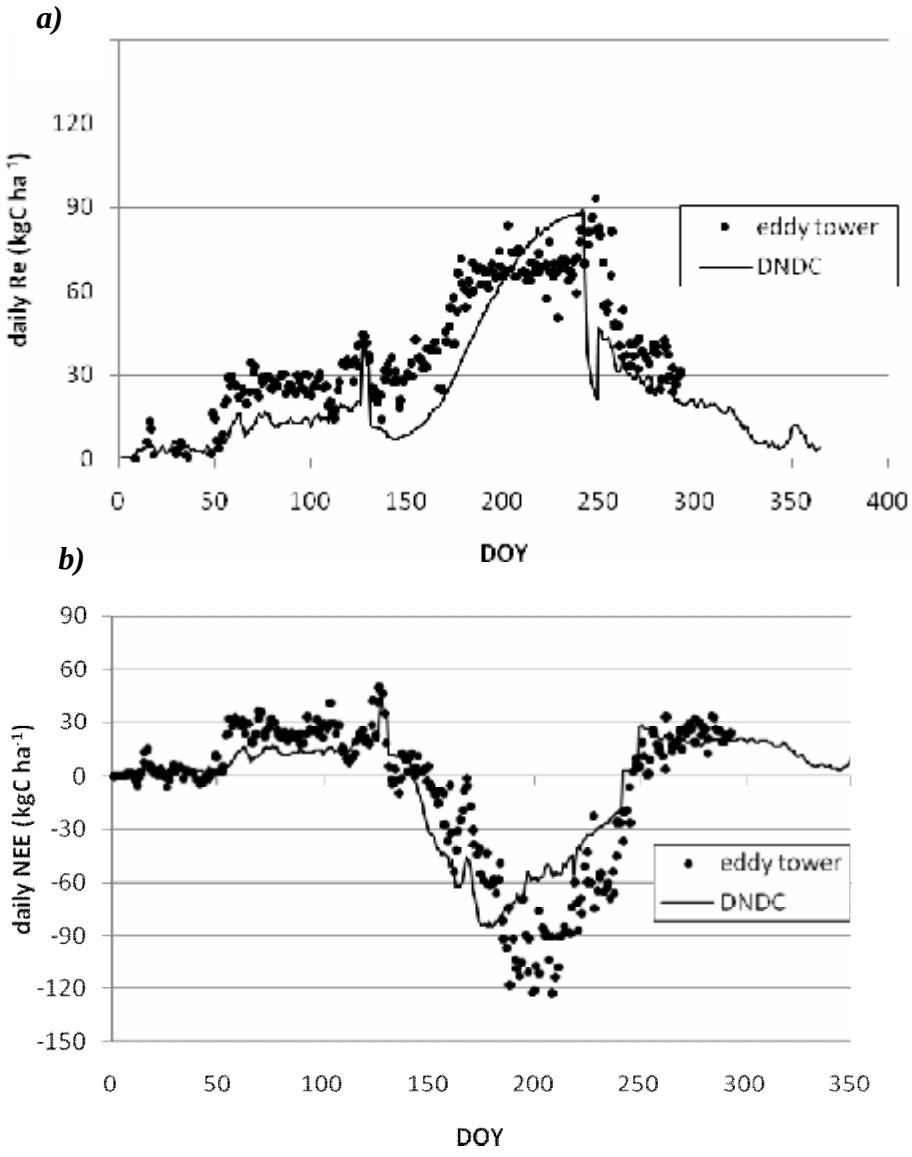

Figure 2.6 Modelled and measured ecosystem respiration-Re (a) and net ecosystem exchange-NEE (b).

About ecosystem data, the agreement between daily observed and simulated values was good considering the fallow period, while major differences were found principally along the crop season.

Discrepancies between predicted and observed values in correspondence of cropping season and therefore in presence of rice plants were also found for soil CO_2 and CH_4 emissions; the empirical approach used for simulating crop growth, on the base of cumulative

temperature, optimum crop biomass, N stress, and water stress at a daily time step, might not be enough.
Annual gas emissions obtained by model simulation were comparable with those obtained by the estimates from field data (table 2.2). The major discrepancy was observed for N_2O emissions, mainly due to the high peak (maximum 81.0 g $N\text{-}N_2O$ $ha^{-1}d^{-1}$) simulated by model after the harvest, for which no field data were available.
Every 3-4 years, rice cultivation is substituted by silage maize cropping. Once tested the DNDC efficiency in simulating site emissions, the model was then applied to estimate gas efflux and compare, in terms of climate forcing, the two different managements.
For the maize-simulation year, climate and soil input data were maintained. The corn management system consisted in ploughing during winter time; the sowing was carried out on 16th April, preceded by N-fertilization (105 kg ha^{-1} of 18/46 fertilizer and 280 kg N ha^{-1} of anhydrous ammonia). Weeding and manure amendment were carried out on May. Three irrigations were carried out on June 29th, July 16th, July 30th with about 800–900 m^3 ha^{-1} each. Corn for silage was harvested on September 23rd.
In terms of CO_2 equivalent, the soil gas emissions from rice were comparable with those from maize (table 2.3). The greater CO_2 and N_2O emissions from maize were counterbalanced by the high CH_4 emissions from rice paddy.

Table 2.3 Modelled soil gases emissions during rice and maize cropping (kg ha^{-1}).
Soil CO_2: heterotrophic respiration.

	$C\text{-}CH_4$	$N\text{-}N_2O$	$C\text{-}CO_2$	CO_2 eq
Rice	197	0.9	3614	19205
Maize	-1	3.6	5223	20876

2.4 CONCLUSION

Soil CH_4, CO_2 and N_2O effluxes, and ecosystem CO_2 exchange, were measured from a paddy soil over a year; the study provided estimates of CH_4 and N_2O emissions during both growing and fallow period. Production and emission of CH_4 largely occurred during the crop growing season, during soil saturation; annual CH_4 fluxes of 268 kg $C\text{-}CH_4$ ha^{-1} were measured, corresponding to 7504 kg CO_2-eq ha^{-1}.
The strong anaerobic conditions in the flooded soil limited N_2O production because of the complete denitrification processes to molecular nitrogen (N_2); N_2O emissions ranged between 0 and 3.4 µg $N\text{-}N_2O$ $m^{-2}h^{-1}$ during flooding and between 0.36 and 23 µg $N\text{-}N_2O$ $m^{-2}h^{-1}$ during fallow season. Annually integrated fluxes were 0.4 kg $N\text{-}N_2O$ ha^{-1}.
CO_2 seasonal trend and annual emission estimates were also obtained. Higher CO_2 emissions occurred in concomitance with the main management interventions; during the

flooding period, CO_2 emissions increased along the cropping growth season. The total CO_2 soil emissions were 1.13 kg CO_2 $m^{-2}y^{-1}$.

The DNDC process-oriented biogeochemical model was then tested against field data. The results indicated that DNDC model was capable of capturing quantitatively CH_4 and CO_2 production and emissions from investigated paddy soil. Model efficiency was high for CH_4 and CO_2 emissions (0.75 and 0.60 respectively) but low (0.01) for N_2O ones. There were some discrepancies between observed and simulated daily fluxes, above all during growing season, in presence of rice plants; for simulating crop growth, an empirical approach was selected: crop growth was calculated based on accumulative temperature, optimum crop biomass, N stress, and water stress at a daily time step. An application of process-based approach could improve the greenhouse gases estimates; if this approach, available in DNDC model is selected, crop development and growth are tracked by photosynthesis, respiration, and C allocation, based not only on the above listed environmental factors but also on several physiological or phenologic parameters, such as initial efficiency of use of absorbed light, maximum rate of leaf photosynthesis, rate of crop development in vegetative stage, rate of crop development in reproductive phase, and initial biomass at emergency.

In terms of CO_2 equivalent, the soil gas emissions from rice were comparable with those from maize.

DNDC model may represent a valid tool to simulate different management sceneries and guide to choose for the most efficient agricultural practice in terms of both climate forcing and crop productivity.

REFERENCES

- Abao, E.B., Bronson, K.F., Wassmann, R., Singh, U., 2000. Simultaneous records of methane and nitrous oxide emissions in rice-based cropping systems under rainfed conditions. Nutrient Cycling in Agroecosystems 58, 131–140.
- Akiyama, H., Yagi, K., Yan, X., 2005. Direct N_2O emissions from rice paddy fields: Summary of available data. Global Biogeochemical Cycles 19 GB 105.
- Aulakh, M.S., Bodenbender, J., Wassmann, R., Rennenberg, H., 2000a. Methane transport capacity of rice plants. I. Influence of CH_4 concentration and growth stage analyzed with an automated measuring system. Nutrient Cycling in Agroecosystems 70, 193-260.
- Aulakh, M.S., Bodenbender, J., Wassmann, R., Rennenberg, H., 2000b. Methane transport capacity of rice plants. II. Variations among different rice cultivars and relationship with morphological characteristics. Nutrient Cycling in Agroecosystems 91, 57-71.

- Aulakh, M.S., Wassmann, R., Rennenberg, H., 2002. Methane transport capacity of twenty-two rice cultivars from five major Asian rice-growing countries. Agriculture, Ecosystems & Environment, 91, 59-71.
- Baldocchi, D.D., Hicks, B.B., Meyers, T.P., 1988. Measuring biosphere–atmosphere exchange of biologically related gases with micrometeorological methods. Ecology 69, 1331–1340.
- Bouwman, A.F., Boumans, L.J.M., Batjes, N.H., 2002. Emissions of N_2O and NO from fertilized fields: Summary of available measurement data. Global Biogeochemical Cycles 16(4), 1058.
- Bronson, K.F., Neue, H., Singh, U., Abao, E.Jr., 1997. Automated chamber measurements of methane and nitrous oxide flux in a flooded rice soil. I. Residue, nitrogen, and water management. Soil Science Society of America Journal 61, 981–987.
- Cai, Z.C., Sawamoto, T., Li, C., Kang, G., Boonjawat, J., Mosier, A.R., Wassmann, R., Tsuruta, H., 2003. Field validation of the DNDC model for greenhouse gas emissions in East Asian cropping systems. Global Biogeochemical Cycles 17, 1107.
- Cai, Z.C., Xing, G.X., Shen, G.Y., Xu, H., Yan, X.Y., Tsuruta, H., Yagi, K., Minami K., 1999. Measurements of CH_4 and N_2O emissions from rice paddies in Fengqiu, China. Soil Science and Plant Nutrition 45, 1–13.
- Cicerone, R.J., Shetter, J.D., 1981. Sources of atmospheric methane: measurements in rice paddies and a discussion. Journal of Geophysical Research 86, 7203–7209.
- Flessa, H., Fischer, W.R., 1992. Plant-induced changes in the redox potentials of rice rhizospheres. Plant and Soil 143, 55–60.
- Jagadeesh Babu, Y., Li, C., Frolking, S., Nayak, D.R., Adhya, T.K., 2006. Field validation of DNDC model for methane and nitrous oxide emissions from rice-based production system of India. Nutrient Cycling in Agroecosystem 74, 157–174.
- Koizumi, H., Kibe, T., Mariko, S., Ohtsuka, T., Nakadai, T., Mo, W., Toda, H., Seiichi, N., Kobayashi, K., 2001. Effect of free-air CO_2 enrichment (FACE) on CO_2 exchange at the flood-water surface in a rice paddy field. New Phytologist 150, 231–239.
- Koizumi, H.,Kibe, T., Mariko, S., Ohtuka, T., Nakadai, T., Mo, W., Toda, H., Seiichi, N., Kobayashi, K., 2001. Effect of free-air CO2 enrichment (FACE) on CO_2 exchange at the flood-water surface in a rice paddy field. New Phytologist 150, 231-239
- IUSS/ISRIC/FAO, 2006. World Reference Base for Soil Resources. World Soil Resources Reports 103, FAO, Rome, pp. 128.
- Leip, A, Seufert, G., Bocchi, S., Conen, F., 2007. Measurements of greenhouse gas emissions from rice cultivation in Italy. 4th International Temperate Rice Conference 2007.

- Leip, A., 2000. Nitrous oxide (N_2O) emissions from a coastal catchment in the delta of the Po river: measurement and modeling of fluxes from a Mediterranean lagoon and agricultural soils, EUR 19052, Luxembourg: European Communities.
- Li, C.S., Frolking, S., Frolking, T.A., 1992. A model of nitrous oxide evolution from soil driven by rainfall events: I. Model structure and sensitivity. Journal of Geophysical Research 97, 9759–9776.
- Li, C., Frolking S., Harriss, R.C., 1994. Modeling carbon biogeochemistry in agricultural soils. Global Biogeochemical Cycles 8, 237–254.
- Li, C., Narayanan, V., Harriss, R.C., 1996. Model estimates of nitrous oxide emissions from agricultural lands in the United States. Global Biogeochemical Cycles 10, 297–306.
- Li, C., Zhuang, Y.H., Frolking, S., Galloway, J.N., Harriss, R.C., Moore, B., Schimel, D., Wang, X.K., 2003. Modeling soil organic carbon change in croplands of China. Ecological Applications 13, 327–336.
- Li, C., Mosier, A., Wassmann, R., Cai, Z., Zheng, X., Huang, Y., Tsuruta, J., Boonjawat, J., Lantin, R., 2004. Modeling greenhouse gas emissions from rice-based production systems: Sensitivity and upscaling. Global Biogeochemical Cycles, 18(1).
- Li, C., Frolking, S., Xiao, X., Moore III, B., Boles, S., Qiu, J., Huang, Y., Salas, W., Sass, R., 2005. Modeling impacts of farming management alternatives on CO_2, CH_4, and N_2O emissions: A case study for water management of rice. Global Biogeochemical Cycles 19.
- Lu, Y., Wassmann, R., Neue, H.U., Bueno, C.S., Huang, C., 2000. Methanogenic responses to exogenous substrates in anaerobic rice soils. Soil Biology and Biochemistry.
- Mayer, D.G., Butler, D.G., 1993. Statistical validation. Ecological Modelling 68, 21–32.
- Minoda, T., Kimura, M., 1994. Contribution of photosynthesized carbon to the methane emitted from paddy fields. Geophysical Research Letters 21, 2007–2010.
- Neue, H.U., 1993. Methane emission from rice fields. Biosciences 43, 466–474.
- Neue, H.U., Wassmann, R., Lantin, R.S., Alberto, M.C.R., Aduna, J.B., 1994. Effect of cultural practices on methane emission. International Rice Research Notes 19(3), 34–35.
- Raimbault, M., Rinaudo, G., Garcia, J.L., Boreau, M., 1977. A device to study metabolic gases in the rhizosphere. Soil Biology and Biochemistry 9, 193–196.
- Reddy, K.R., Patrick, W.H.Jr., 1984. Nitrogen transformation and loss in flooded soils and sediments. CRC Critical Reviews in Environmental Control 13, 273–309.
- Ren, X.E., Wang, Q.X., Tong, C.L., Wu, J.S., Wang, K.L., Zhu, Y.L., Lin, Z.J., Watanabe, M., Tang, G.Y., 2007. Estimation of soil respiration in a paddy ecosystem in the subtropical region of China. Chinese Science Bulletin 52(19), 2722–2730.
- Rennenberg, H., Wassmann, R., Papen, H., Seiler, W., 1992. Trace gas emission in rice cultivation. Ecological Bulletin 42, 164–173.

- Schmidt, J., Seiler, W., Conrad, R., 1988. Emission of nitrous oxide from temperate forest soils into the atmosphere, Journal of Atmospheric Chemistry 6, 95–115.
- Wang, B., Neue, H.U., Samonte, H.P., 1997. Effect of rice plant on seasonal methane emission patterns. Acta Agronomica Sinica 23, 271–279.
- Wang, B., Neue, H.U., Samonte, H.P., 1999. Factors controlling diel patterns of methane emission via rice. Nutrient Cycling in Agroecosystems 53, 229–235.
- Yu, K., Patrick, W.H.Jr., 2004. Redox window with minimum global warming potential contribution from rice soils. Soil Science Society of America Journal 68, 2086–2091.
- Yu, K.W., Wang, Z.P., Vermoesen, P., Patrick, W.H.Jr., Van Cleemput, O, 2001. Nitrous oxide and methane emissions from different soils suspensions: effect of soil redox status. Biology and Fertility of Soils 34, 25–30.
- Zheng, X.H., Wang, M.X., Wang, Y.S., Shen, R.X., Shangguan, X.J., Jin, J.S., Li, L.T., 1997. CH_4 and N_2O emissions from rice paddy fields in southeast China. Scientia Atmospherica Sinica 21, 231–237.

CHAPTER 3

GREENHOUSE GAS EMISSIONS AND MICROBIAL COMMUNITY CHARACTERIZATION BY PHOSPHOLIPID ANALYSIS IN A PADDY RICE SOIL

3.1 INTRODUCTION

Gaseous emissions of N and C from soil are essentially related to microbial activity, which comprises nitrification, denitrification, respiration, methanotrophy and methanogenesis.
A number of factors including temperature, soil water content, pH, redox potential and nutrient availability affect metabolic processes acting either on the enzyme activities or on the proliferation of particular soil microorganisms.
Paddy soils are complex ecosystems characterized by the simultaneous presence and by the alternation of those metabolic processes responsible for production and emissions of different greenhouse gases.
Submerged conditions are usually maintained throughout the growing season; when soils are flooded, the oxygen supply is greatly restricted, resulting in reductive soil environment under which CH_4 production is the final process in the anoxic microbial degradation pathway (Conrad, 1993).
The amount of CH_4 emitted depends on both production and oxidation processes (King, 1992). The overall CH_4 emissions are the result of the contemporary activity of methanogenic and methanotrophic bacteria. A substantial part of methane is consumed by methanotrophs (Reeburgh, 2003) that live in microsites within the rice field, as the shallow oxic layer at the soil water interface and at the surface of rice roots (Frenzel, 2000; Groot at al., 2003).
Rates of nitrification of NH_4 in rice fields, and subsequent denitrification can be substantial (Kirk, 2004). In general, conditions are sufficiently reducing and the availability of organic substrate sufficiently large that denitrification proceeds as far as N_2 is produced.

However, in the middle and at the end of the season, in which the soil is deliberately drained, oxygen can get into the soil profile; these conditions result in a drastic reduction of CH_4 production and are ideal for N_2O emissions.
Microbial community exhibits profound population shifts during the rice cropping cycle, related mainly to soil water content and to soil redox status (Bai et al., 2000; Reichardt et al., 2001; Andersen and Petersen, 2009). Although some changes in soil biological community composition can be characterized using microbial isolation procedures, it is estimated that less than 1% of soil bacteria are culturable using existing techniques (Kennedy, 1999). Alternative approaches and culture independent techniques, based upon structural component analysis, have been developed to characterize changes in soil community diversity (Kennedy and Gewin, 1997) such as fatty acid-based methods (methyl ester (FAME) analysis and phospholipid fatty acid (PLFA) analysis), and PCR-based methods (Øvreas, 2000).
With the DNA approach, total soil DNA is extracted and analyzed for specific marker gene pools with a combination of specific PCR and restriction fragment length polymorphism (RFLP) analyses (Pace, 1996; Widmer et al., 1999). With the fatty acid approach, the total soil fatty acid fraction is obtained and quantitatively analyzed by gas chromatography (GC) and mass spectrometry (MS) (Ratledge and Wilkinson, 1988; Ritchie et al., 2000; Zelles and Bai, 1993; Laczkò et al., 1997).
Fatty acid-based methods such as FAME, PLFA and DNA-based methods can provide insights into microbial community composition at different scales. Fatty acid profiles reflect the general microbial community composition and are quantitative but provide no information on species composition. DNA-based methods have the advantage that the target community (kingdom, species, genes) can be selected. However, they are not quantitative and DNA can also be bound to soil particles (Cai et al., 2006) where it is protected against microbial decomposition. Therefore, DGGE profiles may also include bands from dead organisms.
In this study, we focused the attention on the characterization of microbial community composition in a paddy rice at eight sampling dates during 2008, representative of different soil conditions and crop stages and consequently characterized by distinct soil greenhouse emission rates (see chapter 2).
Microbial community structure was characterized by phospholipid fatty acid analysis (PLFA), and microbiological data were consequently correlated with gaseous emissions.
Phospholipid fatty acids (PLFA) are essential membrane components, and their polar head groups and ester-linked side chains (i.e. FAs) vary in composition between eukaryotes and prokaryotes, as well as among many prokaryotic groups. They are not found in storage products or in dead cells because they are rapidly degraded (Pinkart et al., 2002), making them good indicators of living organisms (White et al., 1979).
Under the conditions expected in natural occurring communities, phospholipids make up a relatively constant proportion of the organisms' biomass, so the sum of all detectable PLFAs is used as an indicator for the total microbial biomass (Lechevalier, 1989). Of the available non–nucleic acid biomarkers, perhaps the PLFAs provide the richest insights into community composition. These insights derive from the fact that various taxonomic

microbial groups synthesize PLFAs of distinctive architecture. Furthermore, PLFAs can also reveal information about the general in situ physiological status of the cells. This concept relies on the observation that bacteria can change their membrane fluidity by modifying their membrane PLFA to adapt to various stimuli. These changes have been found among other causes in response to drought, temperature changes, osmotic stress, starvation and membrane-active substances.
The PLFA community fingerprinting can be used to study changes in community composition in a variety of habitats such as soils, aquifers, lakes, marine sediments and activated sludges among others.
The chemical character of the linkages of the side chains with the glycerol backbone in the phospholipid molecule can give important information about the taxonomical grouping of microorganisms. Ester linkages predominate in aerobic organisms, and amino and ether linkages in anaerobic organisms (monoalkyl) while diether and tetraether compounds were mainly found in domain Archaea, including the methanogens (Kates, 1978).

3.2 MATERIALS AND METHODS

3.2.1 STUDY SITE AND MANAGEMENT PRACTICE

The study area (about 3 hectares) is located in the Po plain (Castellaro de' Giorgi, Lombardy) and is characterized by the presence of rice crop, in rotation with maize (3-4 years rice and 1 year maize).
In order to well characterize the soil properties near gas monitoring points, two pedological profiles (minipit) were opened, described and sampled; the soil samples were taken from the soil horizons for chemical and physical determination (table 3.1).

Table 3.1 Soil chemical and physical properties.

	depth (cm)	OC%	N%	pH	texture
Minipit A					
Apg	0-27	2.8	0.30	7.2	SiL
Bkg	27-48	0.7	0.05	8.4	SiL
Cg	48-120	0.3	0.03	7.6	SL
Minipit B					
Apg	0-28	2.9	0.26	6.8	L
Abg	28-42	3.6	0.27	7.4	CL
Cg1	42-50	0.6	0.05	7.9	CSiL
Cg2	50-65	0.4	0.05	7.9	CSiL
Cg3	65-135	0.4	0.03	8.2	SL

According to the classification system of the World Reference Base (IUSS/ISRIC/FAO, 2006), soils are: Calcic Gleysol (Siltic) and Haplic Gleysol (Calcaric, Humic).
The surface nitrogen content (Ap) is between 0.26 and 0.30%, while surface organic carbon content is 2.8%. The high carbon content is due to a high intensity of accumulation of

organic material; the experimental site is often characterized by surface water excesses and thus the decomposition rate is low; the reduced soil permeability, due to tillage and agricultural practices for rice, causes surface water excesses and poorly drainage also during fallow period.
The soil was prepared for the sowing through a 30 cm-depth ploughing, carried out on February 28th. On May 7th, the manure amendment (16 t ha^{-1} of sugar-beet industrial slops, C/N of 6.4) was distributed on the soil surface and, a few days after, incorporated into the soil through a seed-bed harrow (10 cm depth). The field was leveled and then submerged to prepare sowing; the sowing was carried out in water on May 12th.
The flooding conditions (about 12 cm) were maintained until the distribution of herbicide for weed control, which was carried out on saturated and partially submerged soil on June 11th. The flooding was established again 2-3 days after the distribution and continuously maintained until September 5th. On July 1st, at panicle initiation stage, N fertilization was top-dressed (15 kg ha^{-1} N-NH_3 and 24 kg N_{ureic} ha$^{-1)}$. The crop was harvested on October 17th.
Details about study site and soil characteristics can be found in chapter 1.

3.2.2 GAS SAMPLING

Soil gas emission measurements were performed at two plots (plot 1 and plot 2 of A area, see chapter 2) placed in the middle of the field.
Each plot, 4 meters spaced out, were composed by two measuring points for N_2O and CH_4 fluxes and three points for CO_2 emissions.
For the measurement of N_2O and CH_4 soil fluxes, we used cylindrical chambers of 40 cm diameter which were covered by a Perspex lid and laterally by Teflon foil. The height of chambers was adapted with the proceeding growth season according to the plant heights. We left the chambers closed for 1 hour taking a gas sample every 20 minutes; during the flooding period, as the observed flux rates were high for CH_4 and low for N_2O, we left the chambers closed for 1.5 hour taking a gas sample immediately after closing the chamber, and after 15, 30, and 90 minutes. Unless we observed a zero flux rate, only the measurements with linearity were used.
Gas samples analyses were done with a Shimadzu GC 14B gas chromatograph provided with a 6- port valve to interface with the injection system and a Porapak Q column (2 m x 1/8" x 2 mm SS, 80/100 mesh, Chrompack). Gases were detected with an ECD (N_2O) and an FID (CH_4) (both Shimadzu), mounted in series. The gas chromatographic peaks were evaluated with the software Chrom-Card (CE Instruments, UK). Calibration was done by means of a standard mixture of N_2O and CH_4 in nitrogen, which has been calibrated with a standard mixture (Messer) using a second gas chromatograph.
CO_2 soil fluxes were measured with a portable infrared gas analyzer equipped with a chamber based on the principle of closed dynamic systems (PP-Systems, Hitchin, UK). At each sampling point, a single measurement was performed.
For each gas type, the measurements from points belonging to the same plot were averaged to give soil flux rate.

The analysis presented in this paper is limited to flux data measured at the eight dates in which soil samplings for microbial community study were carried out.
For the overall overview of annual gas emissions and for details about gas sampling method and procedure see chapter 2.

3.2.3 SOIL SAMPLING

Soil sampling was carried out through coring, around the monitoring points of greenhouse gases.
Sampled soils were taken in 8 dates, representative of different soil conditions: the first sampling on February 7th; the second sampling at early spring, on April 7th; the third and the fourth sampling after sowing, before and after weeding practice, on May 28th and June 19th, respectively; the fifth and the sixth samplings were carried out on July 16th (at stem elongation) and on August 6th (at flowering stage), respectively, during flooding period; the seventh sampling, in no flooding conditions, on September 11th at ripening; and the last sampling was carried out after harvest, on November 14th.
With regard to no-flooding period, in the second and in the seventh sampling dates oxic soils prevailed, while in the first and in the last samplings soils were mainly waterlogged due to rainy events and covered by rice straws (4-months old straws for the winter date while fresh residues at the autumn date).
Since the soil sampling causes a disturbance to the natural soil properties we divided each plot area in 30 sub-areas of 2500 cm^2, so that only one sampling was done inside them; we did 3 repetitions and sampled at two depths, 0-15 cm and down the profile to 30 cm, which is the lower boundary of soil tillage.

3.2.4 SOIL PHYSICAL AND CHEMICAL ANALYSES

For each sampling date, nitrate and ammonium contents were determined with ionic chromatography and with indophenol blue method, respectively (Keeney and Nelson, 1982).
The soil samples taken from minipit were air-dried and sieved (2 mm mesh). Soil pH was determined potentiometrically in a soil-to-solution (water and KCl 1N) ratio of 1:2.5. Organic carbon and nitrogen was measured using Thermo Fisher Scientific CN elemental analyzer and soil texture was determined with the method of sedimentation after sieving.

3.2.5 ANCILLARY MEASUREMENTS

For each date, simultaneously with soil fluxes (CO_2, N_2O, CH_4), soil temperature and soil water content were measured; soil temperature was determined with the built-in temperature probes of the CO_2 analyzer, at 5 cm depth, while soil water content was determined gravimetrically for each plot on a bulk sample at 0-15 and 15-30 cm depths and converted to water filled pore space (WFPS).
The soil redox potential was measured in the field using a portable pH/millivolt (mV) meter; the platinum electrode was pushed in the waterlogged soil at the surface; allowing the reading became stable, the voltage was recorded. For the depth layer (15-30 cm), the re-

dox measurements were immediately carried out on sampled soils; since soil exposure to air allows oxidation to occur, electrode was inserted below the oxided surface.

3.2.6 PLFA ANALYSIS

3.2.6.1 Lipid Extraction

Soil samples were frozen and stored at -20 °C. Total FAs were extracted from 4 g of soil in a one-phase mixture of chloroform methanol and citrate buffer (1:2:0.8 v/v/v). After extraction, the lipids were separated into neutral lipids, glycolipids, and polar lipids (phospholipids) on a silicic acid column by elution with chloroform, acetone and methanol, respectively. Two replicates for each samples were done.

3.2.6.2 Determination and identification of Phospholipid Fatty acids (PLFA)

In figure 3.1 the working scheme for PLFA analyses is reported. The phospholipids were transesterified by a mild alkaline methanolysis. The fatty acid methyl esters were detected on a Hewlett-Packard 6890 gas chromatograph equipped with a flame ionization detector. The column used was a HP 5 (50 m x 0.20 mm x 0.33 µm) capillary column. Helium was used as the carrier gas. The temperature of the injector and detector were 280 and 350 °C, respectively. Samples (1 µl) were injected in the splitless mode. An initial oven temperature of 70 °C was maintained for 2 min, then raised to 160 °C at 30 °C min^{-1} and then increased to the final temperature of 280 °C at 3° C min^{-1} for 15 min. The identification of fatty acid methyl esters was based on comparison with chromatograms of fatty acid methyl esters standard compounds (Bacterial Acid Methyl Esters Mix from Supelco and on structural analysis verified by gas chromatography mass spectrometry as described by Fay and Richli (1991) and Spitzer (1997).

3.2.6.3 Fatty Acid Nomenclature

The biomass of groups such as gram-negative bacteria, gram-positive bacteria, actinomycetes, fungi and other soil organisms can be estimated by determining the concentration of so-called signature fatty acids (White, 1993; White et al., 1996) (table 3.2). The fatty acid nomenclature is as follows: total number of carbon atoms: number of double bonds, followed by the position of the double bond from the methyl end of the molecule. Anteiso and iso branching are designated by the prefix a or i. 10Me is a methyl group on the tenth carbon atom from the carboxyl end of the molecule. Cy indicates cyclopropane fatty acids.

3.2.6.4 STATISTICAL ANALYSES

Statistical analyses were performed using the Statistica software (version 7). The mol% and the nmol g^{-1} dm of individual fatty acids were interpreted using principal component analyses (PCA) to elucidate variation patterns and to investigate correlation with gas fluxes, respectively. Moreover, the biomass data were subjected to analyses of variance (ANOVA).

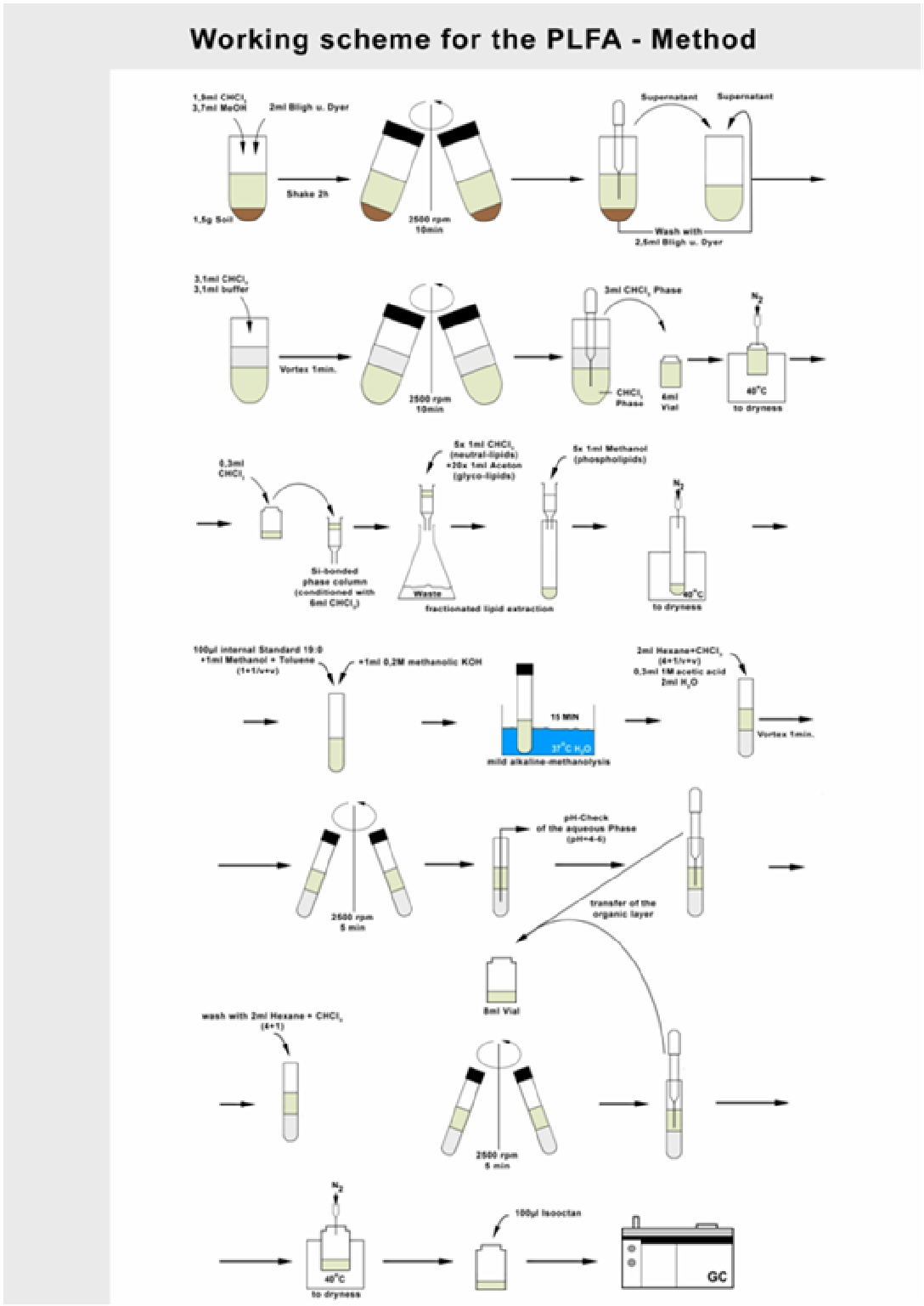

Figure 3.1 Working scheme for PLFA analysis (courtesy of M. Pfeffer - Federal Research and Training Centre for Forests, natural Hazards and Landascape – BFW).

Table 3.2 Fatty acids signature, based on Zak et al. (2000) and Olsson et al. (1997).

Signature of fatty acid		Signature of fatty acid	
i 14:0 i 15:0 a 15:0 i 16:0 i 17:0 a 17:0	Gram + bacteria (also in Gram- bacteria)	10Me 17:0 10Me 18:0	Actinomycetes (Gram +)
		10Me 16:0	Sulfate reducing bacteria (Gram +)
		16:1 (8)	type I methane oxiding bacteria (Gram -)
16:1 (9) cy 17:0 18:1 (11) cy 19:0	Gram - bacteria	18:1 (13)	type II methane oxiding bacteria (Gram -)
18:2 (9, 12)	Fungi	16:1 (11)	Arbuscular mycorrhiza
20:4 (5,8,11, 14)	Microeucaryotes	20:5 (5,8, 11, 14, 17)	Algae and Arbuscular mycorrhiza

3.3 RESULTS AND DISCUSSION

3.3.1 SOIL FLUXES

In figure 3.3 CO_2, CH_4 and N_2O emissions at the sampling dates are shown.

CH_4 fluxes between 411 and 20287 µg C-CH_4 $m^{-2}h^{-1}$ were measured throughout the rice-growing season. Smaller emissions occurred in absence of the rice crop, at the first and at the last sampling dates (6 µg C-CH_4 $m^{-2}h^{-1}$), when soils were covered by straw and were waterlogged due to rainy events. A slight CH_4 oxidation (-2.8 µg C-CH_4 $m^{-2}h^{-1}$) occurred at the second sampling date, at 48% WFPS. At this date, emissions of 36 µg N-N_2O $m^{-2}h^{-1}$ were measured; at the other dates, zero flux rates were measured or N_2O consumption was observed. Denitrification is the major sources for nitrous oxides and molecular nitrogen; it is a form of anaerobic respiration in bacteria which couples the stepwise reduction of nitrate oxides to electron transport with nitrite, nitric oxide, and nitrous oxide as intermediate products (Firestone and Davidson, 1989). Through flooding, conditions are sufficiently reducing and the availability of organic substances is sufficiently large so that denitrification can proceed to N_2; reducing conditions for appreciable N_2 production occur at WFPS above 80%.

As demonstrated by controlled laboratory experiment proposed by Schaufler et al., (submitted), for Castellaro site the N_2O emissions started at WFPS between 30 and 40% and increased with the soil moisture increase, reaching their maximum at about 50-60% WFPS; emissions decreased after 80% WFPS, probably due to the further reduction of N_2O to N_2. The soil moisture in the study site was generally very high: with the exclusion of two dates, characterized by 48 and 86% WFPS (April and September, respectively), the water content ranged between 33 and 100% WFPS (mean value 91±20%) (fig. 3.2). Therefore, we observed mainly a N_2O consumption rather than emission, resulting in a negative correlation (p value <0.05) between N_2O fluxes and soil water content (figure 3.6).

At the investigated sampling dates, CO_2 emissions ranged between 0.4 and 6.1 $\mu molm^{-2}s^{-1}$. The highest value was measured at the end of crop season, at ripening stage, immediately after water removing.

For the overall overview of annual gas emissions and for details about gas sampling method and procedure see chapter 2.

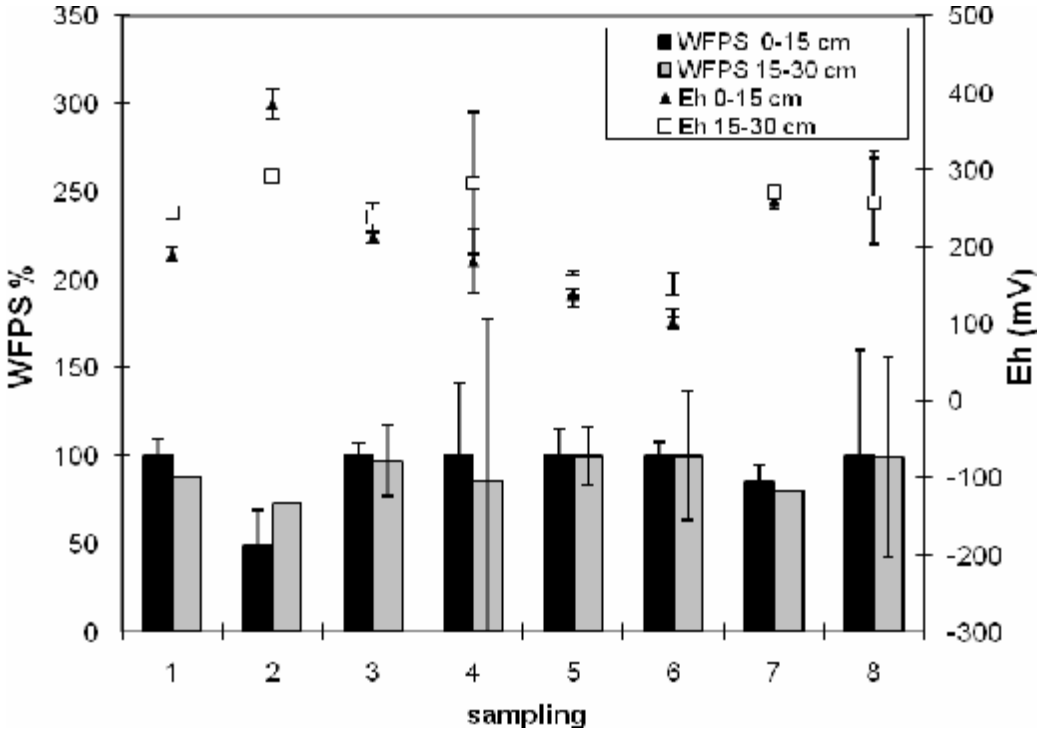

Figure 3.2 Water filled pore space (WFPS) and soil redox potential (Eh) at two depths (0-15 and 15-30 cm).

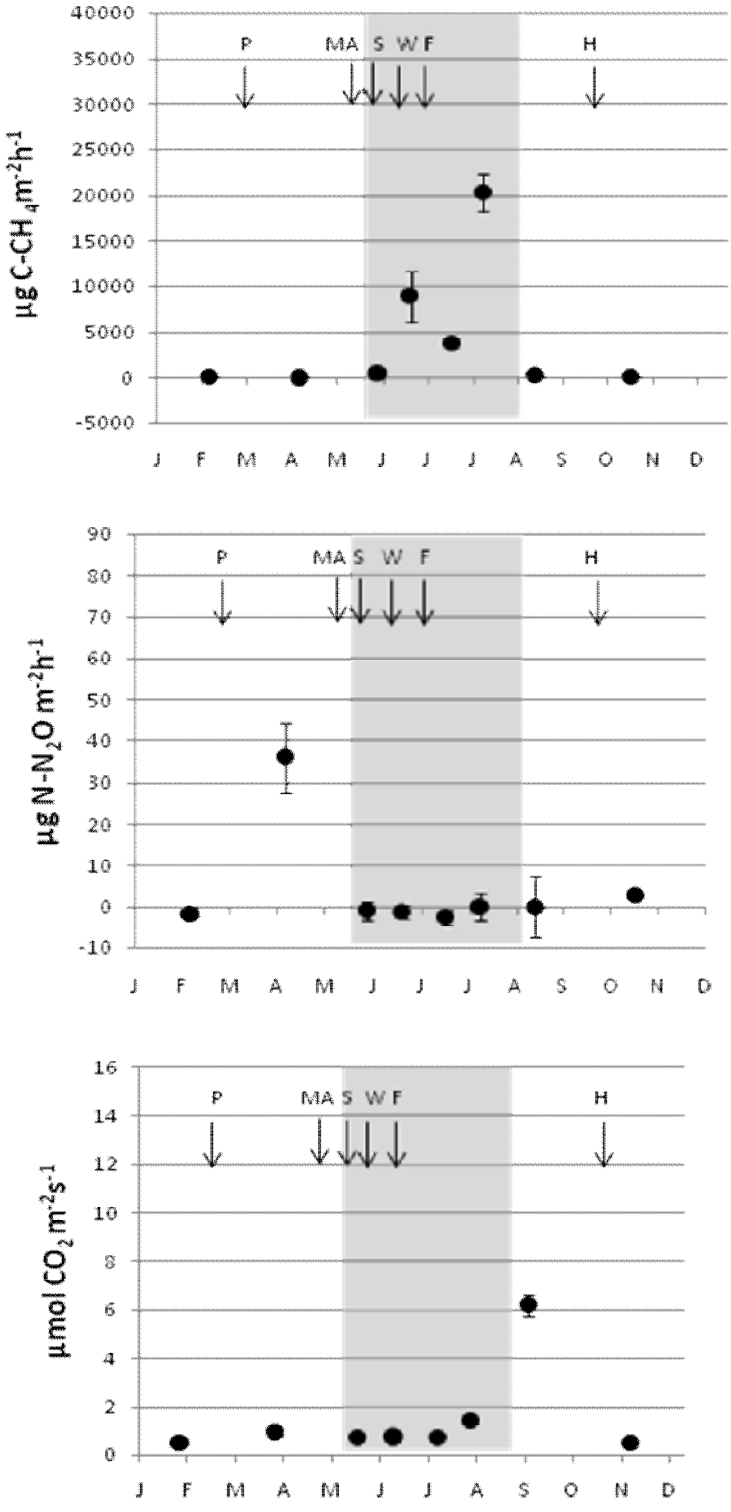

Figure 3.3 Fluxes of (a) CH_4, (b) N_2O and (c) CO_2. Vertical bars are SE. Arrows indicate management (P ploughing; MA manure amendment; S sowing; W weeding; F N-fertilization; H harvesting). Grey rectangles represent flooded period.

3.3.2 PLFA BIOMASS

Figure 3.4 show variation of microbial biomass expressed as nmol g^{-1} dm. The first column represents the weighed mean of the PLFA concentration down the profile to 30 cm. Microbial biomass decreased from 65 nmol g^{-1} dm in the winter sampling to 50 nmol g^{-1} dm in April, and increased again to the highest value in August (68 nmol g^{-1} dm), at the flowering stage; with the crop ripeness (September data sampling) the biomass was 53 nmol g^{-1} dm and increased after harvest to 59 nmol g^{-1} dm.

The lowest biomass was registered at the spring sampling, characterized by the lowest water content (48% WFPS), in absence of straws or rice plants; by ANOVA results, this sampling data and that done at the end of rice growth stage, significantly differed (p value <0.05) from the two samplings carried out at the end of the flooding period.

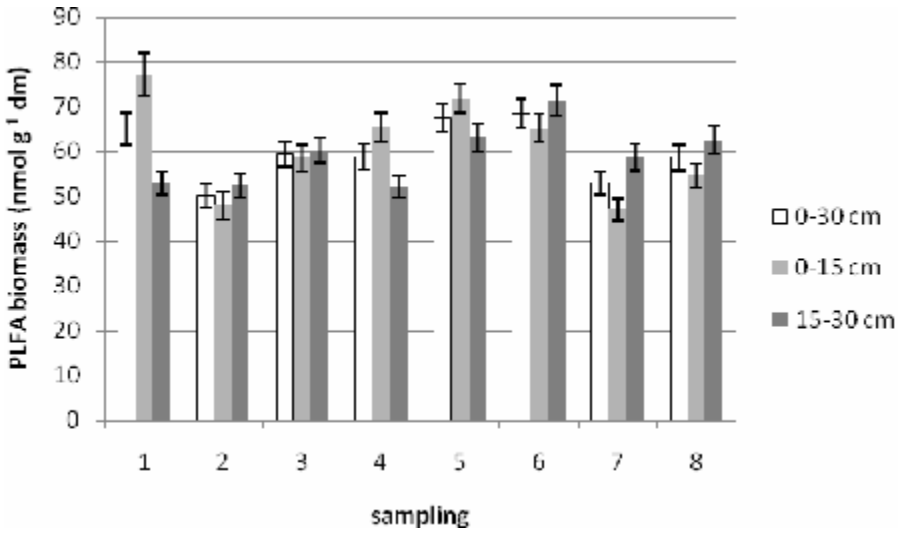

Figure 3.4 PLFA Biomass (nmol g^{-1} dm) data for the marked thicknesses.

A similar trend was obtained for the surface biomass (0-15 cm layer).

No significant differences (p value <0.05) between surface and subsurface biomass were found, with the only exception for the date February 1th, in which the surface PLFA concentration was 77 nmol g^{-1} dm, compared to 53 nmol g^{-1} dm in the deeper layer.

3.3.3 COMMUNITY STRUCTURE

3.3.3.1 Surface Layer (0-15 cm)

Patterns of PLFAs were analyzed for characterization of microbial community composition; single identified fatty acids and their aggregation into microbial groups are shown in table 3.3.

Principal component analysis was carried out to the mol% of single fatty acid values obtained from the first surface layer, comparing the community structure at each investigated

sampling date. As shown in figure 3.5, 91% of the total variance was explained by the first three factors.

Table 3.3 Microbial abundance (mol%) of Gram-positive bacteria, Gram-negative bacteria, fungi, actinomycetes, arbuscular mycorrhiza, microeucaryotes (CH_4ox: methane oxiding bacteria). The asterisk denotes a significant difference between layers.

sampling	cm	Gram+			Gram-			Fungi	Arb.Myc.	MicrEuc
		Gram+	Actino	Tot Gram+	Gram-	CH_4ox	Tot Gram-			
1	0-15	22±0.5 *	23±0.8	45±1.2 *	43±1.4 *	1.8±0.1	45±1.3	3.5±0.1 *	5.5±0.0 *	0.7±0.4 *
	15-30	37±0.9	25±1.9	62±1.0	37±0.6	1.5±0.4	38±0.2	2.9±0.3	5.1±0.4	1.0±0.2
2	0-15	24±0.0 *	19±0.0 *	43±0.0 *	41±0.0 *	2.4±0.0 *	43±0.0	6.2±0.0 *	5.3±0.0	1.2±0.0 *
	15-30	36±1,3	25±0,8	61±2,1	35±1,3	0,9±0,5	36±1,6	3,8±0,4	4,7±0,1	0,3±0,0
3	0-15	38±1,2	21±0,6	59±1,4	32±1,0	2,0±0,1	34±1,0	2,6±0,2	4,3±0,2	0,6±0,0
	15-30	37±5,3	21±2,9	58±2,5	32±2,3	2,0±0,2	34±2,4	2,6±0,4	4,6±0,4	0,6±0,2
4	0-15	40±0,6	22±0,2	62±0,7	29±0,5	1,8±0,3	31±0,2	3,2±1,3	4,1±0,6	0,5±0,2
	15-30	36±1.4	24±1.1	60±0.4	30±0.2	1.8±0.3	32±0.3	3.3±0.2	4.2±0.4	0.5±0.1
5	0-15	38±3.2	20±0.5	58±3.6	29±1.0	1.8±0.1	31±1.0	5.1±2.3 *	3.9±0.2	0.9±0.4
	15-30	37±1.0	24±2.8	61±2.0	29±1.6	1.6±0.1	31±1.6	4.2±0.6	4.1±0.5	0.7±0.2
6	0-15	39±1.4	22±1.3	61±2.1	29±0.6	1.8±0.0	31±0.7	3.6±1.2	3.8±0.3	0.6±0.3
	15-30	37±1.1	25±3.3	62±2.4	28±2.0	1.8±0.4	30±1.6	3.8±0.7	4.0±0.4	0.5±0.0
7	0-15	37±1.8	23±2.1	60±1.4	31±0.9	2.0±0.2	33±0.9	2.1±0.2	4.4±0.6	0.4±0,0
	15-30	39±1.3	22±1.6	61±0.7	31±0.4	1.9±0.3	33±0.6	2.3±0.4	4.2±0.0	0.3±0.2
8	0-15	38±3.5	16±8.0	54±4.8	34±3.0	2.0±0.6	36±3.5	3.6±0.6	5.1±1.0	0.7±0.1
	15-30	38±1.1	23±0.3	61±1.4	31±0.4	1.8±0.2	33±0.3	3.4±1.5	4.6±0.2	0.6±0.1

The results suggest that there was a shift of microbial community correlated with soil conditions and crop growth stage. Sampling done before the rice sowing clearly differed from the others. With regard to the crop period, the early growth stage, characterized by weeding practice, showed PLFA composition slightly different from those of the following two samplings, carried out in stable waterlogged conditions; for these samplings and for the

remaining two last dates, a progressive shift in the PLFA pattern occurred along the third component.

By the loadings values it is evident that the fatty acids 18:1(11), cy17:0, common in Gram-negative bacteria (O'Leary et al., 1988, Zelles, 1999), 10Me18:0, biomarkers of actinomycetes (Kroppenstedt, 1985), 18:2(9,12) and 20:4(5,8,11,14) indicative of fungi and microeucaryotes respectively, were most important for characterization of aerobic and drier conditions of April. On the contrary, flooded conditions showed the lowest relative abundances of such fatty acids but the highest abundances of the saturated fatty acids a15:0, i15:0, i14:0, typically present in Gram-positive bacteria (Brennan, 1988; Haack et al., 1994) and of 10Me17:0 and 10Me16:0, methylbranched fatty acids indicating actinomycetes (Kroppenstedt, 1985; Brennan, 1988; Zelles et al., 1994). The methylbranched 10Me16:0 is a specific biomarker of sulfate reducer bacteria. As shown by flux data, in these anoxic conditions methane production occur; archaebacteria, such as methanogens, cannot be monitored with PLFA analysis, which can detect only ester-linked and no ether-linked lipids. However, it is possible to hypothesize the presence of methanogens by using the biomarker of sulfate reducers since in wetland soils and sediments methane production interact with sulfate reduction (Lovely and Phillips, 1987). Moreover, since the contribution in rice fields of hydrogenotrophic methanogenesis to total CH_4 production is close to the expected ratio of a third or less (Rothfuss and Conrad, 1993; Bilek et al., 1999; Conrad and Klose, 2000), it may be possible that these two anaerobic groups coexist.

The ratio between Gram-positive and Gram-negative bacteria was higher in flooded (1.89-1.99) than in un-flooded (0.99-1.81) soil, suggesting that waterlogged soil contained higher proportion of Gram-positive bacteria, probably connected to the fact that this group include many k-strategists which can survive over long period in soil under harsh conditions.

Despite the fact that fungi were observed to decrease with soil submersion (Bossio and Scow, 1998), after the absolute maximum (6%) registered in April, the fungal PLFA showed a further increase to 5% during the flooding period around the half of June, corresponding to the stem elongation stage (table 3.3).

With water removing it was observed, marked after the harvest, a shift in the FAs composition towards an increase of some biomarkers present in Gram-negative (18:1(11), 16:1(9)) and of arbuscular mycorrhiza (16:1(11)). At the last sampling date, soil was saturated, due to rainy events (100% WFPS), but soil surface was covered by straw. It is known that Gram-negative bacteria include many r-strategists, which are important for the decomposition of fresh material; as shown across a wide variety of soil types and environmental conditions, the monounsaturated group seems to be related to high substrate availability (Zelles et al., 1992; Bossio and Scow, 1998).

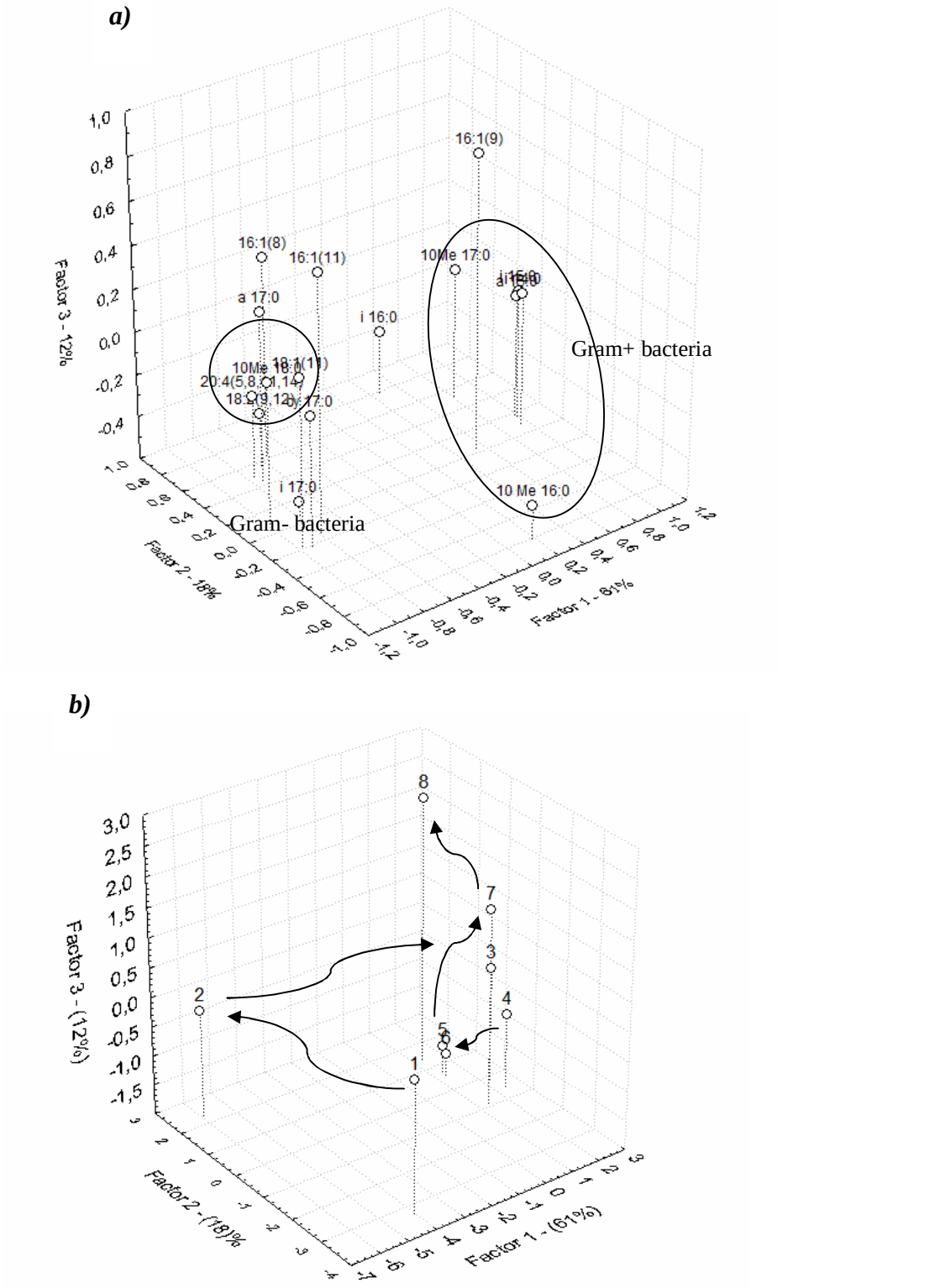

Figure 3.5 Loadings plot (a) and scores plot (b) of the PC Analysis of PLFAs. PCA variables: mol% of single fatty acids. PCA scores: sampling dates (1: 7th February; 2: 7th April; 3: 28th May; 4: 19th June; 5: 16th July; 6: 6th August; 7: 11th September; 8: 14th November).

The monounsaturated fatty acid 16:1(8), representing the specific group I methanotrophs (Bowman et al., 1993) was found in all the samples; its relative abundance was ranging between 1.8 and 2.4% (table 3.3) of the total PLFA. Shrestha and colleagues (2008) demonstrated that both type I and type II methanotrophs coexist in rice paddies even if they occupy different niches, with type I methanotrophs being more important in drained fields, where O_2 reaches deeper soil layers and type II methanotrophs being more important in flooded fields, where CH_4 availability is high. In addition, type I methanotrophs played a particularly important role in the rice field ecosystem and no 18:1(10), specific marker of type II methanotrophs, however, was found in any of our field samples.

3.3.3.2 Depth Layer (15-30 cm)

The change of community structure with soil depth was significant (p value <0.05) for the first sampling date, in relation to mol% of arbuscular mycorrhiza; for the second sampling date, in relation to mol% of CH_4 oxiding bacteria and actinomycetes, while of Gram-positive, Gram-negative, fungi and microeucaryotes for both dates; significant differences were found also between the proportional abundance of surface and subsurface of fungi at the fifth data, during flooding period (table 3.3).

As it was for the biomass, as well as for the community structure, little differences were found between surface and subsurface layers.

Generally, the amount soil microorganisms and the structure of microbial community vary spatially with depth, depending mainly on gradients in organic matter, texture, pH, temperature, and water availability (Fierer et al., 2003). Since the investigated thickness corresponded to the ploughed horizon, the organic carbon content, pH value and soil texture were quite constant (table 3.1). Moreover, also in relation to water content, statistical analysis revealed no significant differences between the two layers.

The agricultural practices, that include straw management or N-fertilizer and manure treatments, can temporarily affect and modify the surface nutrient availability, leading to a vertical separation and differentiation of microbial biomass and structure. Only the samplings, done before the rice sowing, seemed to show a clear distinction of community structure between upper and lower layers.

With regard to the first date, it should be noted that soil surface had been covered for all the winter time by rice straw; at this date, nitrate content in the 0-15 cm layer was particularly high (19.1 mg kg^{-1}), compared with that between 15 and 30 cm depth (6.2 mg kg^{-1}).

3.3.4 MICROBIAL COMMUNITY AND SOIL FLUXES

In figure 3.6 we report the results of the principal component analysis (PCA), carried out comparing the flux rates respective to soil and plant properties (redox potential, water content, nitrate and ammonium content, plant height) and to the concentration of single fatty acids. A total variance of 78% is explained by the first two factors. Aiming at investigating correlations with gas fluxes, the weighed mean of the PLFA concentrations down the profile to 30 cm was considered.

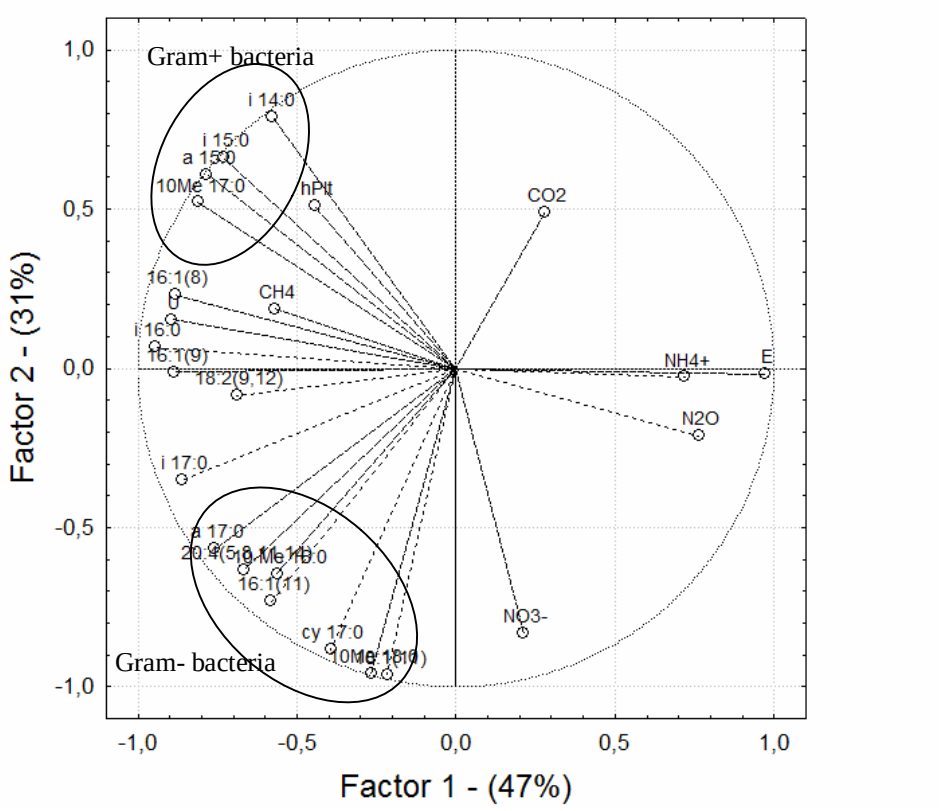

Figure 3.6 Loadings plot of the PCA analysis of PLFAs including soil parameters and plant height. PCA variables: nmol g^{-1} of single fatty acid; E: redox potential; U: soil water content; NO_3^-: nitrate; NH_4^+: ammonium; hPlt: plant height.

There was a balance between conditions favoring methanogenesis and those favoring nitrous oxide production: methane production was positively correlated with soil water content and inversely correlated with redox potential, while for N_2O fluxes the correlations were opposite.

The highest CH_4 fluxes occurred during waterlogged conditions in presence of rice plants. Such soil conditions were also favorable to the presence of type I methanotroph bacteria, as suggested by the increase of the 16:1(8) fatty acid; CH_4 oxidation became active, despite the flooded conditions, perhaps connected with the availability of O_2, coming through roots. The root O_2 availability could also explain the registered fungi increase, not only in term of relative abundances (see paragraph 3.3.3.1) but also in term of nmol g^{-1} of 18:2 (9, 12) fatty acid, in flooded sampling date and in particular at stem elongation. A stable isotope labeling experiment conducted in bulk and rhizosphere rice microcosms (Lu et al., 2007), identified the active microorganisms associated with the carbon dynamics and methane productions: they demonstrated that while some microbial groups were inactive in the wetland rice rhizosphere, others as eukaryotic microorganisms were active and incorporated high amounts of root derived C.

Looking at negative values of N_2O fluxes during the flooding period, we concluded that redox potential and water contents affected denitrification to N_2.

The 16:1(9) saturated fatty acid is the metabolic precursor of cyclopropane fatty acid (cy17:0), which mainly occurs among Gram negative bacteria, including denitrifying (Jantzen, 1984; Grogan and Cronan, 1997).
Although with the PLFA compositions the identification of a specific group, such as nitrifiers and denitrifiers, is not possible, it is known that the most of denitrifiers bacteria belong to the Gram negative group; in relation to this, we also observed a positively relation between the presence of cy17:0 and 18:1(11) fatty acids and nitrate contents. By PCA analysis, an apparently negative relation between CO_2 emissions and monitored fatty acids seems to occur. CO_2 fluxes were low and constant for all the monitored dates, with the only exception of one sampling date (on September 11th), immediately after a long period of flooding. At this date, an increase of emissions was observed; such an increase could be realistically connected with the restarting of soil aerobic conditions and the restarting of plant respiration activity, rather than with the change of microbial biomass, which moreover was one of the lowest monitored.

3.4 CONCLUSION

We studied microbial biomass and community structure in a rice paddy both during the crop growth season and the fallow period and we correlated these data with greenhouse gas fluxes.
Soil conditions and crop stages clearly affected microbial community biomass and structure as well as gaseous emissions of the rice field investigated.
A net change in the composition of the community structure at different sampling times was observed. The ratio between Gram-positive and Gram-negative bacteria was higher in flooded than in un-flooded soils. The saturated fatty acids, such as a15:0, i15:0, i14:0 and the methyl-branched fatty acids 10Me17:0 and 10Me16:0, typically present in Gram-positive bacteria, seemed to be a sensitive indicator of flooded and waterlogged conditions, which were favorable to the production and emission of methane as well as to the complete denitrification to N_2. On the contrary, Gram-negative bacteria were most important for characterization of aerobic and drier conditions and for the decomposition of fresh straw material. In terms of microbial processes, the increase of type I methanotroph bacteria (16:1(8)) during flooding, suggested that CH_4 oxidation was active. Moreover, the 16:1(9), cy17:0 and 18:1(11) fatty acids seemed to be correlated with N_2 production.
The vertical distribution of PLFAs was also investigated; the uniformity in organic C, pH, texture, total N, nitrate and water content of investigated thickness resulted in a vertical homogeneity of microbial biomass and of community composition. Only temporary variations of surface nutrient availability, due to agricultural practices, led to a distinction between microbial populations of the two investigated layers.
In summary, fatty acids composition of microorganisms revealed to be useful as they reflected the response of the microbial community to changes in soil conditions and as they also provided helpful information connected with flux dynamics of gases.

REFERENCES

- Andersen, A.J., Petersen, S.O., 2009. Effects of C and N availability and soil-water potential interactions on N_20 evolution and PLFA composition. Soil Biology and Biochemistry 41(8), 1726–1733.
- Bai, Q., Gattinger, A., Zelles, L., 2000. Characterisation of microbial consortia in paddy rice soil by phosholipid analysis. Microbial Ecology 39, 273–281.
- Batista, A., Vetter, W., Luckas, B., 2001. European Food Research and Technology 212, 377–384.
- Bilek, R.S., Tyler, S.C., Sass, R.L., Fisher, F.M., 1999. Differences in CH_4 oxidation and pathways of production between rice cultivars deduced from measurements of CH_4 flux and ^{13}C of CH_4 and CO_2. Global Biogeochemical Cycles 13, 1029–1044.
- Bossio, D.A., Scow, K.M., 1998. Impact of carbon and flooding on soil microbial communities: phosholipid fatty acid profiles and substrate utilization patterns. Microbial Ecology 35, 265–278.
- Bowman, J.P., Sly, L.I., Nichols, P.D., Hayward, A.C., 1993. Revised taxonomy of the methanotrophs: Description of Methylobacter gen. nov., emendation of Methylococcus, validation of Methylosinus and Methylocystis species, and a proposal that the family Methylococcaceae includes only the group I methanotrophs. International Journal of Systematic Bacteriology 43, 735–753.
- Brennan, P.J., 1988. Mycobacterium and other actinomycetes. In: Ratledge, C., Wilkinson, S.G. (eds.), Microbial Lipids, vol. 1. Academic Press, London, pp. 203–298.
- Cai, P., Huang, Q., Zhang, X., Chen, H., 2006. Adsorption of DNA on clay minerals and various colloidal particles from an alfisol. Soil Biology and Biochemistry 38, 471–476.
- Conrad, R., 1993. Mechanisms controlling methane emission from wetland rice fields. In: Oremland R.S. (ed.), The Biogeochemistry of Global Change: Radiative Trace Gases, Chapman and Hall, New York, pp. 317–335.
- Conrad, R., Klose, M., 2000. Selective inhibition of reactions involved in methanogenesis and fatty acid production on rice roots. FEMS Microbiology Ecology 34, 27–34.
- Fay, L., Richli, U., 1991. Location of double bonds in polyunsaturated fatty acids by gas chromatography—mass spectroscopy after 4,4-dimethyloxazoline derivatization. Journal of Chromatography A 541, 89–98.
- Fierer, N., Schimel, J.P., Holden, P.A., 2003. Variations in microbial community composition through two soil depth profiles. Soil Biology and Biochemistry 35, 167–176.
- Firestone, M.K., Davidson, E.A., 1989. Microbiological basis of NO and N_2O production and consumption in soil. In: Andreae, M.O. and Schimel D.S. (eds.), Exchange of Trace Gases between Terrestrial Ecosystems and the Atmosphere, Wiley, New York, pp. 7–21.
- Frenzel, P., 2000. Plant-associated methane oxidation in rice fields and wetlands: a review. Advances in Microbial Ecology 16, 85–114.

- Grogan, D.W., Cronan, J.E., 1997. Cyclopropane ring formation in membrane lipids of bacteria. Microbiology and Molecular Biology Reviews 61, 429–441.
- Groot, T.T., Van Bodegom, P.M., Harren, F.J.M., Meijer, H.A.J., 2003. Quantification of methane oxidation in the rice rhizosphere using ^{13}C-labelled methane. Biogeochemistry 64, 355–372.
- Haack, S.K., Garchow, H., Odelson, D.A., Forney, L.J. Klug, M.J., 1994. Accuracy, reproducibility and interpretation of fatty acid methyl ester profiles of model bacterial communities, Applied and Environmental Microbiology 60, 2483–2493.
- IUSS/ISRIC/FAO, 2006. World Reference Base for Soil Resources. World Soil Resources Reports 103, FAO, Rome, pp. 128.
- Jantzen, E, 1984. Analysis of cellular components in bacterial classification and diagnosis. In: Odham G, Larsson L, Mardh PA (eds.), Gas chromatography/mass spectrometry—applications in microbiology. Plenum, New York, pp. 257–302.
- Kates, M., Yengoyan, L.S., Sastry, P.S., 1965. A diether analogue of phosphatidyl glycerophosphate in Halobacterium cutirubrum. Biochimica et Biophysica Acta 98, 252–26.
- Kates, M., 1978. The phytanyl ether-linked polar lipids and isoprenoid neutral lipids of extremely halophilic bacteria. Progress in the Chemistry of Fats and Other Lipids 15, 301–342.
- Keeney, D.R., Nelson, D. W., 1982. Nitrogen-Inorganic forms. In Page, A.L., (ed.), Methods of soil analysis, part 2, Chemical and Microbiological Properties - American Society of Agronomy, pp. 643-698.
- Kennedy, A.C., Gewin, V.I., 1997. Soil microbial diversity: present and future considerations. Soil Science 162, 607–617.
- Kennedy, A.C., 1999. Bacterial diversity in agroecosystems. Agriculture Ecosystems and the Environment 74, 65–76.
- King, G.M., 1992. Ecological aspects of methane oxidation, a key determinant of global methane dynamics. Advances in Microbial Ecology 12, 431–468.
- Kirk, G., 2004. The Biogeochemistry of Submerged Soils. Wiley, Chichester, UK, pp. 291.
- Kroppenstedt, R.M., 1985. Fatty acids and menaquinone analysis of actinomycetes and related organisms. In: Goodfellow M. and Minnikin D.E. (eds.), Chemical Methods in Bacterial Systematics. Academic Press, London, pp. 173–199.
- Laczkò, E., Rudaz, A., Aragno, M., 1997. Diversity of antropogenically influenced or disturbed soil microbial communities. In: Insam, H., Rangger, A. (eds.), Microbial Communities - Functional versus Structural Approaches. Springer Verlag, Heidelberg, pp. 57–67.
- Lechevalier, M.P., 1989. Lipids in bacterial taxonomy. In: O'Leary W.M. (ed.), Practical handbook of microbiology. CRC, Boca Raton, Fla., pp. 455–561.
- Lovely, D.R., Phillips, E.P., 1987. Competitive mechanisms for inhibition of sulfate reduction and methane production in the zone of ferric iron reduction in sediments. Applied and Environmental Microbiology 53, 2636–2641.
- Lu, Y., Abraham, W.-R., Conrad, R., 2007. Spatial variation of active microbiota in the rice rhizosphere revealed by in situ stable isotope probing of phospholipid fatty acids. Environmental Microbiology 9, 474–481.
- NRCS, 2004. Soil Survey Laboratory Methods Manual. Soil Survey Investigations Report 42. USDA-NRCS, pp. 700.

- O'Leary, W.M., Wilkinson, S.G., 1988. Gram-positive bacteria. In: Ratledge C., Wilkinson S.G. (eds). Microbial lipids, vol 1. Academic Press, London, pp 117–202
- Olsson, P.A., Baath, E., Jakobsen, I., 1997. Phosphorus effects on the mycelium and storage structures of an arbuscular mycorrhizal fungus as studied in the soil and roots by analysis of fatty acid signatures. Applied and Environmental Microbiology 63, 3531–3538.
- Øvreas, L., 2000. Population and community level approaches for analyzing microbial diversity in natural environments. Ecology Letters 3, 236–251.
- Pace, N.R., 1996. New perspective on the natural microbial world: molecular microbial ecology. ASM News 62, 463–470.
- Pinkart, H.C., Ringelberg, D.B., Piceno, Y.M., Macnaughton, S.J., White, D.C., 2002. Biochemical approaches to biomass measurements and community structure analysis. In: Hurst, C.J., Crawford, R.L., Knudsen, G.R., McInerney, M.J., Stetzenbach, L.D. (eds.), Manual of Environmental Microbiology, 2nd edition. ASM Press, Washington, D.C., pp. 101–113.
- Ratledge, C., Wilkinson, S.G., 1988. Microbial Lipids, vol. 1. Academic Press, London.
- Reeburgh, W.S., 2003. Global methane biogeochemistry. In: Keeling R. F., Holland H. D., Turekian K. K. (eds.), Treatise on Geochemistry: The Atmosphere, vol. 4. Elsevier-Pergamon, Oxford, UK, pp. 65–89.
- Reichardt, W., Briones, A., de Jesus, R., Padre, B., 2001. Microbial population shifts in experimental rice systems. Applied Soil Ecology 17, 151–163.
- Ritchie, N.J., Schutter, M.E., Dick, R.P., Myrold, D.D., 2000. Use of length heterogeneity PCR and fatty acid methyl ester profiles to characterize microbial communities in soil. Applied and Environmental Microbiology 66, 1668–1675.
- Rothfuss, F., Conrad, R., 1993. Vertical profiles of CH_4 concentrations, dissolved substrates and processes involved in CH_4 production in a flooded italian rice field. Biogeochemistry 18, 137–152.
- Shrestha, M., Abraham, W.R., Shrestha, P.M., Noll, M., Conrad, R., 2008. Activity and composition of methanotrophic bacterial communities in planted rice soil studied by flux measurements, analyses of pmoA gene and stable isotope probing of phospholipid fatty acids. Environmental Microbiology 10, 400–412.
- Spitzer, V., 1997. Structure analysis of fatty acids by gas chromatography low resolution electron impact mass spectrometry of their 4,4-dimethyloxazoline derivatives: a review. Progress in Lipid Research 35, 387–408.
- White, D.C., 1993. In situ measurement of microbial biomass, community structure and nutritional status. Philosophical Transactions of the Royal Society of London, Series B, 344, 59–67.
- White, D.C., Davis, W.M., Nickels, J.S., King, J.D., Bobbie, R.J., 1979. Determination of the sedimentary microbial biomass by extractable lipid phosphate. Oecologia 40, 51–62.
- White, D.C., Stair, J.O., Ringelberg, D.B., 1996. Quantitative comparisons of in situ microbial biodiversity by signature biomarker analysis. Journal of Industrial Microbiology 17, 185–196.
- Widmer, F., Shaffer, B.T., Porteous, L.A., Seidler, R.J., 1999. Analysis of nifH gene pool complexity in soil and litter at a Douglas fir forest site in the Oregon Cascade Mountain Range. Applied and Environmental Microbiology 65, 374–380.

- Zak, D.R., Pregnitzer, K.S., Curtis, P.S., Holmes, W.E., 2000. Atmosperic CO_2 and the composition and function of soil microbial communities. Ecological Applications 10, 47–59.
- Zelles, L., Bai, Q.Y., Beck, T., Beese, F., 1992. Signature fatty acids in phospholipids and lipopolysaccharides as indicators of microbial biomass and community structure in agricultural soils. Soil Biology and Biochemistry 24, 317–323.
- Zelles, L., Bai, Q.Y., 1993. Fractionation of fatty acids derived from soil lipids by solid phase extraction and their quantitative analysis by GC-MS. Soil Biology and Biochemistry 25, 495–507.
- Zelles, L., Bai, Q.Y., Ma, R.X., Rackwitz, R., Winter, K., Beese, F., 1994. Microbial biomass, metabolic activity and nutritional status determined from fatty acid patterns and poly-hydroxybutyrate in agriculturally managed soils. Soil Biology and Biochemistry 26, 439–446.
- Zelles, L., 1999. Fatty acid patterns of phospholipids and lipopolysaccharides in the characterisation of microbial communities in soil: a review. Biology and Fertility of Soils 29, 111–129.

CHAPTER 4

TOTAL SOIL CO_2 FLUXES AND SEPARATING OF HETEROTROPHIC AND AUTOTROPHIC RESPIRATION OF A FOREST ECOSYSTEM

4.1 INTRODUCTION

Soil is the major organic carbon pool in terrestrial ecosystems (Schlesinger and Andrews, 2000); it contains larger amount of organic carbon (1500 Pg C) than both terrestrial vegetation (550 Pg C) and the atmosphere (780 Pg C) (Houghton, 2003).

Soils contribute to the carbon budget by acting also as sources; soil respiration is estimated to be within the range of 64–72 Gt C y-1, accounting for the 20-40% of annual input of CO_2–C from terrestrial and marine sources, to the atmosphere (Houghton and Woodwell, 1989; Raich and Schlesinger, 1992). Particularly, forests have been estimated to contain up to 80% of all aboveground C and about 40% of all underground C (Dixon et al., 1994), so that little changes in C pools of such soils can significantly affect the global C cycle.

Several biotic and abiotic factors influence soil CO_2 production: soil temperature and moisture (Keith et al., 1997; Epron et al., 1999; Janssens et al., 1999; Law et al., 1999), soil organic matter quantity and quality (Taylor et al., 1989; Coûteau et al., 1995), root and microbial biomass, root nitrogen content (Ryan et al., 1996), soil acidity, texture and site productivity (Raich and Schlesinger, 1992; Raich and Potter, 1995).

Concerning roots, although many studies have suggested that root respiration significantly contributes to net CO_2 fluxes from soils (Raich and Schlesinger, 1992; Hendricks et al., 1993; Epron et al., 1999; Högberg et al., 2001; Cisneros-Dozal et al., 2006), estimates of such contribution is highly variable and reliable and reproducible quantification remain hard to define.

The contribution of root respiration has been estimated to be between 10 and 90% of the total net CO_2 flux, with an average of 48.6% and 36.7% for forest and non forest vegetation respectively (Hanson et al., 2000).

The total soil CO_2 efflux is the sum of heterotrophic and autotrophic respiration. Heterotrophic respiration includes CO_2 released during microbial decomposition of soil organic matter while autotrophic respiration includes all processes occurring in the rhizosphere

(CO_2 derived from the root metabolism and the activity of microorganisms in the rhizosphere) (Wiant, 1967).
The partitioning of soil respiration in its two components, as well as the knowledge of temperature dependence of each component, are relevant for the comprehension of the soil C balance, for the prediction of ecosystem response to climate change and for the understanding of the potential feedbacks of the global change on soil processes. Moreover, the quantification of the soil respiration components allows to separately enter the autotrophic and heterotrophic contributions into models (Bond-Lamberty et al., 2004).
Methods for the separation and quantification of root and microbial contributions to soil respiration can be direct and indirect.
Component integration, root exclusion and isotope labeling are direct methods (Hanson et al., 2000; Kuzyakov and Larinova, 2005).
With component integration, the CO_2 efflux from each component (litter, roots, sieved soil) is measured, multiplied by respective masses and summed; the obtained total soil respiration is compared with CO_2 efflux measurement done in situ and if they are in good agreement, the calculated component emissions are considered valid. Sometimes heterotrophic respiration is estimated by difference between total CO_2 flux and the other two component fluxes.
A major problem with this approach is that root respiration rates are only measured in vitro, and removal and separation of soil components represent significant soil disturbance particularly of the root–soil interface, altering the soil atmosphere, and often separating roots from most of their associated microbial community (Trumbore, 2006).
With the root exclusion, the root contribution is indirectly estimated by measuring soil respiration with and without roots. The main root exclusion techniques are: root removal (roots are removed, soil is placed back in situ and root growth is prevented by barriers), soil trenching (roots are severed, but not removed, and a barrier is installed to inhibit root growth) and gap analysis (aboveground vegetation is removed from an area in which soil respiration is measured and then compared to respiration rates of the nearby forested area).
The main problem associated with root exclusion methodologies for determining respiration is the soil disturbance, which is the change in soil humidity and the increase of heterotrophic decomposition connected to dead roots, affect CO_2 emissions; it needs to be taken into account or delayed measurements until after the system has returned to the equilibrium.
Compared to component integration and root exclusion methods, isotopic techniques allow partitioning of soil respiration in situ with no soil disturbances, but it presents considerable complexity in experimental setup and analytical measurements as well as it is certainly the most expensive. In isotopic method radioactive 14-C or stable 13-C can be used to estimate the relative contribution of root and soil organic decomposition to total soil respiration; this method can be classified as pulse (single or repeated) or as continuous labeling.
Non-invasive methods separate the total soil respiration into its two components by using regression analysis technique. Heterotrophic respiration is estimated from the y-intercept of the linear regression between CO_2 fluxes and root biomass (Kucera and Kirkam, 1971),

assuming that the CO_2 flux spatial variations are mainly due to spatial variation of root respiration while heterotrophic respiration is spatially homogeneous and considering no interaction between microorganisms and roots (Behera et al., 1990, Xu et al., 2001). In the case variations of soil respiration depend only on the spatial variability in soil carbon, autotrophic component is estimated from the y-intercept of the linear dependence of soil respiration on soil carbon.
Especially in forest ecosystems, the organic carbon is highly heterogeneous; therefore Rodeghiero and Cescatti (2006) adopted a method which accounts for spatial heterogeneity of both autotrophic and heterotrophic respiration. The total soil respiration was expressed as the sum of its two components: the autotrophic component, linearly dependent on the root density, and the heterotrophic components, linearly dependent on soil carbon content. Using the equation R= a x C + b x RD, where R is the total soil respiration at each plot ($\mu molm^{-2}s^{-1}$), a and b regression coefficients, C is the soil organic carbon and RD is the root density, each respiration component was calculated by setting the other to zero and using the site average of RD or C.
The limitation of this method is that it can be applied only in sites where there is an appreciable heterogeneity in both soil organic carbon and root density and that, different coefficients of regression should be established when taking into account different sites from the one in which they were estimated.
The primary objectives of this study were the monitoring of annual soil respiration in a forest site and its partitioning into autotrophic and heterotrophic components applying the indirect linear regression method; moreover the temporal variation of total, autotrophic and heterotrophic respiration rates and consequently their dependence on soil temperature and humidity were investigated.

4.2 MATERIALS AND METHODS

4.2.1 STUDY SITE

The site (about 4.5 hectares), located in the Joint Research Center of Ispra (Varese, Lombardy), is a mixed forest area that before 1960 was a stable grassland in conditions of high water content. The area is crossed along the E-W axis by an artificial concrete pipe, built nearly in the 1960, placed partially above ground but covered with soil and vegetation.
The forest is mainly composed by *Quercus robur*, *Robinia pseudoacacia, Alnus glutinosa* and *Pinus rigida*. *Quercus robur* is dominant while *Alnus glutinosa* prevails in the south-eastern side; *Robinia pseudoacacia* (false acacia) mostly extends along the artificial pipe and *Pinus rigida*, artificially introduced, is principally present at the northern and north-eastern edge of the study site. The forest is also characterized by other minor tree species as *Corylus avellana* (hazel) and *Prunus serotina* (black cherry).
The study about soil types and the spatial variability of soil features (see chapter 1) revealed that the soils (IUSS/ISRIC/FAO, 2006) are Umbrisols (Hypoendogleyic Umbrisol (Hyperdystric, Arenic), Endogleyic Umbrisol (Humic, Hyperdystric, Siltic, Transportic) and Endogleyic Mollic Umbrisol (Arenic, Transportic)).

These soils are weakly-developed, base desaturated and showed gleyic properties in the lower part of the profile. In correspondance of concrete pipe, soils are more thin and have been classified as Haplic Regosol (Dystric, Arenic, Transportic).
The soil surface texture (USDA class) was mainly sandy-loam and loamy-sand; the pHw of the first horizon show high variations, from very acid (3.5) to sub-acid values (6.6). The surface total nitrogen content is between 0.4 and 2% with the mean value of 0.9%, while surface organic carbon content ranges between 4.1 and 23.6% with the mean of 11.4%; when the average organic carbon content is over 5% to a depth of 50 cm, soil takes the qualifier Hyperhumic.
Details about study site and soil characteristics can be found in Chapter 1.

4.2.2 GAS SAMPLING

During 2008 measurements of soil respiration were performed along two cross transects passing for the centre of the area (fig 4.1). Based on detailed mapping of soil properties and on vegetation type, the transects were selected to capture the site conditions described in chapter 1, according to the axes NW-SE and NE-SW.

Figure 4.1 Transects for CO_2 flux measurements (16 points, 1-8 and 9-16). The broken line represents the concrete pipe.
(image from Google Earth)

Each transect was made by 8 measuring points (collars) for a total of 16 sampling points spaced at about 12.5 m one from each other. As the numbering of the plots is sequentially done, we therefore present results from plot 1 (start point of the NW pointing transect) to 8 (endpoint of the NW pointing transect) and from 9 (start point of the NE pointing transect) to 16 (endpoint of the NE pointing transect). The NW-SE transect started from the area where *Alnus glutinosa* prevailed and reached the forest part characterized by the presence of *Quercus robur and Pinus rigida* passing through the central area characterized by the black cherry and, immediately after the artificial pipe, by the pine; along this direction the soil organic carbon content, according the to the spatial distribution study of the main soil characteristics (chapter 1), was 15.61 kg m^{-2} with the higher value (17.95 kg m^{-2}) at the NW end. *Quercus robur* was always present along the second transect, which from the SW extremity (organic carbon: 12.55 kg m^{-2}), pointed to the pine zone (organic carbon: 43.12 kg m^{-2}) passing through plots characterized by the hazel, false acacia and black cherry.

CO_2 soil fluxes were measured with a portable infrared gas analyzer (LI-6400) equipped with a chamber based on the principle of closed dynamic systems.

The LI-6400 is a portable system connected to the Li-6400 soil flux chamber; the chamber is cylindrical with a diameter of 9.5 cm, base area of 76.1 cm^2, and a volume of 991 cm^3. The chamber concentration is automatically scrubbed to just below an ambient target, and then measured as it rises slightly above the ambient target. This maintains the CO_2 concentration gradient to within a few ppm of the natural, undisturbed value. The mixing fan in the sensor head is used to move air through a perforated manifold thoroughly mixing the air in the chamber; a pressure equilibration tube is used to eliminate pressure differentials and avoid chamber leaks.

The permanently installed collars were custom-made from stainless-steel with four rods (20 cm length and 3 mm diameter) helping to fix the collar tightly into the soil. The factory made chamber was slightly modified and an O-ring was added to the base in order to improve its sealing with the collars.

After the insertion, the collars remained in place for all the duration of the experiment. CO_2 soil fluxes were measured every 15-30 days, depending on season. At each sampling point, a single measurement was performed and the measurements from all collars were averaged to obtain the site soil flux rate (mean±SE).

Simultaneously with soil fluxes, soil temperature and soil water content were measured at all sites. Soil temperature was determined with the built-in temperature probe of the analyzer, usually at a depth of 5 cm, while soil water content was measured with a portable TDR system (IMKO Micromodultechnik, GmbH, Ettlingen, Germany) using a 12 cm long trifurcated probe.

The total, the autotrophic and the heterotrophic soil annual respiration rates (g C $m^{-2}y^{-1}$) were computed as the sum of hourly CO_2 fluxes estimated using the dependence of measured respiration from the soil temperature.

The hourly values of soil temperature were estimated by linear regression with soil air temperature data which were registered by the EMEP meteorological station.

4.2.3 SOIL, LITTER AND ROOT SAMPLING

At the end of the year, in correspondence with each respiration collar, a soil observation (minipit) was carried out, described and sampled up to a C horizon.

At each plot a 40 x 40 cm square was sampled from the organic layer (usually only OL, sometimes OL+OF); the litter biomass was converted to carbon content multiplying the dry weight by 0.48 (Nadehoffer and Raich, 1992).

For the determination of root density, core samples of 754 cm^3 was collected in 15 cm layers to a depth of 45 cm, brought to the laboratory, oven dried and weighed; roots were separated into three diameter classes (<2 mm, 2-5 mm, >5 mm) washed and oven dried at 105 °C for 48 hours to determine dry mass.

4.2.4 SOIL CHEMICAL ANALYSES

Carbon and nitrogen contents were determined with a Thermo Fisher Scientific CN elemental analyzer.

C and N concentrations of each described horizon were converted, through soil bulk density to the contents per unit area (kg m^{-2}) and summed to a depth of 15, 30 and 45 cm, including the organic layer too.

4.2.5 SEPARATING OF TOTAL SOIL RESPIRATION

By the results of the study reported in Chapter 1, we assumed the spatially heterogeneity of heterotrophic respiration, due to the large found heterogeneity of soil organic carbon. Therefore, we separated autotrophic (R_A) and heterotrophic (R_H) components applying the indirect method of linear dependence of soil respiration on soil carbon content. The CO_2, attributable to roots, was estimated from the y-intercept of the regression line between total soil respiration (R) and soil organic carbon (mineral soil carbon and litter carbon) expressed as mass per unit area to a depth of 15 cm.

4.3. RESULTS AND DISCUSSION

Figure 4.2 a shows an overview of the averaged CO_2 fluxes, measured during 2008. The fluxes ranged between 0.6 and 8.0 µmol CO_2 $m^{-2}s^{-1}$ with a mean value of 3.5±0.3 µmol CO_2 $m^{-2}s^{-1}$; we observed the highest flux rate during the summer period on 1st of August and the lowest flux values on 23th of December. In fact soil respiration showed a typical seasonal pattern following soil temperature; highly significant correlations were found between the soil respiration and the temperature (R^2= 0.90) (fig. 4.2 b). The absence of water limitations (soil relative water content: 23±5.4%) during the warmer months, resulted into the highest emissions of CO_2 concomitant with the increase of temperature.

A weaker relation (R^2= 0.47) was instead found between soil respiration and soil water content (fig. 4.2c).

We found high CO_2 rates if compared for example with those of a natural old-growth mixed deciduous forest in the Po Valley, which ranged between 0.3 and 3.8µmol$CO_2$$m^{-2}s^{-1}$ (Ferré et al., 2005).

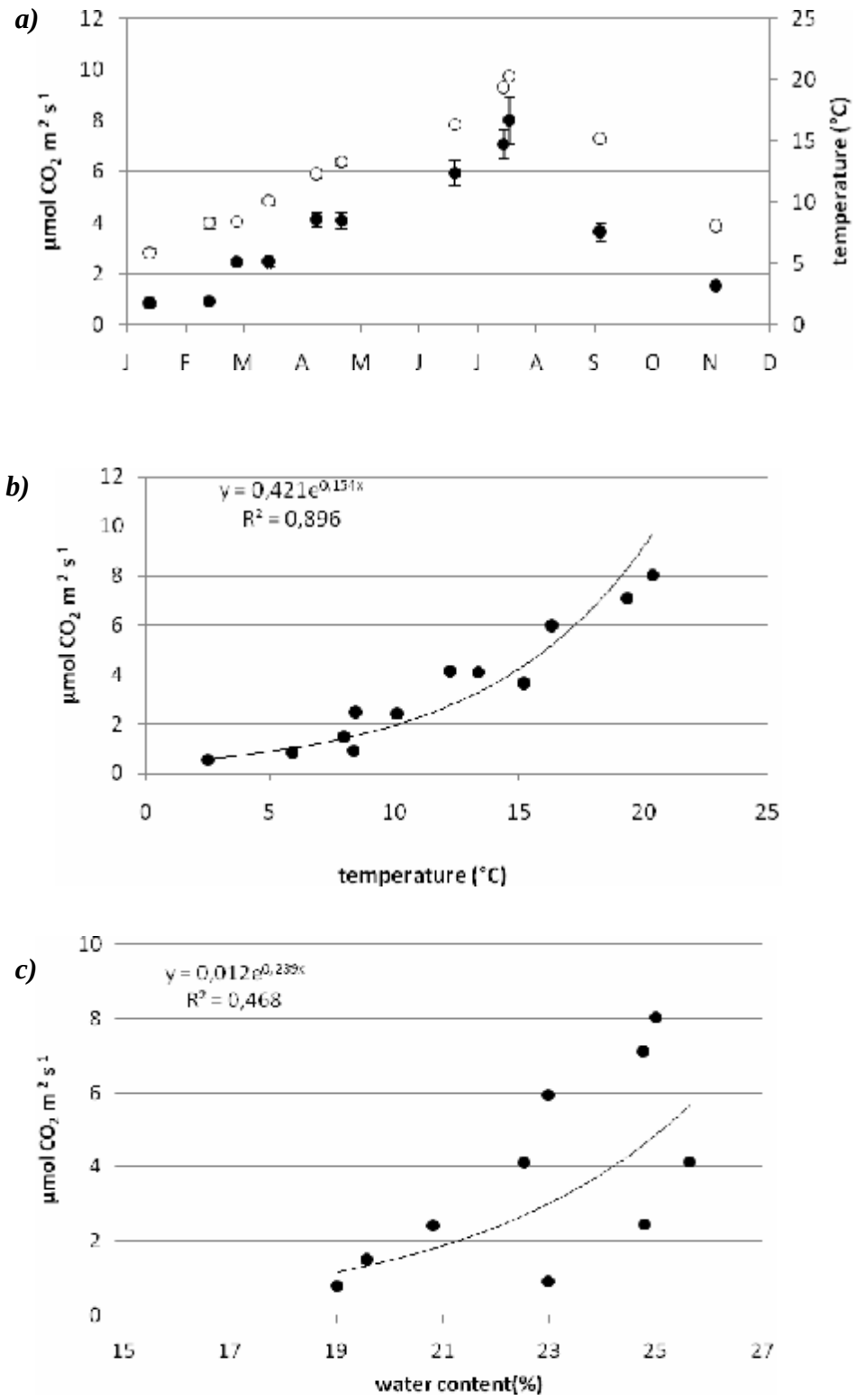

Figure 4.2 Seasonal trend (mean±SE) of CO_2 fluxes from the soil surface and of soil temperature at 5 cm at the EMEP forest site during 2008 (a). Relation between soil respiration and temperature (b) and soil respiration and soil water content (c).

Considering also the annual flux, our estimate (1341± 90 g C $m^{-2}yr^{-1}$) resulted quite elevated in comparison with the average annual value of 647±51 g C $m^{-2}yr^{-1}$ reported for the temperate deciduous forest ecosystems (Raich and Schlesinger, 1992). Important annual flux of 1079 g C $m^{-2}yr^{-1}$ was also found in an oak site in Italian Alps (Rodeghiero and Cescatti, 2006) characterized by lower organic carbon content than our experimental site and affected by drought especially during summer.
The wide range of soil CO_2 efflux estimates in forest ecosystems reflects large differences among different forest types such as from soil organic carbon contents, climate regimes and used measure techniques (Thierron and Laudelout, 1996; Epron et al., 1999; Xu et al., 2001; Borken et al., 2002).
Soil analyses demonstrated that this site was characterized by high soil organic carbon content (table 4.1); it ranged, in the 0-15 cm layer, between 4.22 kg m^{-2} of the antrophic soil placed on the concrete pipe (plot 13) and 10.26 kg m^{-2} of plot 6.

Table 4.1 Soil organic carbon content and humus type according to Référentiel Pédologique (Baize and Girard, 2008).

		OC (kg m^{-2})					
		n°	Mean	St.Dev.	St.Err.	Min	Max
soil	A1	17	9.7	4.3	0.7	1.5	18.5
	0-15 cm	17	8.4	1.6	0.5	4.2	10.3
	15-30 cm	17	5.0	2.3	0.6	0.3	8.3
	30-45 cm	15	2.9	2.2	0.6	0.2	7.0
	0-45 cm	15	16.3	5.1	1.4	6.9	24.7
organic layer		16	0.6	0.3	0.1	0.1	1.2
humus type	Mesomull	2 (plot 3, 7)	0.3	0.2	0.2	0.1	0.4
	Oligomull	6 (plot 1, 2, 4, 10, 11, 14)	0.6	0.2	0.1	0.3	0.8
	Dysmull	7 (plot 5, 8, 9, 12, 13, 15, 16)	0.6	0.3	0.1	0.3	0.9

Moreover, in the site was found humus layer with an average carbon content of 0.60±0.3 kg m^{-2}; according to the Référentiel Pédologique classification (Baize and Girard, 2008), the humus type was generally Mull with differences in the type, thickness and sequence of the organic horizons among the vegetation varieties. Under false acacia and black cherry we found Mesomull, a humus type characterized by high biological activity, principally of annelids; where oak prevails, there was Oligomull, in which the annelids activity is associated with that of arthropods. Above all under pine vegetation, but also under oak, or-

ganic layer was more thick and the biological activity (mainly arthropods) decreased: the humus type was Dysmull. To humus type more thick and less developed, generally characterized by higher CN ratio, correspond soils with higher organic carbon content.
The carbon content of the humus layer was found to be significantly correlated (table 4.2) to the soil annual respiration.

Table 4.2. Correlations between annual soil respiration R (g C $m^{-2}yr^{-1}$) and litter organic carbon (kg C m^{-2}), soil organic carbon (kg C m^{-2}), root density (kg m^{-2}). Significant correlation at p-value < 0.05 is marked with *.

	R
litter OC	0.65*
soil OC (0-15 cm)	0.57*
soil OC (0-30 cm)	0.38
soil OC (0-45 cm)	0.37
litter+OC (0-15 cm)	0.51*
root <2mm (0-15 cm)	0.18
root <2mm (0-30 cm)	0.21
root <2mm (0-45 cm)	0.26
root 2-5mm (0-15 cm)	0.10
root 2-5mm (0-30 cm)	0.12
root 2-5mm (0-45 cm)	0.14

Soil analyses also revealed an high C concentration down the profile to 45 cm; the average organic carbon content was 8.40±1.60 kg m^{-2} in the first 15 cm and 16.49±5.10 kg m^{-2} up to the depth of 45 cm.
While for the 15 cm thickness layer, correlation matrix showed significant relationships (p-value <0.05) between organic carbon content and annual soil respiration (table 4.2), the underlying layers seemed to poorly contribute to CO_2 flux rates. The mineralization in deep horizons was probably lower, connected with the presence of a more stable organic fraction; additionally, since soil bulk density increased with depth, the gas exchanges between atmosphere and deep layers may result quite slow.
Root density was 0.35±0.2 and 0.62±0.3 kg m^{-2} up to a depth of 45 cm for the fine roots (≤2 mm diameter class) and for the overall small roots (<5 mm diameter class) respectively; a worldwide database of measurements of root profiles showed that the average root mass ranged from about 0.2 kg m^{-2} for croplands to about 5 kg m^{-2} for forests, sclerophyllous shrubs and trees (Jackson et al., 1996), and in particular that the fine roots (<2 mm diameter) ranged from 0.27 kg m^{-2} in deserts to 1.5 kg m^{-2} in temperate grasslands, with a temperate deciduous forest value of 0.78 kg m^{-2} (Jackson et al., 1997).
Absence of significant statistical correlation between root density and soil respiration was obtained. We have found a very high organic carbon content (8.4 ± 1.6 in the 0-15 cm layer) which may have hidden the variability effect of root density. A significant correla-

tion between root density and soil respiration was found only for November and December, close to the root sampling data. To avoid disturbances to measurement points, the root sampling was carried out once and the partitioning of soil respiration in its components was applied to yearly data without considering seasonal variations of the investigated parameters. Since the root biomass may change significantly during the year (Lukac et al., 2003), a multiple sampling could have probably provided a more accurate estimation of root contribution to the variation in soil respiration.

Taking into account these results, the dependence of respiration on soil organic carbon (humus layer included) up to a depth of 15 cm was considered at a significant level $p < 0.05$.

For each sampling data, the partitioning of soil respiration components is showed in fig. 4.3. Microbial respiration averaged 1.5±0.3 µmol CO_2 $m^{-2}s^{-1}$ (December) from 0.1 to 4.5 µmol CO_2 $m^{-2}s^{-1}$ (August) while root respiration varied from 0.4 (February) to 3.7 µmol CO_2 $m^{-2}s^{-1}$ (July) with mean value of 1.9±0.4 µmol CO_2 $m^{-2}s^{-1}$.

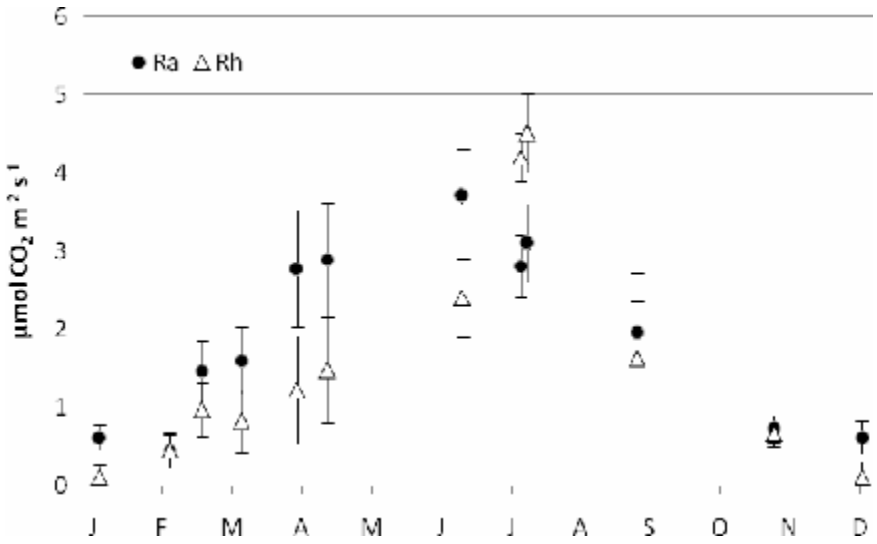

Figura 4.3 Seasonal trend of root (Ra) and microbial (Rh) contributions to the total soil CO_2 efflux. Vertical bars are SE.

The seasonal trend of the heterotrophic component was similar to that of total respiration, with summer peak and lower values during winter time. The seasonal pattern for root contribution was instead slightly different from that of R_H: the rapid increase of the autotrophic respiration during spring and the peak in early summer may be associated with the growing season.

Factors controlling the seasonal change of CO_2 efflux seemed to differ between the two components of soil respiration. Soil temperature controlled both the heterotrophic (R^2 = 0.89) and autotrophic respiration (R^2 = 0.70) (fig. 4.4 a and b) which resulted less correlated with the water content (R^2 = 0.51 and 0.37 respectively) (fig. 4.5 a and b).
During spring and summer time, the increase of the microbial component was mainly connected with temperature (R^2 = 0.98), while the root respiration showed a lower correlation with soil temperature (R^2 = 0.52) suggesting that the autotrophic component was controlled not only by abiotic factors but also by phenology of plants (Epron et al., 2001; Lee et al., 2003).

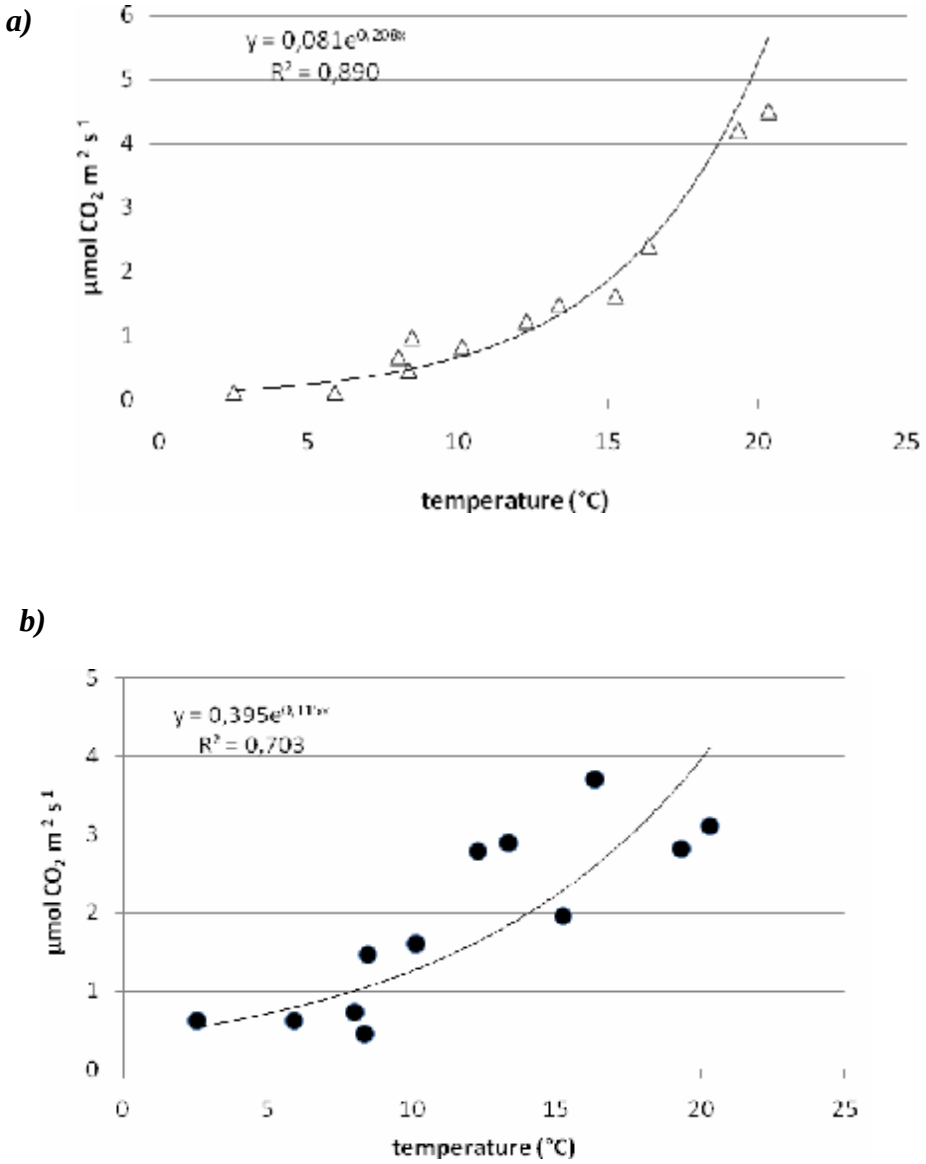

Figura 4.4 Soil temperature dependences of heterotrophic (a) and autotrophic (b) components of soil respiration.

a)

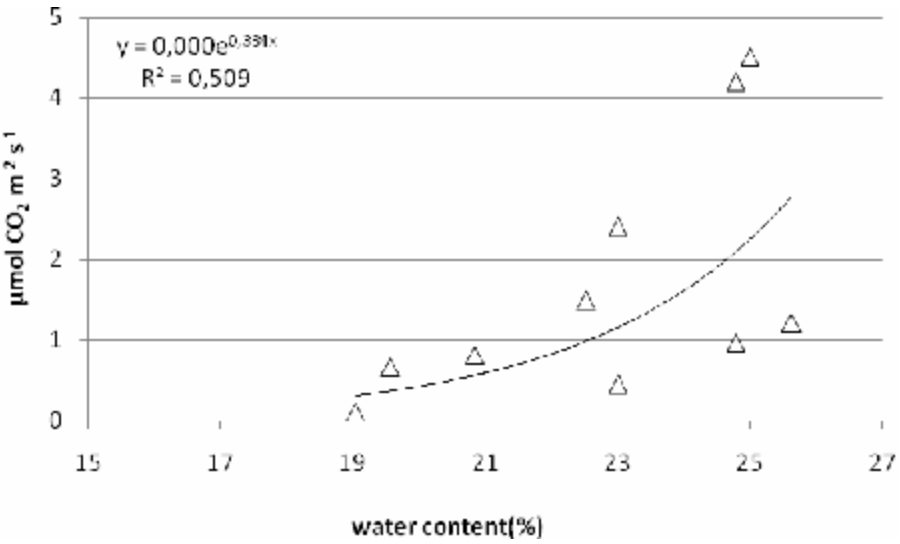

b)

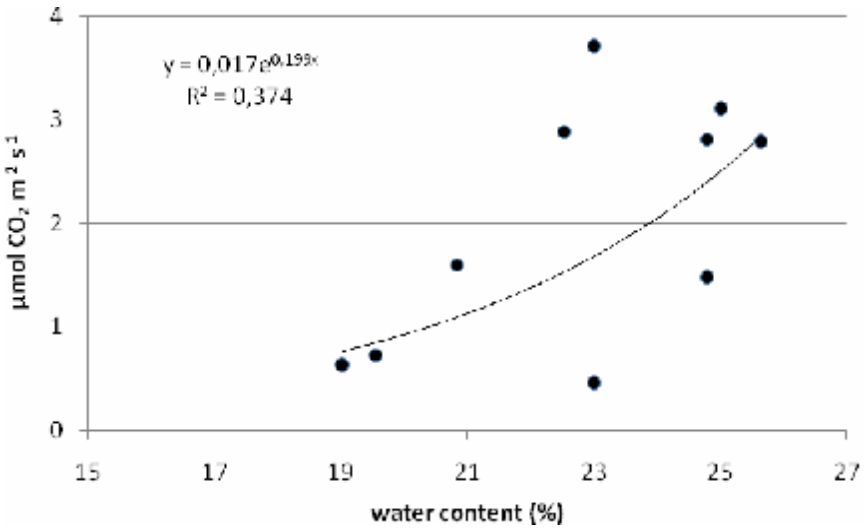

Figura 4.5 Soil water content dependences of heterotrophic (a) and autotrophic (b) components of soil respiration.

The autotrophic and heterotrophic contributions to total soil CO_2 efflux reached their maximum on April (69%) and August (59%), respectively.
The partitioning of the total annual CO_2 flux into its autotrophic and heterotrophic contributions, using temperature dependence of the two components, is shown in figure 4.6; the heterotrophic, with 705 $gCm^{-2}yr^{-1}$ slightly prevailed, counting for 51% of total annual CO_2 efflux, compared with 49% of the autotrophic respiration (670 g C $m^{-2}yr^{-1}$).

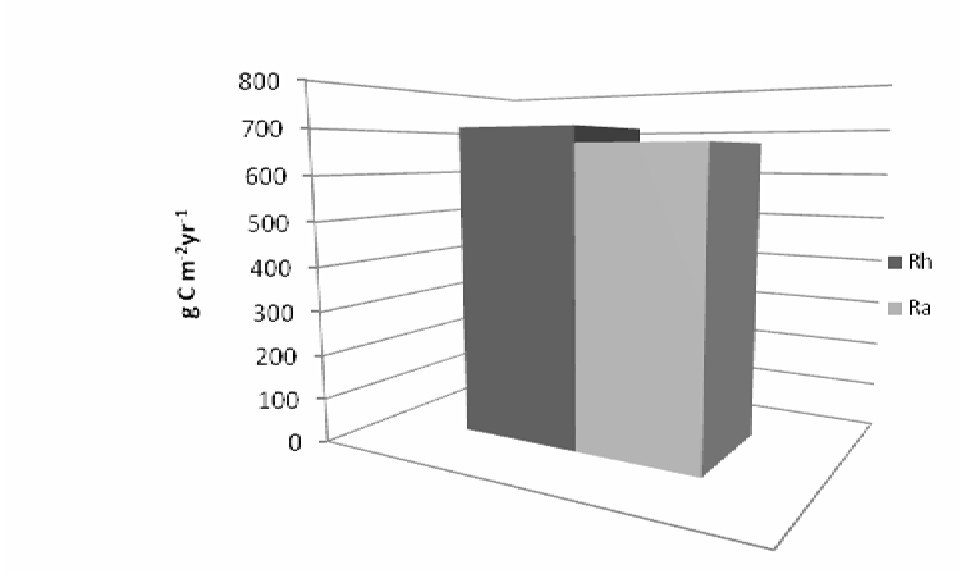

Figure 4.6 Annual autotrophic (Ra) and heterotrophic (Rh) components of soil respiration.

Our results fell in the range reported for forest ecosystems: published estimates of the contribution of root respiration to the total soil respiration, determined with a wide range of methods, vary in the 45–50% range with a mean value of 48% for forest ecosystems; in particular *Quercus* forest showed annual values ranging between 33 and 90% while pine plantation root efflux ranging between 40 and 65% (Hanson et al., 2000).
Applying the standard regression analysis technique, Behera et al. (1990) found that the autotrophic component contributed for 50% to total soil CO_2 efflux in a young mixed forest and Xu et al., (2001) estimated a contribution of 47% in a ponderosa pine plantation; assuming the spatial variation dependence of total soil respiration on spatial variation of both root biomass and soil organic carbon, Rodeghiero and Cescatti (2006) reported that annual autotrophic respiration accounted for 16-58% in seven forest ecosystems.

4.4. CONCLUSIONS

Soil CO_2 efflux was measured in a mixed forest site over a year, to reveal seasonal trend of soil respiration, to separate the respective contributions of root and microbial respiration to the total CO_2 emissions, and to analyze the temperature dependence of the two components.
In this study, the indirect method for separation of soil respiration in its components was applied to investigate the dependence of spatial variation of soil CO_2 efflux on the spatial variation of both soil organic content and root density. However, statistical analysis revealed a significant correlation with soil respiration only for organic carbon. In relation to this, the high organic carbon content that characterized the site may have hidden the variability effect of root density. Additionally, to avoid disturbances to measurement points,

the root sampling was carried out once and the partitioning of soil respiration in its components was applied to yearly data without considering seasonal variations of the investigated parameters; whereas for organic carbon the changes can be considered negligible, root biomass may change significantly during the year, so that an accurate estimation of root contribution through multiple sampling may be advisable.

Through investigation of different soil depths, it was possible to define the layer of soil which principally contributes to total respiration: the surface layer (0-15 cm) primarily contribute to CO_2 flux rates. Despite the fact that a high C concentration was even found down the profile to 45 cm, a significant correlation between soil respiration and organic content in deep horizons was not found. A possible reason of this can be identified in the physical characteristics of such layers (e.g. porosity and bulk density) and in the characteristics of organic matter.

The partitioning of the total annual CO_2 flux into its autotrophic and heterotrophic contributions revealed that the heterotrophic component slightly prevailed, counting for 51% of total annual CO_2 efflux, compared with 49% of the autotrophic one.

Factors controlling the seasonal change of CO_2 efflux seemed to differ between the two components of soil respiration. Several studies have proposed models to predict soil respiration from mainly temperature and soil moisture (Mielnick and Dugas, 2000). We found that soil temperature largely controlled the heterotrophic respiration while the rapid increase of the autotrophic respiration during spring and the peak in early summer suggested that the autotrophic component was affected not only by abiotic factors, but also by plant phenological stages.

REFERENCES

- Baize and Girard, 2008. Référentiel pédologique. AFES (Association française pour l'étude du sol).
- Behera, N., Joshi, S.K., Pati, D.P., 1990. Root contribution to total soil metabolism in a tropical forest soil from Orissa, India. Forest Ecology and Management 36, 125–134.
- Bond-Lamberty, B., Wang, C., Gower, S.T., 2004. A global relationship between the heterotrophic and autotrophic components of soil respiration. Global Change Biology 10, 1756–1766.
- Borken, W., Xu, Y.J., Davidson, E.A., Beese, F., 2002. Site and temporal variation of soil respiration in European beech, Norway spruce, and Scots pine forest. Global Change Biology 8, 1205–1216.
- Cisneros-Dozal, L.M., Trumbore, S., Hanson, P.J., 2006. Partitioning sources of soil-respired CO_2 and their seasonal variation using a unique radiocarbon tracer. Global Change Biology 12, 194–204.
- Coûteau, M.M., Bottner, P., Berg, B., 1995. Litter decomposition, climate and litter quality. Tree 10, 63-66.

- Dixon, R.K., Brown, S., Houghton, R.A., Solomon, A.M., Trexler, M.C., Wisniewski, J., 1994. Carbon pools and flux of global forest ecosystems. Science 263, 185–190.
- Epron, D., Farque, L., Lucot, E., Badot, P.M, 1999. Soil CO_2 efflux in a beech forest: dependence on soil temperature and soil water content. Annals of Forest Science 56, 221–226.
- Epron, D., Le Dantec, V., Dufrene, E., Granier, A., 2001. Seasonal dynamics of soil carbon dioxide efflux and simulated rhizosphere respiration in a beech forest. Tree Physiology 21, 145–152.
- Ferré, C., Leip, A., Matteucci, G., Previtali, F., Seufert, G., 2005. Impact of 40 years poplar cultivation on soil carbon stocks and greenhouse gas fluxes. Biogeosciences Discussions 2, 897–931.
- Hanson, P.J., Edwards, N.T., Garten, C.T., Andrews, J.A., 2000. Separating root and soil microbial contributions to soil respiration: a review of methods and observations. Biogeochemistry 48, 115–146
- Hendricks, J.J., Nadelhoffer, K.J., Aber J.D., 1993. Assessing the role of fine roots in carbon and nutrient cycling. Trends in Ecology & Evolution 8, 174–178.
- Högberg, A., Nordgren, N., Buchmann, A.F.S., Taylor, A., Ekblad, M.N., Högberg, G., Nyberg, M., Ottosson-Löfvenius, Read, D.J., 2001. Large-scale forest girdling shows that current photosynthesis drives soil respiration. Nature 411, 789–792.
- Houghton, R.A., 2003. Revised estimates of the annual net flux of carbon to the atmosphere from changes in land use and land management 1850-2000. Tellus Series B-Chemical and Physical Meteorology 55, 378–390.
- Houghton, R.A., Woodwell, G.M., 1989. Global climatic change. Scientific American 260(4), 36–44.
- IUSS/ISRIC/FAO, 2006. World Reference Base for Soil Resources. World Soil Resources Reports 103, FAO, Rome, pp. 128.
- Jackson, R.B., Canadell, J., Ehleringer, J.R., Mooney, H.A., Sala, O.E., Schulze, E.D., 1996. A global analysis of root distributions for terrestrial biomes. Oecologia 108, 389–411.
- Jackson, R.B., Mooney, H.A., Schulze, E.D., 1997. A global budget for fine root biomass, surface area, and nutrient contents. Proceeding of the National Academy of Sciences, USA, 94, 7362–7366.
- Janssens, I.A., Meiresonne, L., Ceulemans, R., 1999. Mean soil CO_2 efflux from a mixed forest. Temporal and spatial integration. In: Ceulemans, R., Veroustraete, F., Gond, V., Van Rensbergen, J. (eds.), Forest Ecosystem Modelling, Upscaling and Remote Sensing. SPB Academic Publishing, The Hague, pp. 19–33.
- Keith, H., Jacobsen, K.L., Raison, R.J., 1997. Effects of soil phosphorus availability, temperature and moisture on soil respiration in Eucalyptus pauciflora forest. Plant and Soil 190, 127–141.
- Kucera, C.L., Kirkham, D.R., 1971. Soil respiration studies in tallgrass prairie in Missouri. Ecology 52, 912–915.
- Kuzyakov, Y., Larionova, A.A., 2005. Root and rhizomicrobial respiration: a review of approaches to estimate respiration by autotrophic and heterotrophic organisms in soil. Journal of Plant Nutrition and Soil Science 168, 503–520.
- Law, B.E., Ryan, M.G., Anthoni, P.M., 1999. Seasonal and annual respiration of a ponderosa pine ecosystem. Global Change Biology 5, 169–182.

- Lee, M., Nakane, K., Nakatsubo, T., Koizumi, H., 2003. Seasonal changes in the contribution of root respiration to total soil respiration in a cool-temperate deciduous forest. Plant and Soil 255, 311–318.
- Lukac, M., Calfapietra, C., Godbold, D.L., 2003. Production, turnover and mycorrhizal colonization of root systems of three Populus species grown under elevated CO_2 (POPFACE). Global Change Biology 9, 838–848.
- Mielnick, P.C., Dugas, W.A., 2000. Soil CO_2 flux in tallgrass prairie. Soil Biology & Biochemistry 32, 221–228.
- Nadelhoffer, K.J., Raich, J.W., 1992. Fine root production estimates and belowground carbon allocation in forest ecosystems. Ecology 73, 1139–1147.
- Raich, J.W., Schlesinger, W.H., 1992. The global carbon dioxide flux in soil respiration and its relationship to vegetation and climate. Tellus 44B, 81–99.
- Raich, J.W., Potter, C.S., 1995. Global patterns of carbon dioxide emissions from soils. Global Biogeochemical Cycles 9, 23–26.
- Rodeghiero, M., Cescatti, A., 2006. Indirect partitioning of soil respiration in a series of evergreen forest ecosystems. Plant and Soil 284, 7–22.
- Ryan, M.G., Hubbard, R.M., Pongracic, S., Raison, R.J., McMurtie, R.E., 1996. Foliage fine-root, woody-tissue and stand respiration in Pinus radiata in relation to nitrogen status. Tree Physiology 16, 333–343.
- Schlesinger, W.H., Andrews, J.A., 2000. Soil respiration and the global carbon cycle. Biogeochemistry 48, 7–20.
- Taylor, B.R., Parkinson D., Parsons, W.F.J., 1989. Nitrogen and lignin content as predictors of litter decay rates. A microcosm test. Ecology 70, 97–104.
- Thierron, V., Laudelout, H., 1996. Contribution of root respiration to total CO_2 efflux from the soil of a deciduous forest. Canadian Journal of Forest Research 26, 1142–1148.
- Trumbore, S., 2006. Carbon respired by terrestrial ecosystems. Recent progress and challenges. Global Change Biology 12, 141–153.
- Valentini, R., Matteucci, G., Dolman, A.J., Schulze, E.D, Rebmann, C., Moors, E.J., Granier, A., Gross, P., Jensen, N.O., Pilegaard, K., Lindroth, A., Grelle, A., Bernhofer C., Grundwald, T., Aubinet, M., Ceulemans, R., Kowalski, A.S., Vesala, T., Rannik, U., Berbigier, P., Loustau, D., Guomundsson, J., Thorgeirsson, H., Ibrom, A. Morgenstern, K., Clement, R., Moncrieff, J., Montagnani, L., Minerbi, S., Jarvis, P.G., 2000. Respiration as the main determinant of carbon balance in European forests. Nature 404, 861–865.
- Wiant, H.V., 1967. Contribution of roots to forest soil respiration. Advancing Frontiers of Plant Science 18, 163–167.
- Xu, M., De Biase, T.A., Qi, Y., Goldstein, A., Liu, Z., 2001. Ecosystem respiration in a young ponderosa pine plantation in the Sierra Nevada Mountains, California. Tree Physiology 21, 309–318.

CONCLUSIONS AND PERSPECTIVES

The conclusions are the result of each study area developed in this thesis and according to the adopted order.

Study of soil spatial variability: the analysis of the spatial variability of soil properties has revealed to be essential for the identification of the sampling scheme for gas monitoring; without the knowledge of the differences in soil characteristics and their spatial trend, the choice of monitoring points in both experimental sites would have been random. Whereas for forest sites the selection of homogeneous areas can be based on the distribution and composition of vegetation, for the agricultural sites the absence of superficial aspects related to the soil properties, leads to unforeseeable results. According to the spatial survey and due to the necessity, for logistic and economic reasons, of identifying only one sampling area, field parts characterized by extreme soil properties were knowingly excluded, opting for sampling areas with intermediate values of soil characteristics. In conclusion, the study was useful for selecting and assessing most representative plot for measurement points, without, however, taking into account the effect and contribution of revealed soil spatial variability.

Monitoring of CO_2, CH_4 and N_2O and application of DNDC model: with the monitoring of CH_4, N_2O and CO_2, estimation of fluxes from paddy soil relative to the entire year and not only to the growing season was provided. This study represented a contribution in reducing uncertainties and gaps about greenhouse gas emissions, particularly concerning CO_2, for which monitoring data from paddy soils are limited. The DNDC process-oriented biogeochemical model was then tested against field data, revealing the capacity of capturing quantitatively the major aspects of CH_4 and CO_2 production and emissions from investigated paddy soil and of simulating their seasonal trend. The major discrepancies between observed and simulated daily fluxes have regarded the N_2O emissions. Moreover, differences in gas emission rates between model and field data were even found during the growing season, probably connected with the application of the empiric approach in simulating crop growth. Therefore, applying the opportune modifications to improve N_2O flux simulation and selecting the process-based approach for predicting cultivation growth, the model might be used to simulate different management sceneries, guiding the choose for the most efficient agricultural practice in terms of both climate forcing and crop productivity. In addition, it might be possible to evaluate and quantify soil spatial variability effects on greenhouse emissions by applying the DNDC to each area identified with the previous spatial survey of soil properties.

Characterization of microbial community using PLFA analysis: the PLFA method used in this work has already applied in rice ecosystems to observe changes in community structure connected with agricultural management. These studies investigated exclusively surface soil, focusing the attention on the characteristic of fatty acids to be valid indicators of changes in composition of rice soil microbial communities, but the correlation between fatty acids and gas emissions were never investigated.
In this study, microbial biomass and community composition in a rice paddy were examined both during the crop growth season and the fallow period, considering also deeper layers; microbial and gas emission data were compared, revealing that some of the investigated fatty acids can be considered indicators of soil conditions favourable to the production of CH_4 and N_2.

Partitioning of soil respiration in the forest site: the study provided site-specific data on autotrophic and heterotrophic components of soil respiration and their dependence from temperature and soil water content, providing a contribution for the understanding of forest ecosystem carbon balance. Information about autotrophic and heterotrophic respiration are useful to reduce the estimates uncertainty, to predict the forest ecosystem response to climate change and to the understanding of potential feedbacks of the global change on soil processes.
Variation in soil CO_2 fluxes proved to depend on the soil organic carbon (humus layer included); the partitioning of the total annual CO_2 flux into its autotrophic and heterotrophic contributions revealed that the heterotrophic component prevailed slightly. Root density, obtained by yearly sampling, was uncorrelated to soil respiration; a seasonal characterization of the root biomass could be carried out to investigate the root turnover and quantify changes in root biomass, to verify obtained results.

Acknowledgements

This research was sustained by the Institute for Environment and Sustainability of the Joint Research Centre (IES-JRC) of Ispra (VA); I wish to thank the IES-JRC staff: G. Seufert and A. Leip for their kindness, T. Zenone for the helpful support in the soil respiration monitoring, M. Duerr and M. Andersson for logistic assistance during the field campaign. I thank the staff of the Remote Sensing of Environmental Dynamic Laboratory (University of Milano-Bicocca) that provided data on gas emissions at ecosystem level. A special thanks to Sophie Zechmeister-Boltenstern and her Vienna group (Federal Research and Training Centre for Forests, natural Hazards and Landascape - BFW) for assistance in soil microbial analyses. I further thank Annamaria Castrignanò (Research Unit for Cropping Systems in Dry Environments CRA-SCA, Bari) for useful discussions and helpful comments.